INAUGULAR - DISSERTATION

Zur

Erlangung der Doktorwürde

der

Naturwissenschaftlich-Mathematischen Gesamtfakultät

der

Ruprecht – Karls - Universität
Heidelberg

Vorgelegt von

Diplom-Physikerin Soheir El-Derby

aus Ägypten - Kairo

Tag der mündlichen Prüfung: 12-12-2003

2,4,6-Tris(isopropylamino)-1,3,5-trinitrobenzene: Probing the Impact of Crystal Packing Forces in the Dimorphs and the Cocrystals – Experimental and Theoretical Study

Gutachter: Prof. Dr. Hermann Irngartinger

Prof. Dr. Rolf Gleiter

This work was represented :

1. as poster in:

- ICCC 35, Jul. 21-26, 2002. Heidelberg, Germany.
- Workshop on ‘Intermolecular interactions’, Feb. 09-11, 2003. Aachen, Germany.
- INDABA IV, Workshop on Patterns in Nature, Aug. 17-22, 2003. Skukuza, South Africa.
- ECM 21 (European Crystallographic Meeting), Aug. 24-29, 2003. Durban, South Africa.

2. as lecture in:

- Workshop on ‘Intermolecular interactions’, Feb. 09-11, 2003. Aachen, Germany.
- ECM 21 (European Crystallographic Meeting), Aug. 24-29, 2003. Durban, South Africa.

Acknowledgments

I am most grateful to Priv.- Doz. Dr. J. Jens Wolff for the interesting idea of this work and for his kind supervision during the first 18 months of this work, unfortunately he died after this period suddenly. I wish also to express my deep gratitude and thanks to Prof. Dr. Hermann Irngartinger for his kind supervision and assistance. Sincere thanks to all the members of the group: Dr. Thomas Oeser, Mrs. Uta Wiesinger, Dr. Anton Weber and Dr. Oliver Kinderman for their support, with special thanks to Dr. Thomas Oeser for his continuous help, and Mrs. Uta Wiesinger for the performance of the most X-ray single crystal and powder diffraction measurements.

I wish to thank Prof. Dr. Ronald Miletich, Institute of Mineralogy, for given us the chance to perform the high temperature powder diffraction measurements in his institute, with special thanks for his co-worker Mrs. Ilse Glass for her support during the performance of these measurements.

I would like to thank the granting institution DFG (Deutsch Forschunggemeinschft) for financial support of this work.

Finally, I like to express my deepest thanks to my husband for his support and encouragement.

Summary……………………………………………………………………………I

Zusammenfassung……………………………………………………………………I

Introduction …………………………………………………………………………4

1 Theoretical background……………………………………………………………8

1-1Thermal analysis……………………………………………………………………8

1-1-1 Differential scanning calorimetry (DSC) ……………………………………8
1-1-2 Thermogravimetry (TG)…………………………………………………………9
1-1-3 Simultaneous and complementary techniques………………………………9

1-2 Computational methods……………………………………………………………10

1-2-1 Force field method…………………………………………………………………10
1-2-2 Calculating atomic charges: charges derived from the molecular……………11
electrostatic potential. ……………………………………………………………………11
1-2-3 Density functional theory ………………………………………………………12

2 Results and discussions of the experimental part………………………………14

2-1 Dimorphs and cosolvates of **1** ……………………………………………………14

2-2 Ring and molecular conformation ………………………………………………16

2-3 Discussion of the packing……………………………………………………………20

2-3 The influence of packing patterns on molecular parameters of **1**………………30

2-4 Differential scanning calorimetry and thermogravimetry ………………………33

2-5 Powder diffraction ……………………………………………………………………40

3 Energy calculations ……………………………………………………………………42

3-1 Method……………………………………………………………………………………42

3-2 Results and discussion…………………………………………………………………43

3-2-1 The DFT calculations on the molecular level……………………………………43
3-2-2 Force Field calculations in three dimension (on the crystal level) ……………47
3-2-3 Calculation of intermolecular interactions ………………………………………51

4 Deprotonated structures ………………………………………………………………63

4-1 Discussion of the packing………………………………………………………………63

4-2 Ring conformation………………………………………………………………………66

5-1 Synthesis…………………………………………………………………………………69

5-1-1 Synthesis of 2,4,6-tris(2(S)-butylamino)-1,3,5-trinitrobenzenes **5**………………69

5-2 X-ray structure analyses of **5** 69

6 Crystallographic data 71

dimorph **1a** 72

dimorph **1b** 74

benzene as inclusion compound (**1-1**) 75

ethylbenzene as inclusion compound (**1-2**) 76

cumene as inclusion compound (**1-3**) 77

fluorobenzene as inclusion compound (**1-4**) 78

chlorobenzene as inclusion compound (**1-5**) 79

m-difluorobenzene as inclusion compound (**1-6**) 80

o-difluorobenzene as inclusion compound (**1-7**) 81

p-difluorobenzene as inclusion compound (**1-8**) 82

1,2,4-trifluorobenzene as inclusion compound (**1-9**) 83

hexafluorobenzene as inclusion compound (**1-10**) 84

phenol 1 as inclusion compound (**1-11**) 86

phenol 2 as inclusion compound (**1-12**) 88

anisole as inclusion compound (**1-13**) 89

benzonitrile as inclusion compound (**1-14**) 91

trifluorotoluene as inclusion compound (**1-15**) 92

DMF as inclusion compound (**1-16**) 93

hydroquinone as inclusion compound (**1-17**) 94

p-xylene 1 as inclusion compound (**1-18**) 95

p-nitrophenol as inclusion compound (**1-19**) 96

p-fluorotoluene as inclusion compound (**1-20**) 97

o-fluorotoluene as inclusion compound (**1-21**) 98

p-chlorofluorobenzene as inclusion compound (**1-22**) 99

m-fluoronitrobenzene as inclusion compound (**1-23**) 100

o-fluoronitrobenzene as inclusion compound (**1-24**) 101

p-fluoronitrobenzene as inclusion compound (**1-25**) 102

nitroethane as inclusion compound (**1-26**) 103

1-nitropropane as inclusion compound (**1-27**) 104

benzaldehyde as inclusion compound (**1-28**) 105

dioxane as inclusion compound (**1-29**) 106

γ-picoline 2 as inclusion compound (**1-31**) 108

2,4,6-tris(isopropylamino)-1,3,5-trinitrobenzenes with isopropylamine (**1dep-1**) 109

2,4,6-tris(t-butylamino)-1,3,5-trinitrobenzenes with t-butylamine (**3dep-1**) 111

2,4,6-tris(cyclopropylamino)-1,3,5-trinitrobenzenes with t-butylamine (**2dep-1**) 113

2,4,6-tris((S)2-butylamino)-1,3,5-trinitrobenzenes (**5**) 115

Appendix 1 117

References 120

Summary

For a systematic study of crystal packing in a molecular solid, it is advantageous not to change the molecular constitution, but to analyse polymorphs or cosolvates (pseudopolymorphs) of one compound. Cosolvates eliminate the need to work with metastable polymorphs whose available numbers will be quite limited in most cases. Provided a conformationally quite labile molecule is used, packing patterns and their influence on molecular parameters may be studied simultaneously, and also the energetic and structural influence of intermolecular interactions upon the molecular geometry can be examined. We assumed 2,4,6-tris(isopropylamino)-1,3,5-trinitrobezene **1** to be a suitable candidate. We thus attempted to obtain a large amount of solvates and tried to embark on a systematic study (both experimentally and theoretically) of conformational effects of crystal packing. Here we describe their investigation by X-ray diffraction, thermal analysis, and computational methods (force field and ab-initio).

The crystal and molecular structures were determined by X-ray diffraction. For thermal analysis investigations a combination of Differential Scanning Calorimetry (DSC) and Thermogravimetry (TG) measurements were done to ensure better profile and accurate analyses of the changes taking place.

In our work we have calculated the electrostatic potential (ESP) charges and the molecular energies of the experimental molecular structures after the correction of the hydrogen atomic positions, using the Density Functional Theory (DFT) electronic structure program DMOL3 (2.2), with DNP basis set and GGA-BLYP functional. The molecular structures with the calculated charges then have been used to calculate: the crystal, the lattice and individual interaction energies in each structure, within the molecular simulation program Discover, using COMPASS force field.

A wide range of small molecules were found to be incorporated into crystals of **1**: benzene **1-1**, ethyl benzene **1-2**, cumene **1-3**, fluoro- **1-4**, and chlorobenzene **1-5**, *m*- **1-6**, *o*- **1-7** and *p*-difluorobenzene **1-8**, 1,2,4-triflourobenzene **1-9**, hexafluorobenzene **1-10**, two phenol inclusion crystals **1-11, 1-12**, anisole **1-13**, benzonitrile **1-14**, trifluorotoluene **1-15**, DMF **1-16**, hydroquinone **1-17**, *p*-xylene **1-18** , *p*-nitrophenol **1-19**, *p*- **1-20**, and *o*-fluorotoluene **1-21**, *p*-chloro-fluorobenzene **1-22**, *m*- **1-23**, *o*- **1-24** and *p*-fluoronitrobenzene **1-25**, nitroethane **1-26**, 1-nitropropane **1-27**, benzaldehyde **1-28**, dioxane **1-29**, and two γ-picoline inclusion crystals **1-30, 1-31**. in addition to a new dimorph **1b**.

The crystal and molecular structures of the first dimorph **1a** of **1** with two independent molecules (**1a1**, **1a2**) in the asymmetric unit has been found previously, as well as cocrystals with toluene **1-32**, nitrobenzene **1-33**, *p*-chlorotoluene **1-34**, *p*-xylene 2 **1-35**, formic acid **1-36**, acetic acid **1-37**, nitromethane **1-38** and acetonitrile **1-39**. These structural results were included in the discussion of the packing arrangements. The thermal measurements and the energy calculations, for all the structures, were carried out in this present work.

Six different packing arrangements, which have been divided into four groups, for the cosolvates of **1** were found. These different packing arrangements show the adjustable character of our host framework. Only one packing type, group 1, has neither host-host nor host-guest intermolecular hydrogen bonds. 17 structures out of the total of 39 structures adopt this packing type.

For the conformations of the six-membered ring of **1** in the different cosolvates, we have found that :

- three different conformations can be adopted by the host molecule **1**: boat form with two short and four long C—C bonds in the six-membered ring (quinonoid character), twist form with two long and four short C—C bonds (cyanine character) and intermediate twisted-boat form.
- in cosolvates that contain intermolecular hydrogen bonds the host molecule **1** adopts either twist form or twisted-boat forms, except structures with DMF (**1-16**) and *p*-xylene 2 (**1-35**), while in the absence of intermolecular hydrogen bonds (structures of group 1) **1** is more free to adopt twist, boat or twisted-boat form depending on the included molecule.
- in all the 14 structures of group 2, the six-membered ring of molecule **1** adopt twist forms except structures with DMF (**1-16**) (which adopts boat form), *p*-nitrophenol (**1-19**) and *m*-fluoronitrobenzene (**1-23**) (both adopt twisted-boat form). The twist conformation is very suitable for strong van der Waals interactions between the different layers in this structure pattern.
- in all the structures of group 3, the six-membered ring of **1** adopt twisted-boat forms except one of the two independent molecules in the structures with *p*-xylene 2 (**1-35m1**), which adopts boat form.
- the stronger the host-guest interactions, the shorter the $(\text{C—C short})_{\text{ave}}$ and the longer the $(\text{C—C long})_{\text{ave}}$ in the ring of **1**.

The following results were obtained from both DSC experiments and the theoretical calculations of the lattice energy:

1. Substantially high dissolution energy E_{diss} (obtained from DSC measurements) and lattice energy/molecule ELM (obtained from force field calculations) were found for the solvates that have host-guest intermolecular hydrogen bonds (inclusion crystals with phenol, hydroquinone, DMF, benzaldhyde, acetic acid, and formic acid), for solvates that have methyl group in the *para* position (inclusion crystals with *p*-xylene 2, *p*-fluorotoluene, *p*-chlorotoluene and γ-picoline 2) and for inclusion crystals with benzonitrile and nitroethane.

2. Form **1a**, which has chain character of the intermolecular hydrogen bonds system, is more stable than **1b**, which have a dimer character of the intermolecular hydrogen bonds system.
3. The stabilities of the structures with isomeric inclusion molecules are in the following sequence: cosolvates with *para* > *ortho* > *meta* substitution pattern. Guest molecules with substitution in *para* positions fit much better into the holes between the host molecules producing stronger intermolecular interactions with the host molecules as well as with the other guest molecules and consequently more stable packing.
4. The first structure with phenol 1 (host: guest = 2:1) is more stable than the second structure phenol 2 (host: guest = 1:2), the second structure with γ-picoline 2 (host: guest = 1:1.5) is more stable than the first structure γ-picoline 1 (host: guest = 1:1) and the first structure with *p*-xylene 1 (host: guest = 1:1) is more stable than the second structure *p*-xylene 2 (host: guest = 1:1/4). The close packing structure is always more stable then the other structure.

For every structure powder diffraction measurements have been performed at room temperature and at temperature higher than the guest dissolution temperature. All the cosolvate structures changes to structure **1a** after the evaporation of the solvent, except that of anisole which change to structure **1b**. The anisole structure has a unique packing arrangement.

The ab-initio single point calculations for the molecular structures of **1** in the dimorphs show that the stabilities of the different molecular conformations of **1** are in the order of **1opt** > **1a1** > **1a2** > **1b**. In other words, the stabilities of the molecules are in the order of, isolated molecule > molecule free of intermolecular hydrogen bonds > molecule connected with one intermolecular hydrogen bond > molecule connected with two intermolecular hydrogen bonds, which illustrate the effect of the packing patterns on the molecular structure. This relation is not applied for the conformations of **1** in the different inclusion structures, since in these structures there are additional host-guest interactions, which also have influence on the conformation of **1**.

Detailed calculations of the interaction energies between the different molecules in each structure have been done to understand the factors affecting the crystal packing forces. The following results have been found:

- In the structures without solvent (the dimorphs) the largest interaction in the crystal has been calculated to be between the pair of molecules that connected with intermolecular hydrogen bonds.
- For the cosolvate structures in group 2, there are a dimer (two neighbouring molecules that are connected with intermolecular hydrogen bonds) or a pair (two neighbouring molecules sitting in the analogue position as the dimer but not connected with intermolecular hydrogen bonds) character structure of the host molecules. The largest interaction has been calculated to be between the host molecules of different dimers or pairs, which are not connected with intermolecular hydrogen bonds. This is because the intermolecular hydrogen bonds within the dimer are of week type, their lengths (NH—O) range between 3.20 Å and 3.43 Å. On the other hand, strong dispersion interactions in addition to considerable electrostatic interactions, have been calculated between the molecules of the different dimers or pairs, which can be attributed to the many close contacts between the methyl···methyl, nitro···methyl and nitro···nitro groups of these molecules. The nitro group free of intramolecular hydrogen bond and the methyl groups of the neighbouring isopropylamino groups are generally the groups that responsible for this interaction.
- The twist or the twisted boat six-membered ring conformations of the host **1**, which are the forms adopted by **1** in the most cosolvates structures, are very suitable for the generation of many van der Waals interactions between the different layers within the packing patterns of our cosolvate structures.

Zusammenfassung

Für die systematische Untersuchung der Kristallpackung in einem molekularen Festkörper ist es vorteilhaft, nicht die molekulare Konstitution zu ändern, sondern die Polymorphe oder Cosolvate (Einschlusskristalle) einer Verbindung zu analysieren. Cosolvate machen es überflüssig, mit metastabilen Polymorphen zu arbeiten, deren verfügbare Zahl in den meisten Fällen begrenzt ist. Unter der Voraussetzung von labilen Konformationen des zu untersuchenden Moleküls kann man die Packungen und ihren Einfluss auf die molekulare Struktur gleichzeitig untersuchen. Zusätzlich kann man den energetischen und strukturellen Einfluss der intermolekularen Wechselwirkungen auf die Geometrie des betreffenden Moleküls studieren. Wir schlagen hier 2,4,6–Ttris(isopropylamino)–1,3,5–trinitrobenzol (**1)** als einen geeigneten Kandidaten für das systematische Studium von Kristallpackungseffekten vor. Deshalb haben wir versucht eine große Menge von Cosolvaten herzustellen und (sowohl experimentell als auch theoretisch) eine systematische Studie der Konformationseffekte, hervorgerufen durch die Kristallpackung, durchzuführen. Hier beschreiben wir ihre Untersuchung durch Röntgenstrukturanalyse, Thermoanalyse und theoretische Berechnungen (Kraftfeld und abinitio).

Die Kristall- und Molekularstrukturen wurden mit Hilfe von Röntgenbeugungsuntersuchungen ermittelt.

Für thermoanalytische Untersuchungen wurde eine Kombination von Differential scanning calorimentry (DSC) und Thermogravimetry (TG) durchgeführt, um ein besseres Profil und eine genaue Analyse der Veränderungen, die stattgefunden haben, zu erhalten.

In der vorliegenden Arbeit haben wir das elektrostatische Potential (ESP) und die molekularen Energien der experimentell ermittelten Strukturen nach Korrektur der Wasserstoffatompositionen berechnet. Dazu haben wir das Dichtefunkuntions-Programm DMOL3 mit dem DNP-Basissatz und den GGA-BLYP-Funktionen verwendet. Die Strukturen mit den berechneten Ladungen wurden verwendet, um die Kristall-, die Gitter- und die individuelle Wechselwirkungsenergie in jeder Struktur zu berechnen, unter Benutzung des Simulationsprogramms Discover mit dem COMPASS Kraftfeld.

Eine große Vielzahl kleiner Moleküle wurden in Einschlusskristallen von **1** eingebaut: Benzol **1-1**, Ethylbenzol **1-2**, Cumol **1-3**, Fluor- **1-4**, and Chlorbenzol **1-5**, *m*- **1-6**, *o*- **1-7** and *p*-Difluorbenzol **1-8**, 1,2,4-Trifluorbenzol **1-9**, Hexafluorbenzol **1-10**, zwei Phenol-Einschlusskristall-Strukturen **1-11, 1-12**, Anisol **1-13**, Benzonitril **1-14**,

Trifluortoluol **1-15**, DMF **1-16**, Hydrochinon **1-17**, *p*-Xylol **1-18** , *p*-Nitrophenol **1-19**, *p*- **1-20**, and *o*-Fluortoluol **1-21**, *p*-Chlor-fluorbenzol **1-22**, *m*- **1-23**, *o*- **1-24** and *p*-Fluornitrobenzol **1-25**, Nitroethan **1-26**, 1-Nitropropan **1-27**, Benzaldehyd **1-28**, Dioxan **1-29**, and zwei γ-Picolin-Einschlusskristall-Strukturen **1-30, 1-31**.

Die Kristall- und Molekular-Strukturen der ersten Dimorphs **1a** von **1** mit zwei unabhängigen Molekülen (**1a1**, **1a2**) in der asymmetrischen Einheit wurde bereits zuvor gefunden, ebenso wie Cokristalle mit Toluol **1-32**, Nitrobenzol **1-33**, *p*-Chlortoluol **1-34**, *p*-Xylol 2 **1-35**, Ameisensäure **1-36**, Essigsäure **1-37**, Nitromethan **1-38** and Acetonitril **1-39**. Das zweite Dimorph **1b** von **1** haben wir bei Untersuchungen des Einschlussverhaltens von **1** gefunden. Struktur **1b** hat nur ein Molekül (**1b**) in der asymmetrischen Einheit. Die Strukturergebnisse aller Cosolvate wurden in die Pakungsdiskussionen miteinbezogen, die thermischen Messungen und die Energieberechnungen wurden für alle Strukturen in dieser Arbeit durchgeführt.

Sechs verschiedene Packungen der Cosolvate von **1** wurden gefunden und in vier Gruppen eingeteilt. Diese unterschiedlichen Packungen zeigen den Anpassungscharakter des host-Systems. Nur ein Packungstyp (Gruppe 1) hat weder host-host noch host-guest intermolekulare Wasserstoffbrückenbindungen. 17 Strukturen der insgesamt 38 Strukturen nehmen diesen Packungstyp ein.

Für die Konformationen des Sechsrings von **1** in den unterschiedlichen Cosolvaten haben wir gefunden dass:

- drei unterschiedliche Konformationen des Wirtsmoleküls **1** eingenommen werden können: Bootsform mit zwei kurzen und vier langen C—C Bindungen im Benzolsechsring substituiert mit Elektronen-Donor- und Akzeptorgruppen (chinoider Charakter), Twistform mit zwei langen und vier kurzen C—C Bindungen (Cyanin-Charakter) und intermediäre Twist-Boot-Form.

- in den Strukturen, die intermolekulare Wasserstoffbrückenbindungen enthalten, **1** entweder eine Twist-Form oder eine Twist-Boot-Form annimmt, außer in Strukturen mit DMF (**1-16**) und *p*-Xylol 2 (**1-35**). In Abwesenheit von intermolekularen Wasserstoffbrückenbindungen (Strukturen der Gruppe 1) kann **1** leichter eine Twist-, Boot- oder Twist-Boot-Form annehmen jeweils in Abhängigkeit vom eingeschlossenen Molekül.

- in allen 14 Strukturen von Gruppe 2 der Sechsring von **1** eine Twist-Form einnimmt, außer Strukturen mit DMF (**1-16**) (die Wannen-Form annehmen), *p*-Nitrophenol (**1-19**) und Fluornitrobenzol (**1-23**) (die beide Twist-Boot–Form annehmen). Die Twist-Konformation ist gut geeignet für starke van der Waals-Kräfte zwischen unterschiedlichen Schichten.

- in allen Strukturen der Gruppe 3 der Sechsring von **1** eine Twist-Boot-Form annimmt, außer eines der beiden unabhängigen Moleküle in den Strukturen mit *p*-Xylol 2 (**1-35m1**), welches eine Boot-Form annimmt.
- je stärker die host-guest-Wechselwirkung ist, desto kleiner $(\text{C-C short})_{\text{ave}}$ and desto größer $(\text{C-C long})_{\text{ave}}$ im Ring von **1** ist.

Die Ergebnisse der DSC-Experimente und der theoretischen Berechnungen der Gitterenergie beweisen Folgendes:

1. Hohe Desolvatationsenergie (erhalten von DSC-Messung) und Gitterenergie pro Moleküle (ELM) (erhalten von Kraftfeldberechnungen) sind nötig für: die Solvate, die host-guest intermolekulare Wasserstoffbrückenbindungen haben (wie Einschlusskristalle mit Phenol, Hydrochinon, DMF, Benzaldhyd, Essigsäure, Ameisensäure), die Solvate, die Methyl-Gruppen in der *para*-Position besitzen (wie *p*-Xylol 2, *p*-Flurotoluol, *p*-Chlorotoluol und γ-Picolin) und für Strukturen mit Benzonitil und Nitroethan.

2. Form **1a** ist stabiler als **1b**.

3. Die Stabilitäten der Strukturen mit isomeren Einschlussmolekülen haben folgende Reihenfolge: Kosolvate mit *para-* > *ortho-* > *meta-* Substitutionsmuster. Die *para*-Struktur des Gast-Moleküls passt besser in die Hohlräume zwischen den Wirts-Molekülen und ergibt folglich eine stabilere Packung.

4. Die erste Struktur mit Phenol 1 (host:guest = 2:1) ist stabiler als die Struktur mit Phenol 2 (host:guest = 1:2), die Struktur mit γ-Picolin 2 (host: guest = 1:1,5) ist stabiler als die mit γ-Picolin 1 (host:guest = 1:1) und die Struktur mit *p*-Xylol 2 (host:guest = 2:½) ist stabiler als die mit *p*-Xylol 1 (host: guest = 2:1). Mit anderen Worten: die dichtere Packung ist immer die stabilere.

Für jede Struktur wurden Pulver-Diffraktions-Messungen bei Zimmertemperatur und einer Tempereatur, die höher ist als die Desolvatationstemperatur, durchgeführt. Alle Cosolvat-Strukturen verwandeln sich zur Modifikation **1a** nach der Verdunstung des Lösungsmittels, außer die von Anisol, welche sich zu Struktur **1b** umwandelt. Die Anisol-Struktur hat eine einzigartige Packung.

Die ab-initio-Berechnungen der Molekülstruktur von **1** bei den Dimorphen zeigt, dass die Stabilitäten der verschiedenen molekularen Konformationen von **1** die Reihenfolge **1opt** > **1a1** > **1a2** > **1b** besitzen. Mit anderen Worten: Die Stabilitäten der Moleküle besitzen die Reihenfolge isoliertes Molekül > Molekül ohne intermolekularer Wasserstoffbrückenbindung > Molekül mit einer intermolekularen Wasserstoffbrückenbindung > Molekül mit zwei intermolekularen Wasserstoffbrückenbindungen. Dies zeigt den Effekt der Packung auf die molekulare Struktur. Diese Beziehung gilt nicht für die Konformationen von **1** in den unterschiedlichen Einschlussstrukturen. Die Ursache ist, dass in diesen Strukturen zusätzliche host-guest-Wechelwirkungen existieren, die auch Einfluss auf die Konformationen von **1** haben.

Detaillierte Berechnungen der Wechselwirkungsenergien zwischen den unterschiedlichen Molekülen in jeder Struktur wurden durchgeführt, um die Faktoren, die die Kristallpackungskräfte beeinflussen, zu verstehen. Die folgenden Ergebnisse wurden gefunden:

- In den Strukturen ohne Lösungsmittel (den Dimorphen) wurde die größte Wechselwirkung in den Kristallen zwischen den zwei Molekülen, welches mit den intermolekularen Wasserstoffbrückenbindungen verbunden sind, berechnet.

- In den Cosolvatstrukturen (Gruppe 2) können Dimere von **1** vorliegen, die mit Wasserstoffbrückenbindungen verknüpft sind oder Paare von **1** vorliegen, die nicht mit Wasserstoffbrückenbindungen verknüpft sind. Die stärksten Wechselwirkungen werden jedoch für Kontakte zwischen den Dimeren oder Paaren berechnet. Diese sind keine Wasserstoffbrückenbindungen. Das kommt daher, dass die intermolekularen Wasserstoffbrückenbindungen innerhalb der Dimere bzw. Paare vom schwachen Typ sind. Ihre Längen (NH-O) liegen zwischen 3,20 Å und 3,43 Å. Andereseits wurden starke Dispersions-Wechselwirkung zusätzlich zu (erheblichen) elektrostatischen Wechselwirkungen zwischen den Molekülen der verschiedenen Dimere oder Paare berechnet, die den vielen engen Kontakten zwischen den Methyl$\cdots$ Methyl- und Nitro$\cdots$ Methyl- und Nitro$\cdots$Nitro-Gruppen dieser Moleküle zugeschrieben werden können. Nitro-Gruppen, ohne intramolekulare Wasserstoffbrückenbindungen und Methyl-Gruppen der benachbarten Isopropylamino-Gruppen sind im allgemeinen die Gruppen, die für diese Wechselwirkungen veranwortlich sind.

- Die Twist- oder die Twist-Boot-Form der Sechsringe, die von **1** am häufigsten in den Cosolvatstrukturen vorkommen, eignen sich besonders gut zur Erzeugung von Schichtstrukturen, die durch van der Waals Wechselwirkungen zusammengehalten werden.

Introduction

Investigation of crystal structures formed by molecular solids by diffraction methods yield an unparalleled wealth of information about molecular parameters. In most cases, only one crystal out of several possibly existing polymorphs is examined by X-ray diffraction. There are tendencies then to regard one structure of a molecule thus obtained as the single possible structure, i.e., the molecule is considered to behave as an unperturbed, isolated species. Molecular parameters in disagreement with this assumption are believed to originate from "crystal packing forces". Only in rare cases can these forces be quantified; strategies for evaluation of crystal fields include: (i) comparison with gas-phase data, (ii) comparison of crystallographic independent molecules within the same crystal, (iii) comparison of different polymorphic crystals, and (iv) computational procedures (empirical, semi-empirical and ab-initio calculations). However, most molecules are either not volatile enough or too complex to obtain information from spectroscopy in the gas phase; many are available only in one crystal form with crystallographically identical molecules. Comparing chemically closely related molecules, a method so successful in classical correlation analysis methods of physical organic chemistry, fails to yield useful information for molecular crystals. Rather minor changes on the molecular level can lead to pronounced alterations at the supramolecular level, the crystal structure. Quantification of "crystal packing forces" is highly desirable, and closely related to a central problem in the solid-state chemistry of molecular crystals as well as being of practical importance in designing new molecular materials with desirable physical properties[1].

The crystal packing adopted by organic molecules reflects the intermolecular forces, which act between the molecules and it also determines many physical properties of the solid, ranging from solubility to non-linear optical activity. For a systematic study of crystal packing in a molecular solid, it is advantageous not to change the molecular constitution, but to analyse polymorphs or cosolvates of one compound. Cosolvates eliminate the need to work with metastable polymorphs whose available numbers will be quite limited in most cases.

In the last years many efforts have been done which aimed at explaining and predicting the existence of polymorphic structures[2,3,4], and improvements in computational techniques have led to the developments of programs which intend to predict the crystal structures, and thus possible polymorphism, of organic compounds[5,6,7]. Despite some success, the field is still in its infancy and more experimental data and theoretical studies are required.

A time opportunity to discuss the state of the art in the field of crystal engineering has been provided by the first CrystEngComm discussion meeting[8]. The broad rang of topics discussed at the meeting reflected the strong interdisciplinary character of this field.

In 1998, C. B. Aakeröy et. al.[9] have investigated, theoretically, the lattice energies of three polymorphs of 2-Amino-5-nitropyrimidine, while Lian Yu et. al.[10] in 2000 have used calorimetric data of melting to examine the thermodynamic stability relationships between six polymorphs of 5-Methyl-2- [(2-nitrophenyl)amino]-3-thiophenecarbonitrile. In 2000, Luigi R. Nassimbeni et. al.[11] have used lattice energy calculations in addition to thermal analysis measurements to examine the relative stability of the inclusion structures of Aminobenzonitrile isomers by a diol host compound.

Provided a conformationally quite labile molecule is used, packing patterns and their influence on molecular parameters may be studied simultaneously, and also the energetic and structural influence of intermolecular interactions upon the structure can be examined. We assumed 2,4,6-tris(isopropylamino)-1,3,5-trinitrobezene **1** to be a suitable candidate. We thus attempted to obtain a large amount of solvates, using different kinds of solvents: aromatic, aliphatic, alcohol, acids or esters, and tried to embark on a systematic study (both experimentally and theoretically) of conformational effects of crystal packing. Here we describe their investigation by X-ray diffraction, thermal analysis (differential scanning calorimetry (DSC) and thermalgravimetry (TG)), high temperature powder diffraction, and computational methods (force field and ab-initio).

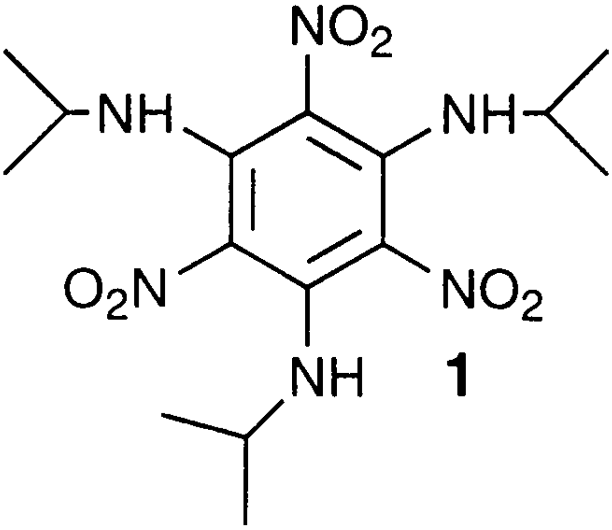

1

Scheme 1. 2,4,6-tris(isopropylamino)-1,3,5-trinitrobezene

Although most benzene derivatives show a strong tenacity to retain a planar ring, hexa-substituted benzene derivative with donor and acceptor groups in alternating positions show ring geometries widely distorted from planarity. In 1989 Siegel et al.[12] provided the first example of strong distortions of a neutral benzene derivative of this type. In 1991, J. J. Wolff et. al.[13] have examined the distortion in the benzene rings of three 1,3,5-tris(alkylamino)-2,4,6-trinitrobenzene.

The reason why the ring, in hexa-substituted benzene derivative with donor and acceptor groups in alternating positions, may retain conjugation at the expense of ring planarity may be explained as follows: the push-pull between donor and acceptor groups shifts π electron density to the substituents, and therefore depletes π electron density from the ring. A radialene resonance form gains and this facilitates bending of the ring. However, the non-dipolar radialene form is not the only alternative to the benzenoid resonance form. Two dipolar forms may be envisioned where electron density is shifted to the substituents, namely a cross-conjugated quinonoid form and a form similar to a coupled bis-trimethinecyanine as shown in Scheme 2.

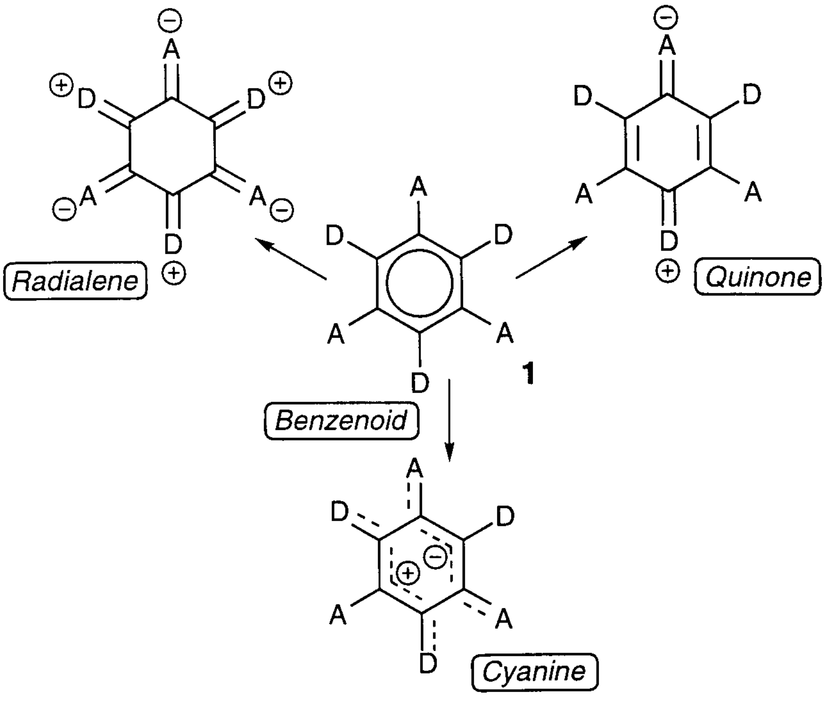

Scheme 2. Limiting resonance forms for the π system.

Thermal analysis techniques are useful in measuring compound stability. TG and DSC are convenient methods for monitoring the dissolution reaction of an inclusion compound and the identification of intermediate phases[14].

Dealing with molecule **1** on the computational level is very attractive because: (i) although being a benzene derivative it is not planar, (ii) it contains several potential donor and acceptor groups for both weak C-H…X, and strong N-H…X, (X=O or N) hydrogen-bond interactions, (iii) in the crystal structure, both inter- and intramolecular hydrogen bonds can be found, (iv) it has the ability to form inclusion compounds, and (v) it is small enough to make it accessible to ab-initio calculations.

Intermolecular interactions play a crucial role in determining the three-dimensional structures of large molecules[15,16] including proteins[17] and polymers[18]. The calculations of the intermolecular interactions rely on the atomic charges, but there is considerable debate about which is the best way to determine atomic charges to simulate condensed-phase properties. A number of approaches have been used. One of the most common approaches is to determine the atomic charges by fitting them to reproduce the molecular electrostatic potential (ESP)[19]. Numerous applications of ESP-fitted charges in simulations of biochemical systems prove the usefulness of this technique[20,21]. The ESP-derived charges can reproduce the intermolecular interaction properties of molecules well with a simple two-body additive potential. On the other hand, the use of the Density Functional Theory (DFT) approach with the numerical DNP (Double Numerical plus Polarization) basis sets to calculate ESP charges of DNA bases has been prove to be better than the ab-initio Hartree-Fock (HF) method and similar to the MP2 method[20]. Since the DFT approaches require less computational time than the calculation at the MP2 level, the DFT method is recommended for these calculations.

In our work we have calculated the ESP charges and the molecular energies of the experimental structures after the correction of the hydrogen atomic positions, using the DFT electronic structure program DMOL3 (2.2)[22,23] . DMOL3 uses numerical orbitals for the basis function; each function corresponds to an atomic orbital. We have performed these calculations using the DNP basis set, which includes a polarization p-function on all hydrogen atoms, and the GGA-BLYP[24,25] functional. These structures have been then used to calculate: the crystal, the lattice and individual interaction energies in each structure, within the molecular simulation program Discover[26], using the COMPASS (condensed-phase optimised molecular potentials for atomistic simulation studies)[27,28] force field. COMPASS is the first ab-initio force field that has been parameterized and validated using condensed-phase properties, in addition to various ab-initio and empirical data for isolated molecules, and it also has been expanded to include high energy nitro functional, which is very important for our molecule. The parameters were derived with an emphasis on the non-bonded parameters, which include a Lennard-Jones 9-6 function for the van der Waals term and columbic term for the electrostatic interactions. The graphical displays generated with the Materials Visualizer[26].

1 Theoretical background

1-1Thermal analysis

Thermal analysis (TA) is defined as: A group of techniques in which a property of the sample is monitored against time or temperature while the temperature of the sample, in a specified atmosphere, is programmed. The programme may involve heating or cooling at a fixed rate of temperature change, or holding the temperature constant, or any sequence of these[29]. In many thermal methods the results obtained may depend upon the conditions used during the experiment, the reason for this is the dynamic nature of the processes involved. The signal generated by the sensors will depend on the extent and the rate of reaction, or the extent and rate of the property measured. The transfer of heat by conduction, convection and by radiation around the sample all affects these changes. It is therefore essential, whenever a thermal analysis experiment is reported, that the precise conditions used are included in the report. Similarly, comparison of samples should only be made when their curves are run under the same conditions, or when differences in conditions are clearly stated.

1-1-1 Differential scanning calorimetry (DSC)

According to the International Confederation for Thermal Analysis and Calorimetry (ICTAC) the definition of Differential Scanning Calorimetry (DSC) is: A technique in which the heat flow rate (power) to the sample is monitored against time or temperature while the temperature of the sample, in a specified atmosphere, is programmed[30]. Differential techniques involve the measurement of a difference in the property between the sample and a reference.

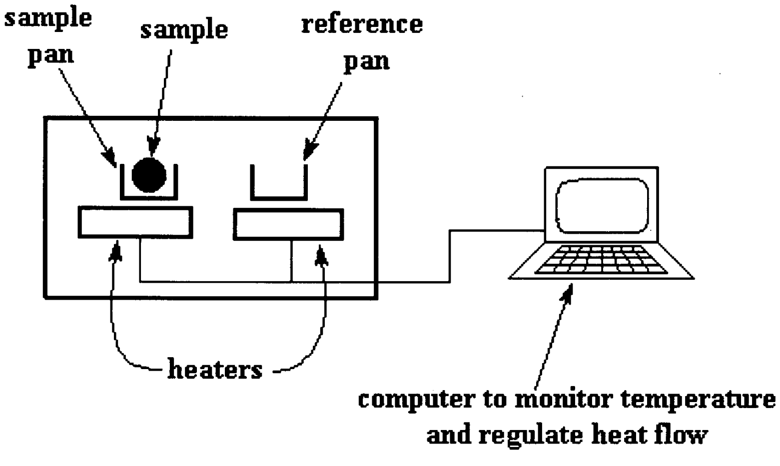

Figure 1-1. Schematic diagram of DSC apparatus

There are large number and variety of application of DSC. The applications may be divided roughly into two categories:

- Physical changes and measurements, such as melting, crystalline phase changes, phase diagrams, heat capacity and glass transitions.
- Chemical reactions, such as dehydrations, decompositions, polymer curing, glass formation and oxidative attack.

1-1-2 Thermogravimetry (TG)

Thermogravimetry (TG)[31] is a technique in which the mass of the sample is monitored against time or temperature while the temperature of the sample, in a specified atmosphere, is programmed. The origins of thermogravimetry have been fully documented by Duval[32], Keattch and Dollimore[33], and Wendlandt[34]. The most significant contribution was made by Honda[35] in 1915 who used a lever-arm balance fitted with an electrical furnace to investigate manganese oxide. Simple experimental apparatus has been described which uses modified manual analytical balances and controlled electric furnaces[36].

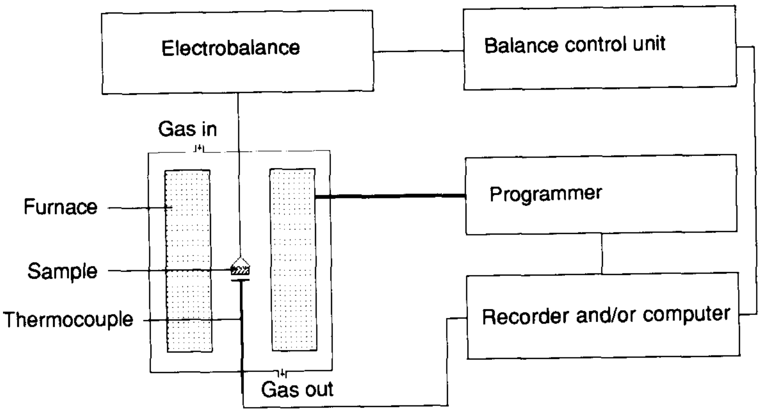

Figure 1-2. Schematic diagram of TG apparatus.

The range of applications of thermogravimetry is very large, a selection of some of these applications are; analysis of mixtures, oxidation studies, and reduction studies.

1-1-3 Simultaneous and complementary techniques

A single thermal method dose not always gives sufficient information to allow the analyst to be sure what is occurring. For example, a ‘downward’ peak produced by a Differential Thermal Analysis (DTA) experiment means that an endothermic event occurs over this temperature range. It dose not tell whether this is a chemical reaction or a physical change such as melting, or whether any gases are evolved. A (TG) experiment on the same sample may show a mass loss over this temperature range, thereby ruling out melting. Conversely, if the TG curve showed no mass loss, the process of melting could be confirmed by direct observation of the sample. It is clear that combining several analytical methods gives a better profile of the changes taking place. If the two techniques are performed on different samples, or at very different times, then the method are referred as complementary. If the techniques are performed on a single sample at the same time, then they are simultaneous techniques.

1-2 Computational methods

1-2-1 Force field method

Quantum mechanical methods deal with the electrons in a system, so that even if some of the electrons are ignored, a large number of particles must still be considered, and the calculation is time-consuming. Force field methods ignore the electronic motions and calculate the energy of a system as a function of the nuclear positions only. In some cases force fields can provide answers that are as accurate as even the highest-level quantum mechanical calculations, in a fraction of the computer time. However, force field calculations cannot of course provide properties that depend upon the electronic distribution in a molecule[37].

Many of the molecular modelling force fields can be interpreted in terms of a relatively simple four-component picture or intra- and inter-molecular forces within the system. Energetic penalties are associated with the deviation of bond lengths and bond angles away from their reference or equilibrium values, there is a function that describes how the energy changes with torsion parameters, and finally the terms that describe the interaction between non-bonded parts of the system.

The Non-bonded interactions

Independent molecules and atoms interact through non-bonded forces, which also play an important role in determining the structure of individual molecular species. The non-bonded terms in a force field are usually considered in two groups, one comprising electrostatic interactions and the other van der Waals interactions.

(I) Van der Waals interactions

The interactions between uncharged atoms and molecules, in the absence of an appreciable exchange of electrons, consist of weak forces, which are generally known as van der Waals forces[38]. At large interatomic distances this energy is zero, and for small distances it be-comes very repulsive. The repulsive part of van der Waals interaction is proportional to $1/r^{12}$. At intermediate distance there is a slight attraction. The physical meaning of this attraction is that, even in such atoms or molecules, whose electrical multipole moments are on the average equal to zero, there exist certain fluctuating multipole moments which depend on the instantaneous electric field associated with these moments leads to the appearance of induced multipole moments in neighbouring atoms. The averaged interaction between the electrical moments of the initial atom or molecule and the induced moment of neighbouring atoms or molecules gives rise to attractive forces between the particles. London has shown that the dominating part of this effect is due to the outer, most loosely bound electrons, the same electrons that are responsible for optical dispersion. This explains why this effect called dispersion effect[35].

(II) Electrostatic interactions

This is due to internal distribution of the electrons, creating positive and negative parts of the molecule.

The electrostatic interaction between two molecules (or between different parts of the same molecule) is then calculated as a sum of interactions between pairs of point charges, using Coulomb's law:

$$E_{el} = q_i\, q_j / \varepsilon\, r_{ij}$$

Where ε is a dielectric constant.

1-2-2 Calculating atomic charges: charges derived from the molecular electrostatic potential.

The electrostatic potential at a point is the force acting on a unit positive charge placed at that point. The electrostatic potential is an observable quantity that can be determined from a wave function using the equation:

$$\phi(\vec{r}) = \phi_{nucl}(\vec{r}) + \phi_{1ec}(\vec{r}) = \sum_{A=1}^{M} \frac{Z_A}{\left|\vec{r} - \vec{R}_A\right|} - \int \frac{d\vec{r}\,'\,\rho(\vec{r})}{\left|\vec{r}\,' - \vec{r}\right|}$$

The electrostatic potential is a continuous property and is not easily represented by an analytical function. Consequently, it is necessary to derive a discrete representation for use in numerical analysis. The objective is to drive the set of partial charges, that best reproduce the quantum mechanical electrostatic potential at a series of points surrounding the molecule. A solution of this problem was suggested by Cox and Williams in 1981. The electrostatic potential at each of the chosen points is calculated from the wavefunction. A least-squares fitting procedure is then employed to determine the set of partial atomic charges that best reproduce the electrostatic potential at the points. The fitting procedure minimises the sum of squares of the difference in the electrostatic potential. Thus if the electrostatic potential at a point is φ_i^0 and if the value from the charge model is φ_i^{calc}, then the objective is to minimise the following function:

$$R = \sum_{i=1}^{N_{points}} w_i \left(\varphi_i^0 - \varphi_i^{calc}\right)^2$$

N_{points} is the number of points and w_i is a weighting factor that enables different points to be given different degrees of importance in the fitting process. One of the charges is dependent on the value of the others (because the sum must equal Z, the molecular charge). This *N*th charge has a value given by:

$$q_N = Z - \sum_{j=1}^{N-1} q_j$$

The electrostatic potential due to the charges q_j at the point *i* is given by Coulomb's law:

$$\varphi_i^{calc} = \sum_{j=1}^{N-1} \frac{q_j}{4\pi\varepsilon_0 r_{ij}} + \frac{Z - \sum_{j=1}^{N-1} q_j}{4\pi\varepsilon_0 r_{iN}}$$

r_{ij} is the distance from the charge *j* to the point *i*. At a minimum value of the error function, *R*, the first derivative is equal to zero with respect to all charges q_k :

$$\frac{\partial R}{\partial q_k} = -2 \sum_{i=1}^{N_{points}} w_i \left(\varphi_i^0 - \varphi_i^{calc}\right)\left(\frac{\partial \varphi_i^{calc}}{\partial q_k}\right) = 0$$

This equation can be written in the following form:

$$\sum_{i=1}^{N_{points}} w_i \left(\varphi_i^0 - \frac{Z}{r_{iN}}\right)\left(\frac{1}{r_{iK}} - \frac{1}{r_{iN}}\right) = \sum_{j=1}^{N-1}\left[\sum_{i=1}^{N_{points}} w_i \left(\frac{1}{r_{iK}} - \frac{1}{r_{iN}}\right)\left(\frac{1}{r_{ij}} - \frac{1}{r_{iN}}\right)\right]\frac{q_j}{4\pi\varepsilon_0}$$

when expressed in this way, then the set of equations can be recast as a matrix equation of the form **Aq** = **a**. The charges q are then determined using standard matrix method via $\mathbf{q} = \mathbf{A}^{-1}\mathbf{a}$

1-2-3 Density functional theory

A rule which assigns a number to a function is called a *functional.* Phrased differently, we can say that a functional is a function whose argument is itself a function.

The probability $\rho(\vec{r}_1)$ of finding any of the N electrons within the volume element dr_1 but with arbitrary spin while the other N-1 electrons have arbitrary positions and spin in the state represented by Ψ, is defined as following[39]:

$$\rho(\vec{r}_1) = N\int \ldots \int \left|\Psi(\vec{x}_1, \vec{x}_2, \ldots, \vec{x}_N)\right|^2 ds_1 d\vec{x}_1 d\vec{x}_2 \ldots d\vec{x}_N .$$

Strictly speaking $\rho(\vec{r}_1)$ is a probability density, but calling it the electron density is common practice. This represent the probability for one particular electron is within the volume element $d\vec{r}_1$. However, since electrons are indistinguishable the probability of finding any electron at this position is just N times the probability for one particular electron.

$$\rho(\vec{r} \to \infty) = 0,$$
$$\int \rho(\vec{r}_1) d\vec{r}_1 = N$$

Unlike the wave function, the electron density is an observable and can be measured experimentally, e.g. by X-ray diffraction. One of its important features is that at any position of an atom, $\rho(\vec{r}_1)$ exhibits a maximum with a finite value, due to the attractive force exerted by the positive charge of the nuclei. However, at these positions the gradient of the density has a discontinuity and a cusp results. This cusp is a consequence of the singularity in the $-\frac{Z}{r_{iA}}$ part in the Hamiltonian as $r_{iA} \to 0$. Actually, it has long been recognized that the properties of the cusp are intimately related to the nuclear charge Z of the nucleus according to:

$$\lim_{r_{iA}\to 0}\left[\frac{\partial}{\partial r} + 2Z_A\right]\overline{\rho}(\vec{r}) = 0$$

where $\overline{\rho}(\vec{r})$ is the spherical average of $\rho(\vec{r})$.

Thus, the electron density already provides all the ingredients that we identified as being necessary for setting up the system specific Hamiltonian and it seems at least very plausible that in fact $\rho(\vec{r})$ suffices for a complete determination of all molecular properties.

2 Results and discussions of the experimental part

2-1 Dimorphs and cosolvates of 1

The crystal and molecular structures of the first form **1a**[40] of **1** with two independent molecules (**1a1**, **1a2**) (Figure 2-1) in the asymmetric unit has been found previously, as well as cocrystals with toluene **1-32**, nitrobenzene **1-33**, *p*-chlorotoluene **1-34**, *p*-xylene 2 **1-35**, formic acid **1-36**, acetic acid **1-37**, nitromethane **1-38** and acetonitrile **1-39**[41]. In the first published structure of **1a**, which has been measured at room temperature, disorder effects appeared at the isopropyl groups. The dimorphic form **1b** of **1** has been discovered in investigations concerning the inclusion behaviour of **1**. Structure **1b** has only one molecule (**1b**) (Figure 2-2) in the asymmetric unit.

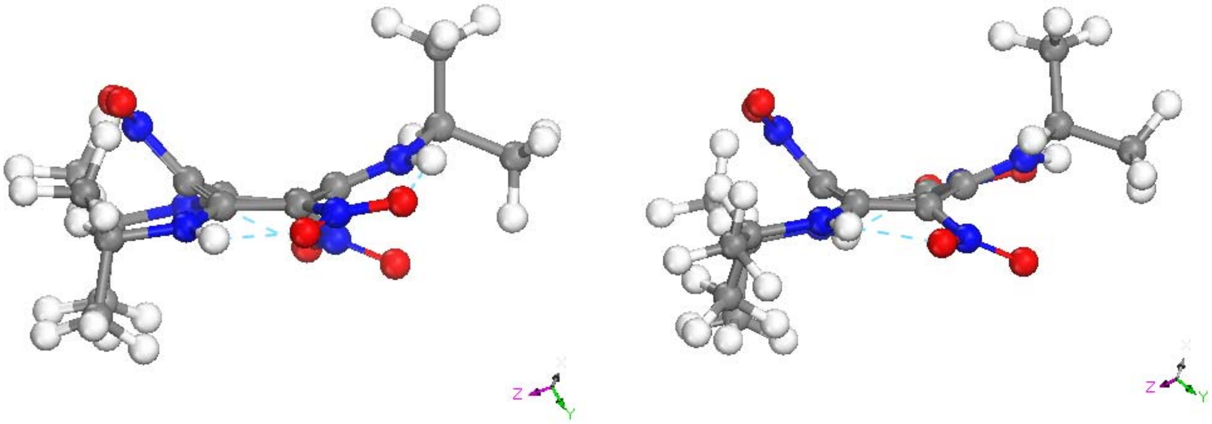

1a1 **1a2**

Figure 2-1. Molecular structure of 1a1 and 1a2

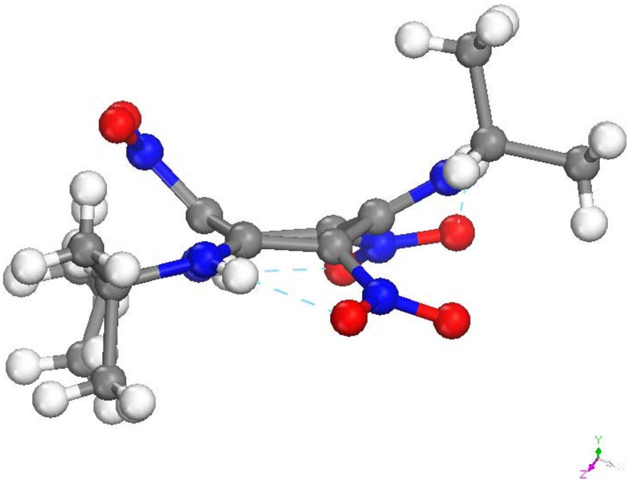

Figure 2-2. Molecular structure of 1b

Since disorder effects in the room temperature structure of **1a**[40] complicate the theoretical calculations, we have recrystallized compound **1** from ethanol and performed the X-ray diffraction measurement at low temperature (100 K). This low temperature structure is free from disorder, the thermal parameters are reduced, the agreement factor (R-factor) is improved, and the positions of the hydrogen atoms could be determined unequivocally by experimental difference density analysis. Additionally, new refinements, using the modern programs which are now available, have been performed for the previously determined structures (**1-32** to **1-39**) resulting in the improvements of the agreement factor (R-factor) and even the correction of the space group in the structure with *p*-chlorotoluene **1-34** from P1 to Cc.

We thus attempted to obtain a large amount of solvates, using different kinds of solvents; aromatic, aliphatic, alcohol, acid or ester, and tried to embark on a systematic study of conformational effects of crystal packing. A wide range of small molecules were found to be incorporated into crystals of **1**: benzene **1-1**, ethylbenzene **1-2**, cumene **1-3**, fluoro- **1-4**, and chlorobenzene **1-5**, *m*- **1-6**, *o*- **1-7** and *p*-difluorobenzene **1-8**, 1,2,4-triflourobenzene **1-9**, hexafluorobenzene **1-10**, two phenol structures **1-11, 1-12**, anisole **1-13**, benzonitrile **1-14**, trifluorotoluene **1-15**, DMF **1-16**, hydroquinone **1-17**, *p*-xylene 1 **1-18** , *p*-nitrophenol **1-19**, *p*- **1-20**, and *o*-fluorotoluene **1-21**, *p*-chloro-fluorobenzene **1-22**, *m*- **1-23**, *o*- **1-24** and *p*-fluoronitrobenzene **1-25**, nitroethane **1-26**, 1-nitropropane **1-27**, benzaldehyde **1-28**, dioxane **1-29**, and two γ-picoline structures **1-30, 1-31**.

Crystallization was done by slow evaporation of solution in the cocrystallizing liquid or as solutions in 1,3,5-trimethylbenzene (mesitylene) for solids except crystallization form dioxane. In this crystallization process crystals have been grown at 80°C over two days, the solution with the formed crystals has then to cool down very slowly to room temperature.

No incorporation could be found of aliphatic alcohols and of esters for example isopropanol, cyclohexanol, ethanol, benzylalcohol ethylacetat, formic acid methylester, *o*-formic acid tri-methyleester. Furthermore no inclusion crystals could be found of pentane, heptane, THF, 2-nitropropane, *o*-, *m*-, *p*-dichlorobenzene, chloroform, DMSO, mesitylene, 1,3,5-trifluorobenzene, 1,2,3-trimethylamine, dimethylamine diethylamine, diispropylamine, benzonic acid, benzoylacetone, *p*-benzochinon, resorcinol, phloroglucin, and water. From most not cocrystallizing solvent, form **1a** was formed.

2-2 Ring and molecular conformation

Substantially different conformations for the six-membered ring of **1** have been found which cover the gamut of boat and twist forms. Deviations from planarity are most easily quantified by the summation of absolute torsional angles within the ring $\sum |\text{Tors.}|$, while the geometries of six-membered rings may be described in terms of a linear combination of three basic forms, chair, boat and twist. In this work the ring conformations were calculated using the Zefirov, Palyulin, and Dashevskaya (ZPD) method[42], in which the puckering parameters dependent on endocyclic torsional angles ϕ_j, where for six-membered ring this is given by:

$$\Phi_j = \Phi_0 + \Phi_1\cos(P_1 + 2\pi j/6) + \Phi_2\cos(P_2 + 4\pi j/6) + \Phi_3\cos(\pi j); \qquad j=0,1,\ldots,5$$

Where:

$$\Phi_0 = \frac{1}{6}\sum_{j=0}^{5}\Phi_j \cos(\pi j/3)$$

$$\Phi_1 \sin P_1 = -\frac{1}{3}\sum_{j=0}^{5}\Phi_j \sin(\pi j/3) \qquad and \qquad \Phi_1 \cos P_1 = \frac{1}{3}\sum_{j=0}^{5}\Phi_j \cos(\pi j/3)$$

$$\Phi_2 \sin P_2 = -\frac{1}{3}\sum_{j=0}^{5}\Phi_j \sin(\pi j/3) \qquad and \qquad \Phi_2 \cos P_2 = \frac{1}{3}\sum_{j=0}^{5}\Phi_j \cos(\pi j/3)$$

$$\Phi_3 = \frac{1}{6}\sum_{j=0}^{5}\Phi_j \cos(\pi j)$$

Φ_0, Φ_1 and P_1 can be neglected because they are very small, while Φ_2 and Φ_3 will be used to define another two parameters Q and θ, where;

$$Q = \sqrt{\Phi_2^2 + \Phi_3^2} \qquad and \qquad \theta = \arctan\frac{\Phi_2}{\Phi_3} \qquad 0 \le \theta \le \pi$$

Consequently, the conformation of the six-membered ring can be completely described in terms of the three parameters Q ,θ and P_2 .

- Q; is the puckering amplitude which measure the deviation of the ring from planarity

- θ; differentiates between the chair (θ= 0°, 180°) and the twist/boat families (θ = 90°).
- P_2; differentiates between boat and twist forms; ideal boat conformations occur for P_2 =(30+n*60)° and twist conformations for P_2 =(0+n*60)°.

The calculated ring conformations of **1** in the different inclusion structures are summarized in Table 1.

29 molecular structures of **1** out of the 46 different once have been found to adopt twist form, while the rest adopt highly distorted boat form with relatively high deviation from the ideal form.

The ring conformations of **1** were found to adopt;

- *nearly ideal twist form* in the inclusion structures with phenol 1 (**1-11m1**) (**1-11m2**), anisole (**1-13m1**), hydroquinone (**1-17**), and dioxane (**1-29**) with $\Delta(P_2)$= 1.5, 0.2, 1.5, 3.5, and 1.2 respectively. In these structures the host:guest ratio has found to be 2:1 (for phenol & anisole 2:1, and for hydroquinone & dioxane 1:1/2), which illustrate the effect of the structure density on the resulting molecular structure.
- *twist form* in the inclusion structures with *p*-subsituted benzene derivatives [*p*-difluorobenzene (**1-8**), *p*-nitrophenol (**1-19**), *p*-fluorotoluene (**1-20**), *p*-chlorofluorobenzene (**1-22**), *p*-fluorornitrobenzene (**1-25**), *p*-chlorotoluene (**1-34**)] except with p-xylene 1 and 2 (**1-18)** (**1-35m1**), and mono- substituted benzene derivatives [ethylbenzene (**1-2**), cumene (**1-3**), chlorobenzene (**1-5**), benzonitrile (**1-14**), benzaldhyde (**1-28**), toluene (**1-32**), and nitrobenzene (**1-33**)].
- *boat form* with high deviation from the ideal form in the inclusion structures with *m*- and *o*-fluorobenzene derivatives (structures with *m*- and *o*-difluorobenzene (**1-6**) and (**1-7**), *m*- and *o*-fluoronitrobenzene (**1-23**) and (**1-24**), and *o*-fluorotoluene (**1-21**), especially for the *meta* derivatives ($\Delta(P_2)$= 13.8 for *m*-difluorobenzene and 14.9 for *m*-fluoronitrobenzene) (see Table 1).
- *nearly ideal boat form* in the inclusion structures with *p*-xylene (*p*-xylene 1 (**1-18)** with $\Delta(P_2)$ = 3.3 and *p*-xylene 2 (**1-35m1)** with $\Delta(P_2)$ = 4.2), which should to be an effect of the host/guest intermolecular interaction.

It is convenient to introduce a third ring conformation form to our classification of the different ring forms of **1**. This is the twisted-boat form with ($\Delta(P_2)$>10).

Table 1 . Six membered ring conformation of 1 (m1 and m2 for two independent molecules in the asymmetric unit).

Inclusion Compound	**Twist form**	**Boat form**	$\sum\lvert_{\mathrm{Tors}}\rvert$ [°]	**Q / θ [°] / P_2 [°]**	**$\Delta(P_2)$ from ideal form**
1a1		☒	137.4	0.54 / -78.8 / 101.4	11.4
1a2	☒		144.4	0.57 / 86.8 / 106.5	13.5
1b		☒	152.2	0.45 / -86.6 / 101.5	11.5
1-1 benzene		☒	129.6	0.52 / -82.8 / 101.1	11.1
1-2 ethylbenzene	☒		138.0	0.53 / 78.5 / 111.8	8.2
1-3 cumene	☒		136.5	0.53 / -75.8 / 111.0	9.0
1-4 fluorobenzene		☒	129.8	0.52 / -77.0 / 102.3	12.3
1-5 chlorobenzene	☒		143.0	0.54 / -86.8 / 111.3	8.7
1-6 *m*-difluorobenzene		☒	128.8	0.52 / 76.2 / 103.8	13.8
1-7 *o*-difluorobenzen		☒	129.5	0.53 / -72.8 / 81.2	8.8
1-8 *p*-difluorobenzene	☒		145.5	0.56 / 79.6 / 112.0	8.0
1-9 1,2,4-trifluorobenzene	☒		137.6	0.54 / -82.0 / 107.8	12.2
1-10m1 hexafluorobenzene	☒		145.5	0.56 / -85.2 / 108.7	11.3
1-10m2 hexafluorobenzene	☒		127.4	0.49 / 83.3 / 108.7	11.3
1-11m1 phenol 1	☒		154.8	0.43 / -86.8 / 58.5	1.5
1-11m2 phenol 1	☒		153.5	0.58 / 83.6 / 119.8	0.2
1-12 phenol 2	☒		155.3	0.59 / -83.9 / 109.4	10.6
1-13m1 anisole	☒		144.4	0.58 / -85.1 / 118.5	1.5
1-13m2 anisole		☒	144.6	0.58 / -82.5 / 99.3	9.3
1-14 benzonitrile	☒		152.2	0.57 / -87.5 / 114.4	5.6
1-15 trifluorotoluene	☒		136.7	0.53 / -80.4 / 109.3	10.7
1-16 DMF		☒	154.1	0.62 / 88.9 / 98.3	8.3
1-17 hydroquinone	☒		158.3	0.60 / -83.4 / 116.5	3.5
1-18 *p*-xylene 1		☒	135.7	0.42 / 86.7 / 145.7	3.3
1-19 *p*-nitrophenol	☒		131.9	0.51 / 86.5 / 106.4	13.6
1-20 *p*-fluorotoluene	☒		143.5	0.56 / -78.9 / 110.1	9.9
1-21 *o*-fluorotoluene		☒	124.4	0.51 / 76.9 / 99.3	9.3
1-22 *p*-chloro-fluorobenzene	☒		144.1	0.55 / 79.7 / 111.5	8.5
1-23 *m*-fluoronitrobenzene		☒	130.0	0.52 / 78.2 / 104.9	14.9
1-24 *o*-fluoronitrobenzene		☒	140.3	056 / -85.5 / 101.7	11.7
1-25 *p*-fluoronitrobenzene	☒		139.6	0.53 / -85.6 / 113.9	6.1
1-26 nitroethane		☒	140.9	0.55 / 86.8 / 104.8	14.8
1-27 1-nitropropane		☒	142.6	0.57 / -87.5 / 100.9	10.9
1-28 benzaldhyde	☒		153.2	0.58 / -87.6 / 112.1	7.9
1-29 dioxane	☒		149.9	0.56 / 84.0 / 118.8	1.2
1-30 γ-picoline 1		☒	129.8	0.52 / -77.8 / 102.3	12.3
1-31 γ-picoline 2	☒		153.8	0.59 / 80.9 / 112.5	7.5
1-32 toluene	☒		143.8	0.56 / -83.5 / 124.3	4.3

Inclusion Compound	**Twist form**	**Boat form**	$\sum\lvert\text{Tors.}\rvert$ **[°]**	**Q / θ [°] / P_2 [°]**	**$\Delta(P_2)$ from ideal form**
1-33 nitrobenzene	☒		150.2	0.56 / -88.9 / 115.4	4.6
1-34 *p*-chlorotoluene	☒		143.4	0.54 / 81.4 / 111.1	8.9
1-35m1 *p*-xylene 2		☒	135.9	0.57 / 86.6 / 145.8	4.2
1-35m2 *p*-xylene 2		☒	135.7	0.54 / 86.2 / 139.1	10.9
1-36 formic acid	☒		158.7	0.60 / -86.4 / 112.8	7.2
1-37 acetic acid	☒		157.1	0.59 / -85.9 / 115.2	4.8
1-38 nitromethane	☒		144.8	0.56 / -87.7 / 107.0	13.0
1-39 acetonitrile	☒		142.2	0.54 / -81.5 / 113.5	6.5

Table 2 summarize the data of the averaged C—C (in the ring), C—NO_2, C—NH, and N—O bond lengths over all the structures in the boat, twisted boat, and twist forms of **1**, in addition to the values of these bonds in the aromatic system for comparison.

Table 2. Selected average bond lengths

	C—C	C—NO_2	C—NH	N—O
boat	1.443(4)	1.396(8)	1.316(5)	1.252(1)
twisted boat	1.443(5)	1.400(5)	1.316(7)	1.249(6)
twist	1.442(8)	1.395(12)	1.316(12)	1.251(5)
aromatic system	1.381(13)	1.468(14)	1.355(13)	1.218(13)

The averaged C—C bond length within the six-membered ring markedly increased (in comparison with the aromatic system), both types of average C—N bond length decreased and the average N—O bond length increased. These results support the idea that the π electron density is shifted from the ring to the substituents.

2-3 Discussion of the packing

Intramolecular hydrogen bonds are asymmetric in all cases, which have been established as a general phenomenon in non-planar 2,4,6-tris-monoalkylamino-1,3,5-trinitrobenzenes[43]. One nitro group is connected with both neighbouring NH groups by hydrogen bonds, and the second nitro group takes part in only one intramolecular hydrogen bond leaving the third nitro group free from intramolecular hydrogen bonding (Figure 2-3). The nitro group which dose not accept a hydrogen bond is always the one at the bowsprit (N5).

Both dimorphic structures adopt the centrosymmetric space group C2/c with 16 molecules in the unit cell for structure **1a** (two independent molecules in the asymmetric unit: **1a1**, **1a2**, Figure 2-1) and with 8 molecules for structure **1b** (one molecule in the asymmetric unit **1b**, Figure 2-2).

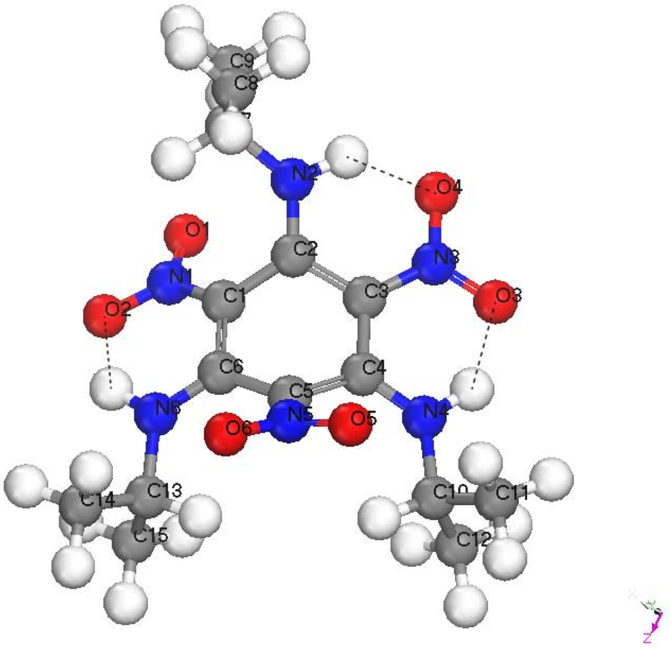

Figure 2-3. The intramolecular hydrogen bonds in 1

Intermolecular hydrogen bonds also were found in both structures which in this case implies the existence of bifurcated hydrogen bonds. The packing arrangement and structure system of the molecules connected with the intermolecular hydrogen bonds in both structures are completely different. In form **1a**, there are a Zig-Zag columns of antiparallel, hydrogen bonded **1a2**, molecules neighboured another Zig-Zag columns of parallel not bonded mole cules **1a1**. Namely, we have a chain character of the hydrogen bond system, which connects only one of the two independent molecules (**1a2**) and extends in the b direction (Figure 2-4). In dimorph **1b** we have a dimer character of the structure, every two molecules are connected with two symmetry equivalent hydrogen bonds forming units of isolated pairs. These units arranged in layer form structure (Figure 2-5).

Although some times it is difficult to explain the reason of a polymorphic system, it is known that the strength and directionality of the intermolecular hydrogen bonds might suggest a high incidence of polymorphism for those compounds which contain a number of potential hydrogen bond donors and acceptors, since they might be combined in different ways[44]. To this point we expect structure **1a** to be more stable than **1b**, because of the chain nature of the intermolecular hydrogen bond system, which proved to be true by DSC measurements and calculations.

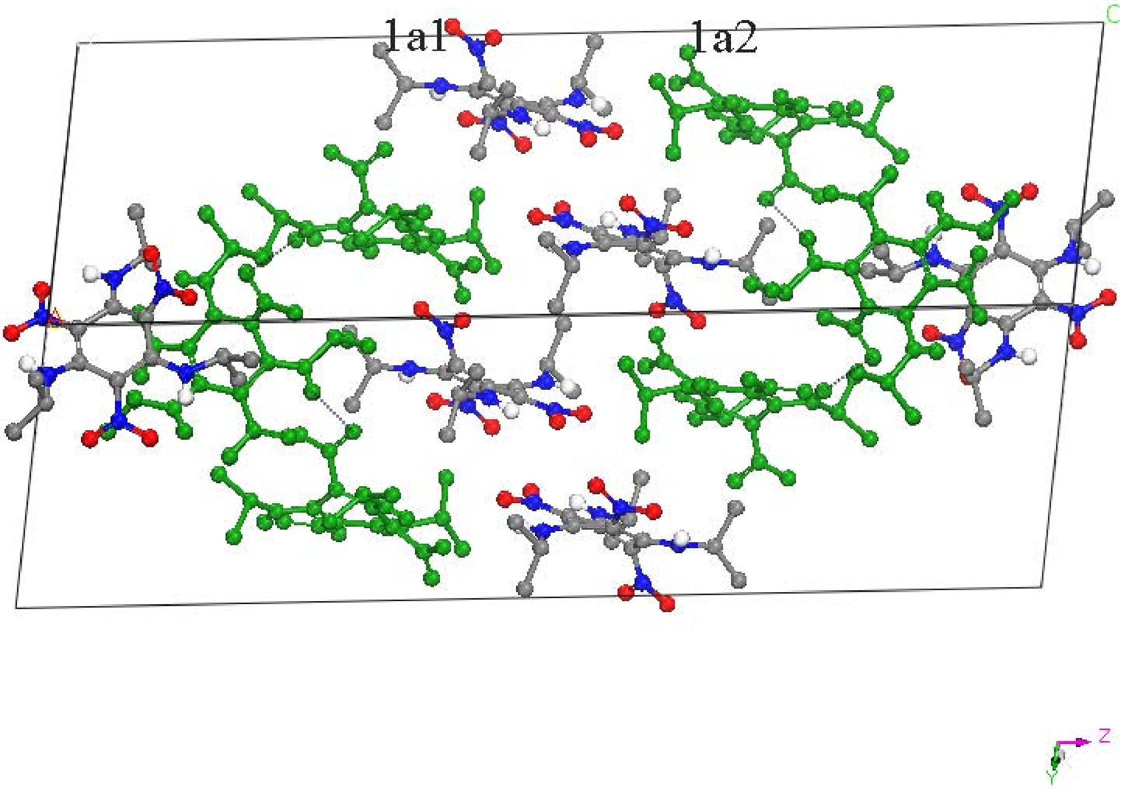

Figure 2-4. Packing pattern of 1a

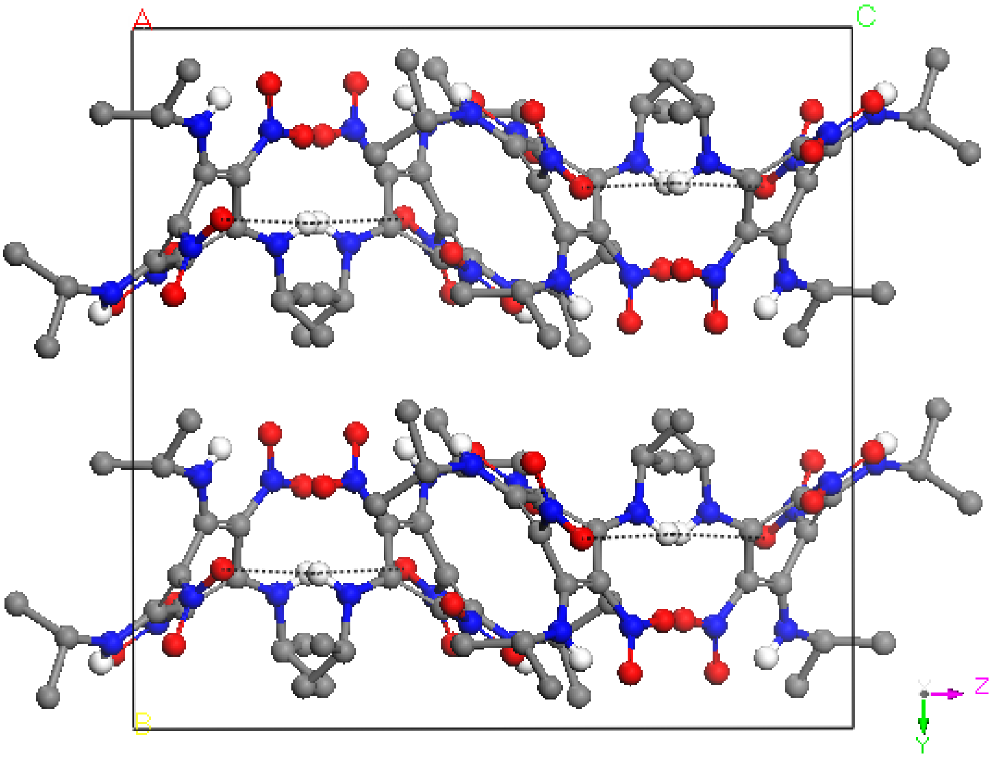

Figure 2-5. Packing pattern of 1b

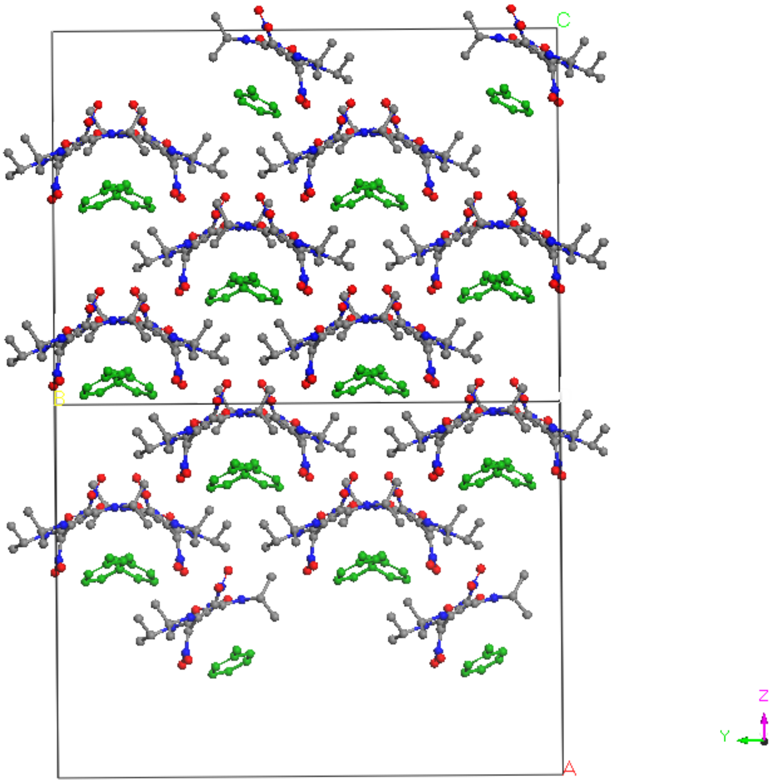

Figure 2-6. Packing pattern of structure with fluorobenzene (1-4)

Six different packing arrangements for the cosolvates of **1** were found. The most cosolvates, as with benzene, alkyl- and halogenbenzene derivatives, and γ-picoline (17 structures **1-1, 1-2**, **1-3**, **1-4**, **1-5**, **1-6, 1-7**, **1-8**, **1-9**, **1-15**, **1-18**, **1-20**, **1-21**, **1-22**, **1-30, 1-32, 1-34**) crystallize in the non-centrosymmetric space group Cc.

All crystal structures of this group (group 1) have nearly the same packing arrangement Figure (2-6), in which the inclusion molecules (green molecules) are sitting in canals, in the (101) direction, between the host molecules. The canals dimension change slightly according to the volume of the guest molecule. In this packing arrangement no intermolecular hydrogen bond was found.

Another favourite space group for the cosolvates is the space group P–1. 16 inclusion compounds have been found to adopt this space group. These inclusion compounds are, phenol and its derivatives, anisole, benzonitrile, DMF, *m*- and *p*-fluoronitrobenzene, benzaldahyde, dioxane, nitrobenzene, formic acid, acetic acid and acetonitrile (**1-11, 1-13**, **1-14**, **1-16**, **1-17, 1-19**, **1-23**, **1-25**, **1-28**, **1-29, 1-33, 1-36, 1-37, 1-39**). These 14 cosolvates (group 2) packed in three different packing arrangements, subgroups 2-1, 2-2, and 2-3, Figures (2-7, 2-8 and 2-9).

The first packing type in this group (subgroup 2-1), which include structures with benzonitrile (**1-14**), hydroquinone (**1-17**), *p*-nitrophenol(**1-19**), *p*-fluoronitrobenzene (**1-25**), benzaldhyde (**1-28**), dioxane (1-**29**), DMF (**1-16**) and nitrobenzene (**1-33**), is a structure with Zig-Zag channels of non connected layers of dimers of host molecules (the host dimers are connected with two intermolecular hydrogen bonds forming with the intramolecular hydrogen bonds a square or parallelogram form), while the guest molecules are sitting in a pair character between these channels one time parallel (structures with hydroquinone, *p*-nitrophenol, and *p*-fluoronitrobenzene), (Figure 2-7a) and another perpendicular (structures with benzonitrile, benzaldhyde, dioxane, and nitrobenzene) to the host dimer (Figure 2-7b). In the structure with DMF, a clasters of four guest molecules caused total distortion of the host pattern (Figure 2-7c).

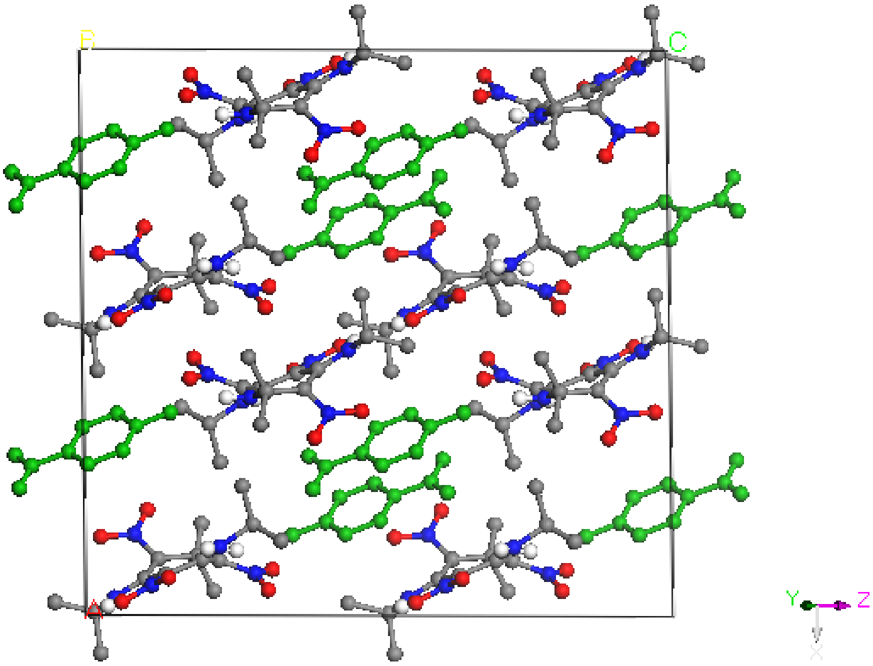

Figure 2-7a. Packing pattern of structure with p-fluoronitrobenzene (1-25)

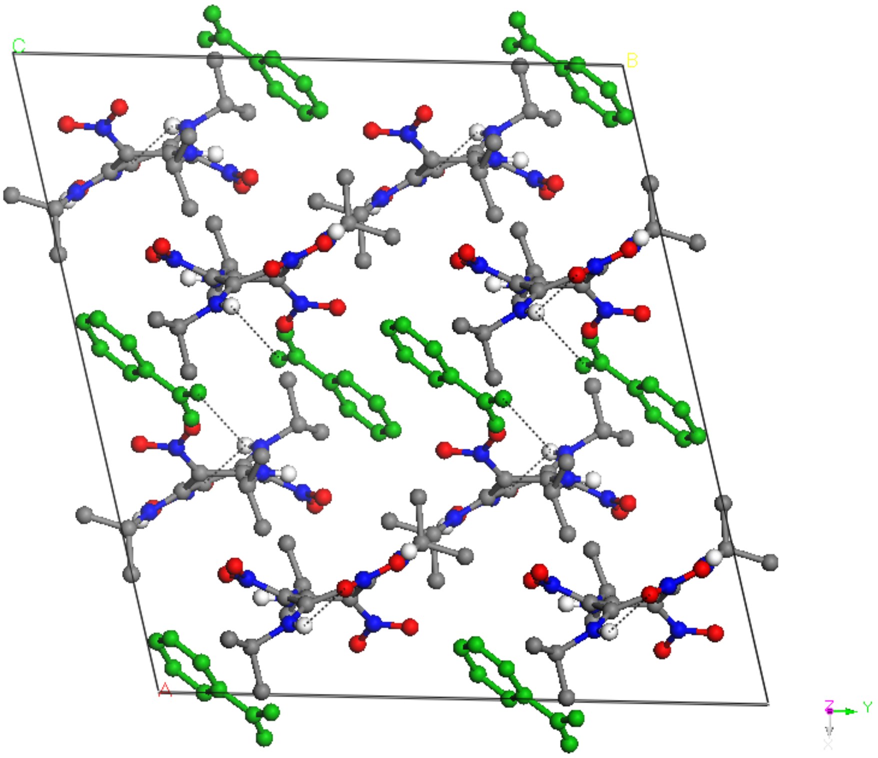

Figure 2-7b. Packing pattern of structure with benzaldhyde (1-28)

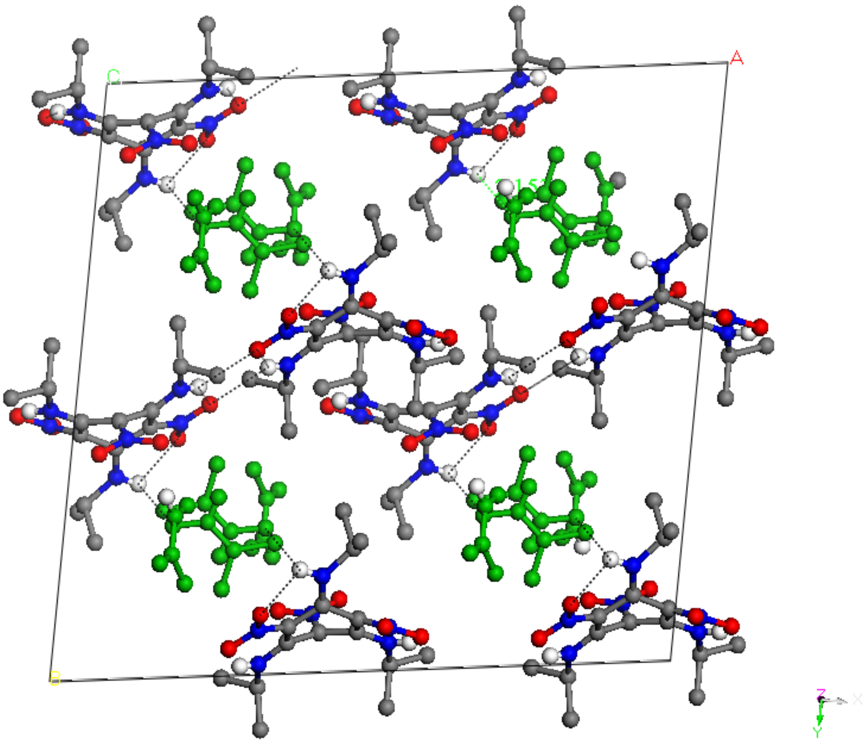

Figure 2-7c. Packing pattern of structure with DMF (1-16)

One can clearly see the adjustable character of the host framework. The host molecules can slide mutually and be locked in several distinct positions differing in the degree of overlap. Two adjacent host layers will adjust mutually, moving sideways according to the size of the molecule being included in between.

The second packing type of this group (subgroup 2-2), include structures with phenol (**1-11**), *m*-fluoronitrobenzene (**1-23**), acetonitrile (**1-39**), acetic acid (**1-3**7), and formic acid (**1-36**), (Figure 2-8a, 2-8b and 2-8c). This packing type has again a channel structure consisted of parallel dimers of host molecules (each two host molecules are connected with two intermolecular hydrogen bonds forming with the intramolecular hydrogen bonds a square or parallelogram form), while the guest molecules are sitting in a pair character between these channels with different motifs as seen in Figures.

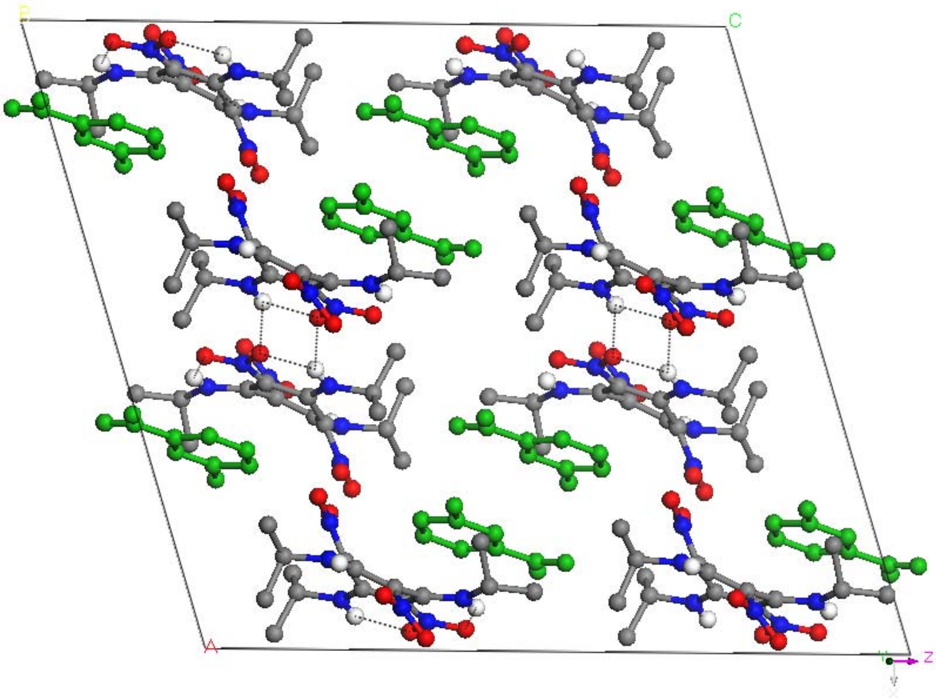

Figure 2-8a. Packing pattern of the structure with *m*-fluoronitrobenzene (1-23)

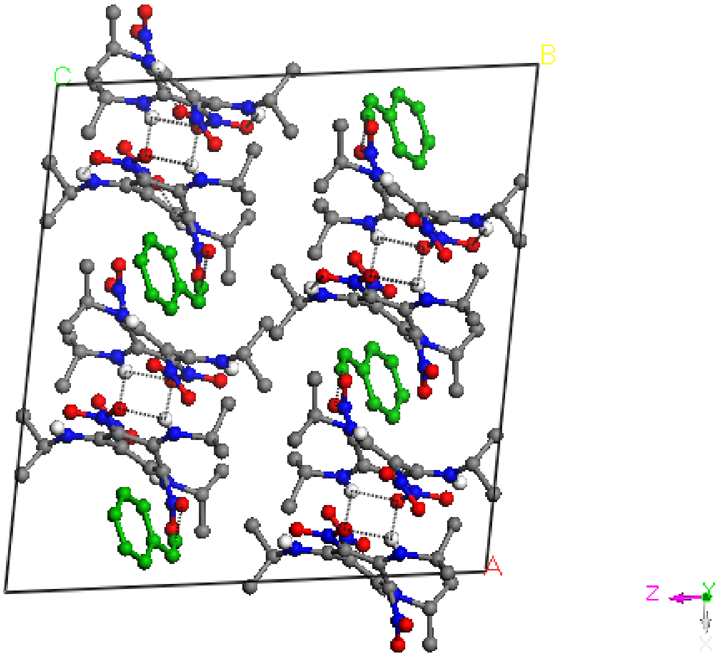

Figure 2-8c. Packing pattern of the structure with phenol (1-11)

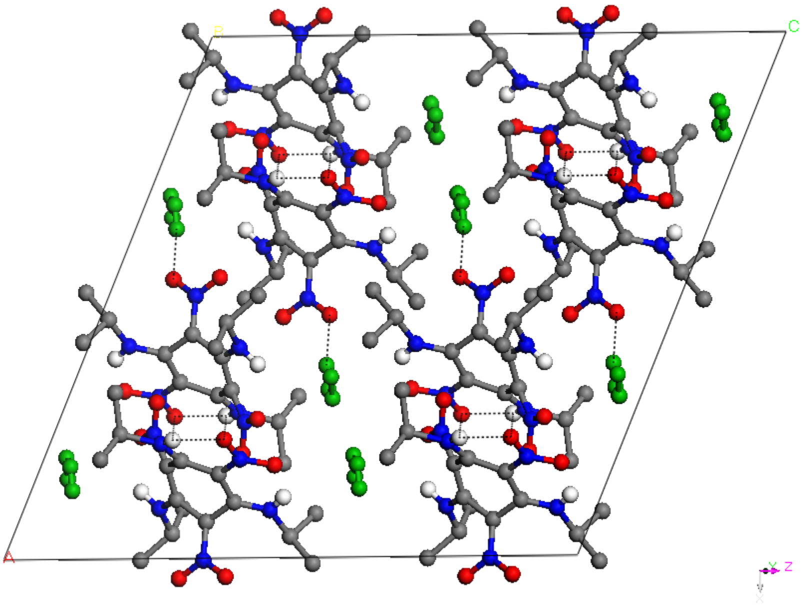

Figure 2-8c. Packing pattern of the structure with formic acid (1-36)

In the third packing type of this group (subgroup 2-3), which include structure with anisole (**1-13**), there is a kind of combination between the last two packing types. There are both types of the host pairs, the one in which the two host molecules lie beside each other and the other one in which the two host molecules lie parallel to each other. Both kinds of pairs sitting in alternating position in channels, while the host molecules are sitting in the free gaps in between (Figure 2-9).

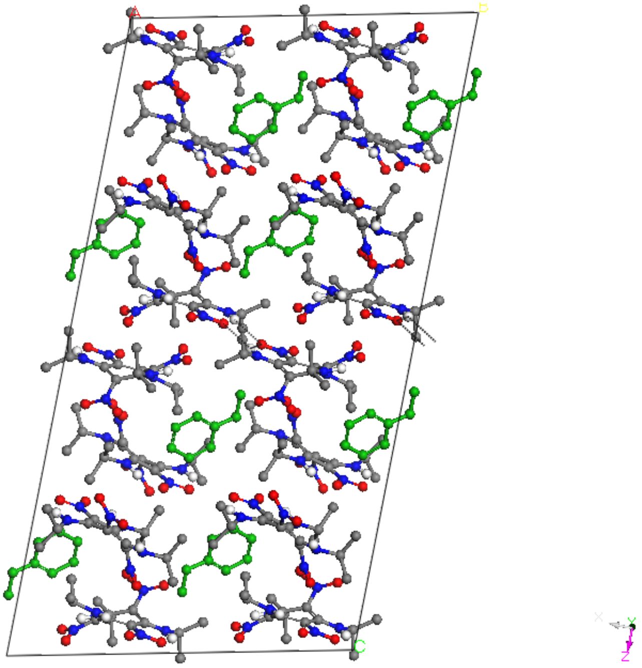

Figure 2-9. Packing pattern of structure with anisole (1-13)

The fifth type of packing arrangement include structures in the space groups $P2_1/n$, $P2_1/a$, and $P2_1/c$; this comprise structures with nitroethane (**1-26**), 1-nitropropane (**1-27**), hexafluorobenzene (**1-10**), *o*-fluoronitrobenzene (**1-24**), and *p*-xylene 2 (**1-35**), in addition to the second structure with phenol 2 (**1-12**), which crystallize in the space group P-1. The dimer character for host molecules can also be found in this packing arrangement, except for the structure with hexafluorobenzene (**1-10**). Each two host molecules are connected with two symmetry equivalent hydrogen bonds. The host molecules lie in planes parallel to the bc plane, while the guest molecules lie in between in a parallel sheets (Figure 2-10).

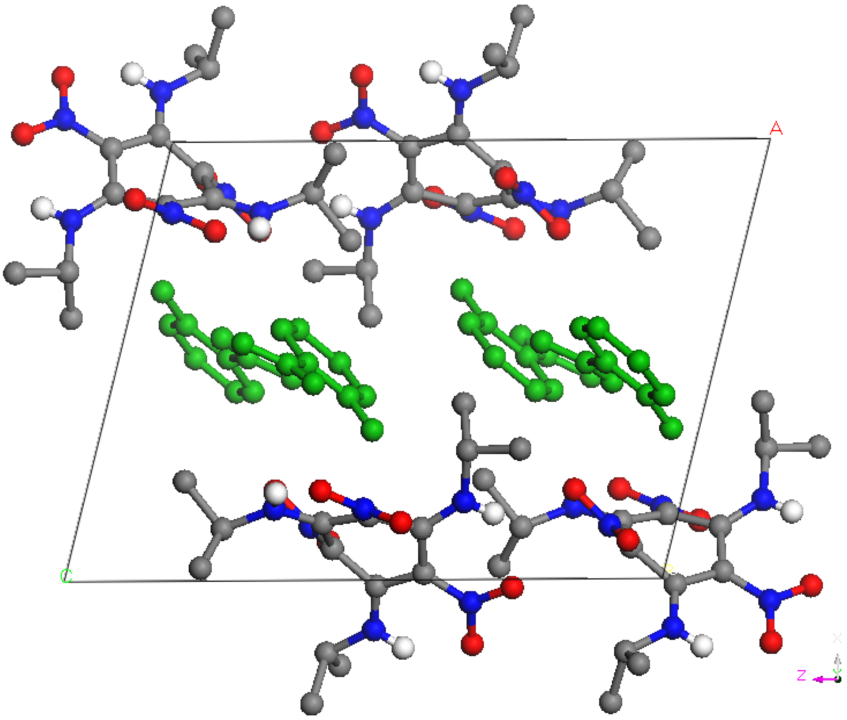

Figure 2-10. Packing pattern of the structure with *o*-fluoronitrobenzene (1-24)

Only one structure has been found in the hexagonal space group P $3(2)2_1$. This is the second structure with γ- picoline 2 (**1-31**) (Figure 2-11). In this structure there is a very stable net of hydrogen bonded host molecule, each molecule is connected by hydrogen bonds with three neighbouring molecules. A hydrogen bond system with chain character was found, which extend in the c direction. The different chains of host molecules also are connected by hydrogen bonds.

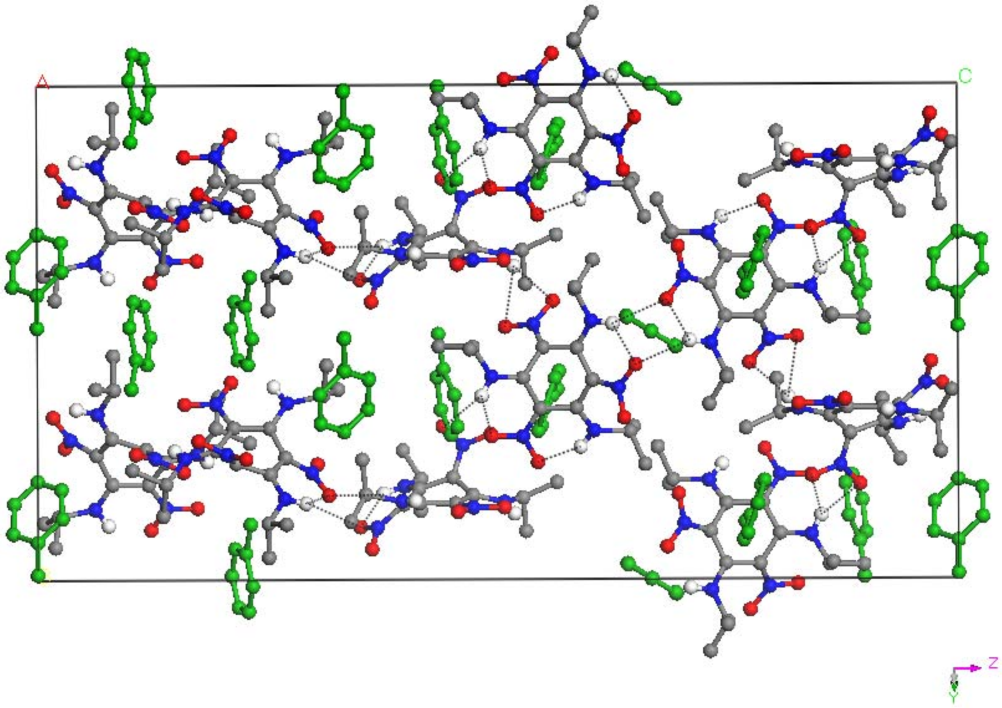

Figure 2-11. Packing pattern of the second structure with γ- picoline 2 (1-31).

In all the structures of group 2, the six-membered ring of the host molecule **1** adopts twist forms except structures with DMF (**1-16**) (which adopt boat form), *p*-nitrophenol (**1-19**) and *m*-fluoronitrobenzene (**1-23**) (both adopt twist form). This conformation is very suitable for strong van der Waals interactions between the different layers in this structure pattern.

In all the structures of group 3, the six-membered ring of **1** adopts twisted-boat forms except one of the two independent molecules in the structures with *p*-xylene 2 (**1-35m1**), which adopt boat form.

2-3 The influence of packing patterns on molecular parameters of 1

All three forms (boat, twist, and twisted-boat forms), show distinct bond length alternation within the ring. Quinonoid forms are compatible with boat geometries, where the formal double bonds are located at the sites of no twisting (torsional angle at this bond close to 0°). Thus, there are two short and four long bonds (Scheme 2.1). The six-membered ring conformations of **1** in the structures with *o*-difluorobenzene (**1-7**), DMF (**1-16**), *o*-fluorotoluene (**1-21**), *p*-xylene 1 (**1-18**) and one of the two independent molecules in the structure with *p*-xylene 2 (**1-35m1**) have found to adopt this conformation. The average of the summation of the two short and the four long bonds over all these structures are 1.427 Å and 1.451 Å respectively. The average of the two short $(\text{C—C short})_{\text{ave}}$ and the four long $(\text{C—C long})_{\text{ave}}$ bonds in each structure are given in Table 3. Structure with DMF (**1-16**) has relatively low value for $(\text{C—C short})_{\text{ave}}$ and high value for $(\text{C—C long})_{\text{ave}}$. In this structure the host:guest ratio is 1:2 and in addition host-guest intermolecular hydrogen bonds has been found in this structure. On the other hand, structure with *p*-xylene 2 (**1-35**) has relatively high value for $(\text{C—C short})_{\text{ave}}$ and low value for $(\text{C—C long})_{\text{ave}}$. In this structure the host:guest ratio is 1:1/4 and no host-guest intermolecular hydrogen bonds has been found in this structure. Consequently, in the structure with DMF (**1-16**) host molecules have strong interaction to guest molecules, because of the host-guest intermolecular hydrogen bonds and the higher number of guest molecules to the number of the host molecules, than the host molecules in the structure with *p*-xylene (**1-35**). Therefore we can conclude that, the stronger the host-guest interaction, the shorter the $(\text{C—C short})_{\text{ave}}$ and the longer the $(\text{C—C long})_{\text{ave}}$ in the ring of the host molecule and vice versa.

Table 3. The average C—C bond lengths in boat form conformation structures of 1

	o-difluorobenzene (**1-7**)	DMF (**1-16**)	*o*-fluorotoluene (**1-21**)	*p*-xylene 1 (**1-18**)	*p*-xylene 2 (**1-35m1**)
$(\text{C—C short})_{\text{ave}}$/ $(\text{C—C long})_{\text{ave}}$	1.430/1.450	1.421/1.457	1.419/1.450	1.433/1.451	1.434/1.446

In contrast to boat forms, twist forms cannot be quinonoid since twisting is largest at the sites where it is smallest for boat forms. Now the pattern of bond length alternation is reversed, there are four short and two long bonds (Scheme 2.1). The six-membered ring conformations of **1** in the structures with ethylbenzene (**1-2**), cumene (**1-3**), chlorobenzene (**1-5**), *p*-difluorobenzne (**1-8**), phenol 1 (**1-11**), anisole (**1-13m1**), benzonitrile (**1-14**), hydroquinone

(**1-17**), *p*-chlorofluorobenzene (**1-22**), *p*-fluoronitrobenzene (**1-25**), benzaldhyde (**1-28**), dioxane (**1-29**), γ-picoline 2 (**1-31**), toluene (**1-32**), nitrobenzene (**1-33**), *p*-chlorotoluene (**1-34**), formic acid (**1-36**), acetic acid (**1-37**), and acetonitrile (**1-39**) have found to adopt this conformation. The average of the summation of the four short and the two long bonds in these structures is 1.456 Å and 1.435 Å respectively. The average of the four short (C—C short)$_{\text{ave}}$ and the two long (C—C long)$_{\text{ave}}$ bonds in each of these structures are given in Table 4.

The following structures have relatively high value for (C—C long)$_{\text{ave}}$. These are the structures with:

- phenol 1(**1-11m2**), hydroquinone (**1-17**), formic acid (**1-36**) and acetic acid (**1-37**). These structures have host-guest intermolecular hydrogen bonds.
- benzonitrile (**1-14**), benzaldhyde (**1-28**), and nitrobenzene (**1-33**). These structures belong to one packing type (group 2).
- γ-picoline 2 (**1-31**). This structure has unique packing pattern with three host-host intermolecular hydrogen bonds.

The reason for this could be strong host-guest interaction, which will examined both experimentally and theoretically in the next parts.

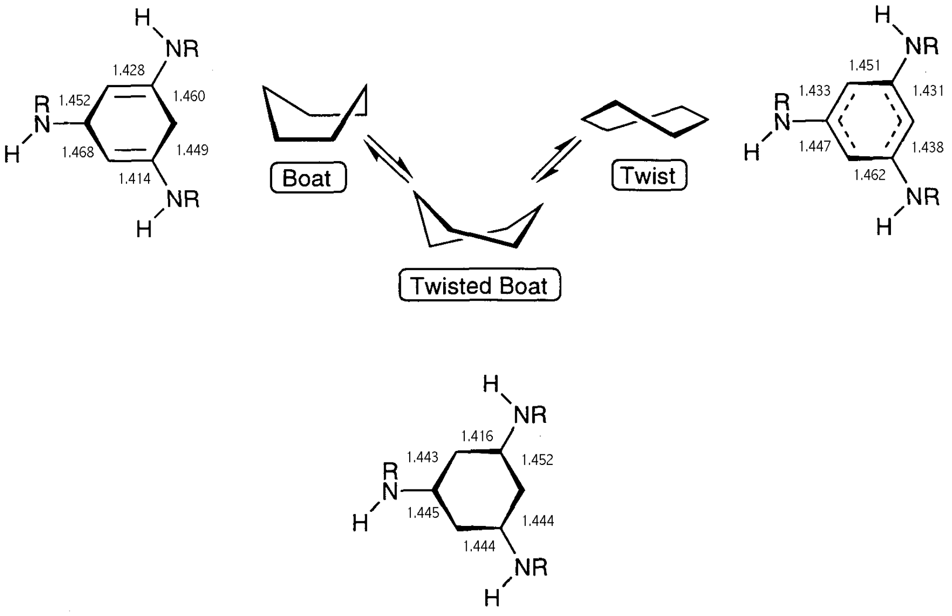

Scheme 2.1 The different possible conformations of 1, boat form in structure with DMF (1-16), twist form in structure with nitrobenzene (1-33), and twisted-boat form in structure with 1,2,4-trifluorobenzene (1-9).

Table 4. The average C—C bond lengths in twisted-boat form conformation of 1

	ethylbenzene (**1-2**)	cumene (**1-3**)	chlorobenzene (**1-5**)	*p*-difluorobenzne (**1-8**)	phenol 1 (**1-11m1**)
(C—C short)$_{ave}$/ (C—C long)$_{ave}$	1.437/1.454	1.438/1.452	1.435/1.451	1.437/1.454	1.435/1.451
	phenol 1 (**1-11m2**)	anisole (**1-13m1**)	benzonitrile (**1-14**)	hydroquinone (**1-17**)	*p*-chlorofluorobenzene (**1-22**)
(C—C short)$_{ave}$/ (C—C long)$_{ave}$	1.433/1.458	1.436/1.449	1.436/1.457	1.437/1.461	1.436/1.45
	p-fluoronitrobenzene (**1-25**)	benzaldhyde (**1-28**)	dioxane (**1-29**)	γ-picoline 2 (**1-31**)	toluene (**1-32**)
(C—C short)$_{ave}$/ (C—C long)$_{ave}$	1.439/1.452	1.437/1.461	1.436/1.454	1.436/1.457	1.429/1.454
	nitrobenzene (**1-33**)	*p*-chlorotoluene (**1-34**)	formic acid (**1-36**)	acetic acid (**1-37**)	acetonitrile (**1-39**)
(C—C short)$_{ave}$/ (C—C long)$_{ave}$	1.437/1.457	1.436/1.455	1.439/1.470	1.434/1.459	1.422/1.455

For twisted-boat forms, there are one bond long, one bond short and the other four bonds in between.

Conclusion 1

In general we can conclude that :

- The six-membered ring conformations of the host molecule **1** in structures that contain intermolecular hydrogen bonds were found to adopt either twist form or twisted-boat forms, except structures with DMF (**1-16**) and *p*-xylene 2 (**1-35**), while in the absence of the intermolecular hydrogen bonds (structures of group 1) **1** is free to adopt twist, boat or twisted-boat form depending on the included molecule.
- In the structures with phenol 1(**1-11m2**), benzonitrile (**1-14**), DMF (**1-16**), hydroquinone (**1-17**), benzaldhyde (**1-28**), γ-picoline 2 (**1-31**), nitrobenzene (**1-33),** formic acid (**1-36**), and acetic acid (**1-37**), the average of the long bond lengths (four bonds for boat form and two bonds for twist form) (C—C long)$_{ave}$ in the six-memdered ring of **1** have relatively high value. This should be a result of strong host-guest interaction.
- The stronger the host-guest interaction, the shorter the (C—C short)$_{ave}$ and the longer the (C—C long)$_{ave}$ in the ring of the host molecule.

2-4 Differential scanning calorimetry and thermogravimetry

Differential Scanning Calorimetry (DSC) method has been used to measure the energies needed to evaporate the different solvents (dissolution energy, E_{diss}) and to examine the relative stability of the two forms **1a** and **1b**.

Heating our samples, which placed in crimped but vented aluminium pans, at a rate of 5 °C min^{-1} with a purging steam of dry nitrogen flowing at 150 mL min^{-1} and over a temperature range of 30-600 °C. Two different forms of the DSC output curves were found. The first form, which occurs in most of the cases, has two endothermic peaks; we assume that the first peak is associated with the evaporation of the solvent, while the second one corresponds to the melting or decomposition of the pure host (Figure 2-12).

The second form of the DSC curves, has three endothermic peaks (Figure 2-13a). Now we have an additional peak and our first assumption, that one peak is associated with the evaporation of the solvent, while the second one correspond to the melting or decomposition of the pure host, can not be applied directly. A peak produced by DSC experiment means that a thermal event occurs over this temperature range. It dose not tell whether this is a chemical reaction or a physical change such as melting, or whether any gases are evolved. A performance of thermogravimetry (TG) experiment on the same sample may show a mass loss over this temperature range, thereby ruling out melting or phase transition. Conversely, if the TG curve showed no mass loss, the process of melting or phase transition could be confirmed. It is clear that a combination of DSC and TG measurements for our samples gives better profile of the changes taking place.

The performance of TG measurements have confirmed our analysis of the first form of the DSC curves to be correct. The first peak is associated with the evaporation of the solvent, while the second one correspond to the melting or decomposition of the pure host. The energy needed to evaporate the solvent calculated directly from the area under the first peak.

For structures with anisole (**1-13**), DMF (**1-16**), *p*-xylene 1 and 2 (**1-18**) (**1-35**), γ-picoline 1and 2 (**1-30**) (**1-31**), and *p*-chlorotoluene (**1-34**), the first two peaks in the DSC curves correspond to the evaporation of the solvent, which takes place in two steps because the TG curves show two stages that occur at the same corresponding temperature as in DSC measurements (Figure 2-13b). Namely, only a part of the guest molecules leaves the structure (the exact ratio of the evaporated part can be calculated from the height of the step in the TG curve) at certain temperature. New structure will then be formed with less number of guest molecules. At higher temperature the rest of the guest molecules will be able to leave the structure as well. Consequently, one can expect to find more than one structure with these solvents, which exactly what we got, there are two structures with *p*-xylene as well as with γ-picoline. The energy associated with the evaporation of the solvent in these cases should be calculated over the area of the two peaks (Figure 2-13b).

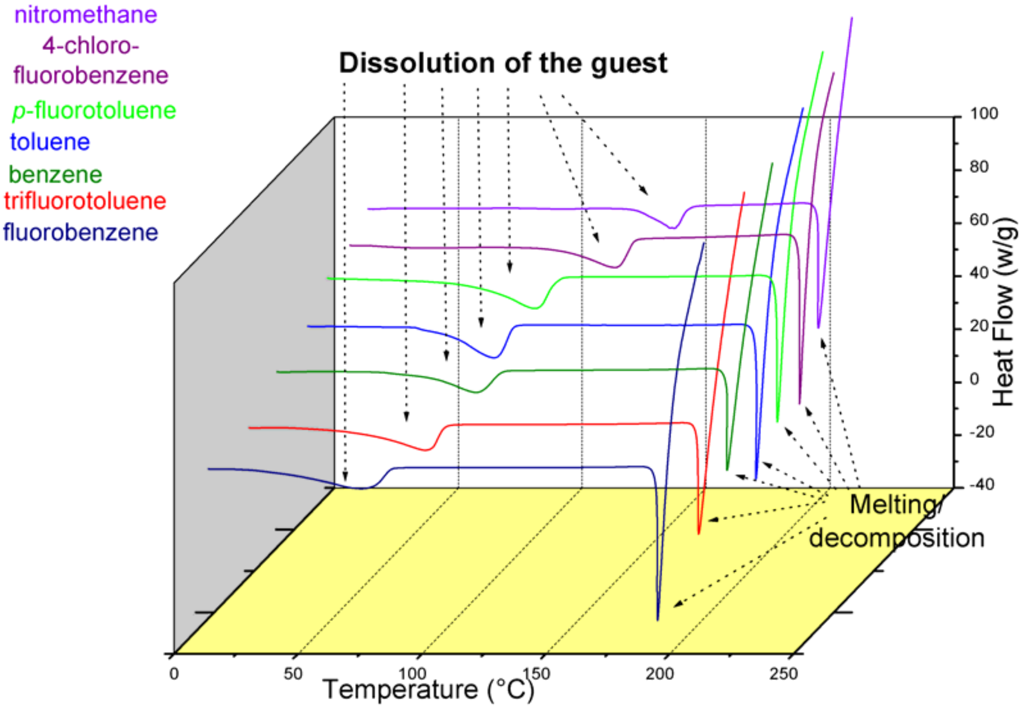

Figure 2-12. DSC output curves

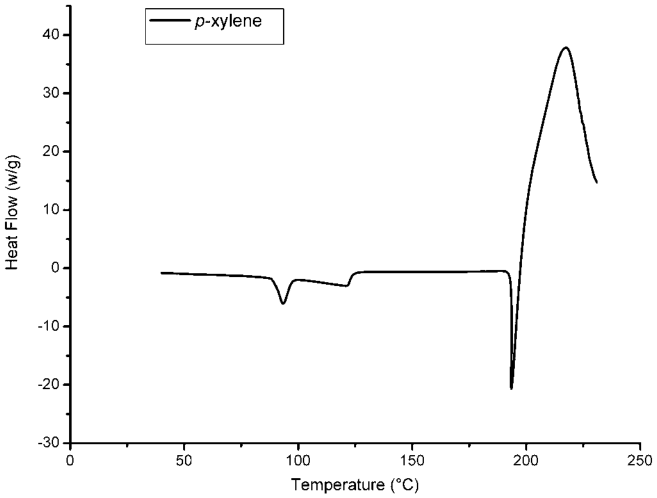

Figure 2-13a. DSC output curves of structure with *p*-xylene (1-18)

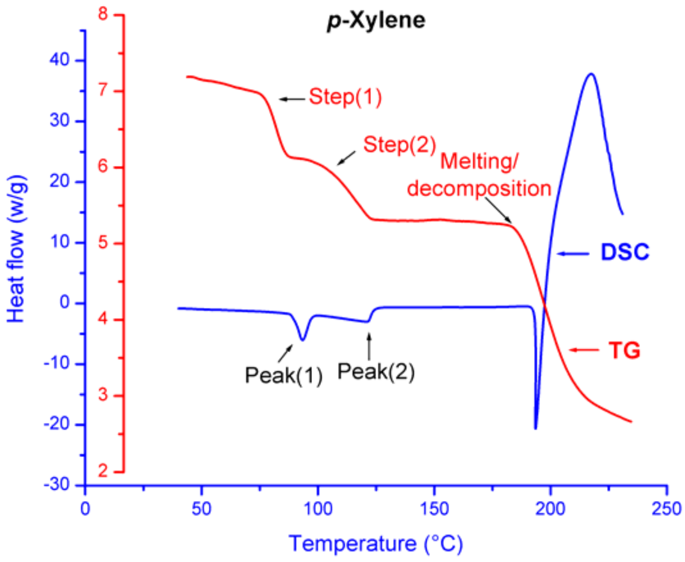

Figure 2-13b. DSC and TG output curves of structure with *p*-xylene (1-18)

In other cases, as for structures with benzonitrile (**1-14**) (Figure 2-14) and ethylbenzene (**1-2**), the TG curve shows only one step that occur at the same temperature as the first peak in the DSC curve, then only this peak of the DSC curve correspond to the evaporation of the solvent (and only this peak should be used in the energy calculation), while the second one correspond to phase change of the host structure that takes place after the evaporation of the solvent, which has also been tested by performing powder diffraction at this range of temperature.

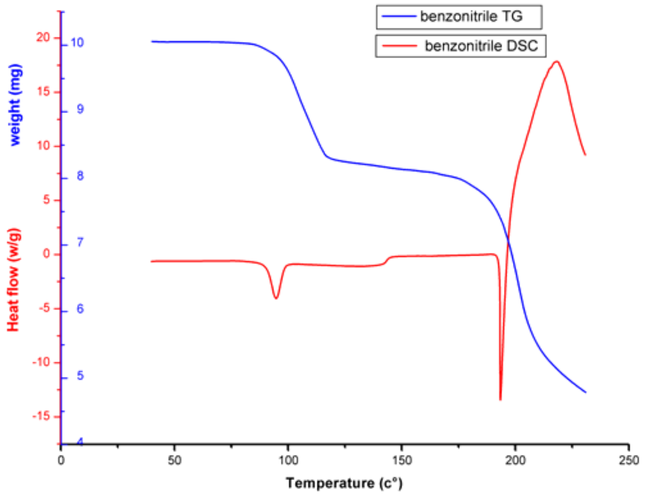

Figure 2-14 . DSC and TG curves of structure with benzonitrile (1-14)

The energy needed to evaporate the different solvents is given in Table (5). The energy associated with the evaporation of the solvent for structure with hydroquinone could not be determined, because the structure was very stable till melting. For structure with benzaldhyde, we could not get the enough amount of powder needed to perform the measurements.

Table 5. DSC and TG results

Inclusion structure	DSC			TG	
	No. of peaks other than melting	Onset temp.	Dissolution Energy E_{diss} kcal/mol	No. of steps	% of the weight loss
1a	-	193.7	7.6	-	-
1b	-	187.3	2.9	-	-
1-1 benzene	1 peak	85.6	10.8	1 step	17.1
1-2 ethylbenzene	2 peaks	81.6	7.0	1 step	21.1
1-3 cumene	2 peaks	34.4	8.8	1 step	22.5
1-4 fluorobenzene	1 peak	59.7	12.1	1 step	20.1
1-5 chlorobenzene	1 peak	116.1	12.7	1step	22.9
1-6 *o*-difluorobenzene	1 peak	74.4	12.0	1 step	23.6
1-7 *m*-difluorobenzene	1 peak	60.0	10.7	1step	23.5
1-8 *p*-difluorobenzene	1 peak	78.0	12.7	1 step	23.6
1-9 1,2,4-trifluorobenzene	1 peak	60.1	7.2	1 step	28.6
1-10 hexafluorobenzene	1 peak	68.6	13.3	1 step	32.0
1-11 phenol 1	1 peak	142.0	12.7	1step	11.4
1-12 phenol 2	1 peak	78.4	7.8	1step	38.2
1-13 anisole	2peaks	77.3	11.4	2steps	12.1
1-14 benzonitrile	2 peaks	90.5	16.7	2 steps	19.2
1-15 trifluorotoluene	1 peak	71.3	12.4	1 step	27.2
1-16 DMF	2 peaks	46.4	15.2	2 steps	18.4
1-17 hydroquinone	x	x	x	x	x
1-18 *p*-xylene 1	2 peaks	89.8	5.1	2 steps	26.3
1-19 *p*-nitophenol	1 peak	135.5	12.3	1 step	24.4
1-20 *p*-fluorotoluene	1 peak	87.0	15.4	1 step	23.6
1-21 *o*-fluorotoluene	1 peak	81.4	12.2	1 step	23.4
1-22 *p*-chlorofluorobenzene	1 peak	110.3	8.9	1 step	25.9
1-23 *m*-fluoronitrobenzene	1 peak	56.2	2.5	1step	27.1
1-24 *o*-fluoronitrobenzene	1 peak	86.7	3.4	1 steps	26.4
1-25 *p*-fluoronitrobenzene	1 peak	119.3	8.1	1 step	25.7
1-26 nitroethane	2 peaks	82.6	14.1	2 steps	15.3
1-27 1-nitropropane	2 peaks	77.3	6.0	1 step	18.6
1-28 benzaldhyde	x	x	x	x	x
1-29 dioxene	1 peak	122.3	9.6	1 step	10.9
1-30 γ-picoline 1	2 peaks	94.7	8.6	2 steps	19.9
1-31 γ-picoline 2	2peaks	63.4	13.4	2 steps	25.9
1-32 toluene	1 peak	85.6	12.3	1 step	19.9
1-33 nitrobenzene	1 peak	96.4	3.4	1 step	25.9
1-34 *p*-chlorotoluene	2 peaks	109.1	15.8	2 steps	29.2

Inclusion structure	DSC			TG	
	No. of peaks other than melting	Onset temp.	Dissolution Energy E_{diss} kcal/mol	No. of steps	% of the weight loss
1-35 *p*-xylene 2	2 peaks	88.8	15.3	2 steps	15.3
1-36 formic acid	2 peaks	126.6	16.4	2 steps	12.2
1-37 acetic acid	2 peaks	107.5	17.5	2 steps	13.5
1-38 nitromethane	1 peak	142.7	5.9	1 steps	14.3
1-39 acetonitrile	1 peaks	68.8	12.0	1 steps	15.8

Substantially high dissolution energies E_{diss} (more than 13 Kcal/mol) are needed for;

- solvates that have host-guest intermolecular hydrogen bonds as acetic acid (**1-37**) (17.5 Kcal/mol), formic acid (**1-36**) (16.4 Kcal/mol), and DMF (**1-16**) (15.2 Kcal /mol).
- solvates that have methyl group in the *para* position as *p*-xylene 2 (**1-35**) (15.3 Kcal/mol), *p*-fluorotoluene (**1-20**) (15.4 Kcal/mol), *p*-chlorotoluene (**1-34**) (15.8 Kcal/mol) and γ-picoline 2 (**1-31**) (13.4 Kcal/mol).
- benzonitrile (**1-14**) (16.7 Kcal/mol) and nitroethane (**1-26**) (14.1 kcal/mol).

These results show strong host-guest interaction in these inclusion crystals. This has been conformed by the detailed calculation of the intermolecular interactions in each structure, which will be shown in the next chapter.

As mentioned before the DSC method has been used to examine the relative stability of the two forms **1a** and **1b**. Figure (2-15) shows the DSC curves for **1a** and **1b**. Both structures show no features in the trace, other than the melting endothermic peak at 193.72±0.06 °C for structure **1a** and at 187.33±0.06 °C for structure **1b**, indicating no phase changes occurring in the structures upon heating. Details of the onset temperature, peak temperature, and the enthalpy of melting are given in Table 5. We note that **1a** should be more stable than **1b**, because it has higher enthalpy of melting, which has been proved to be correct from the theoretical calculations of the lattice energy.

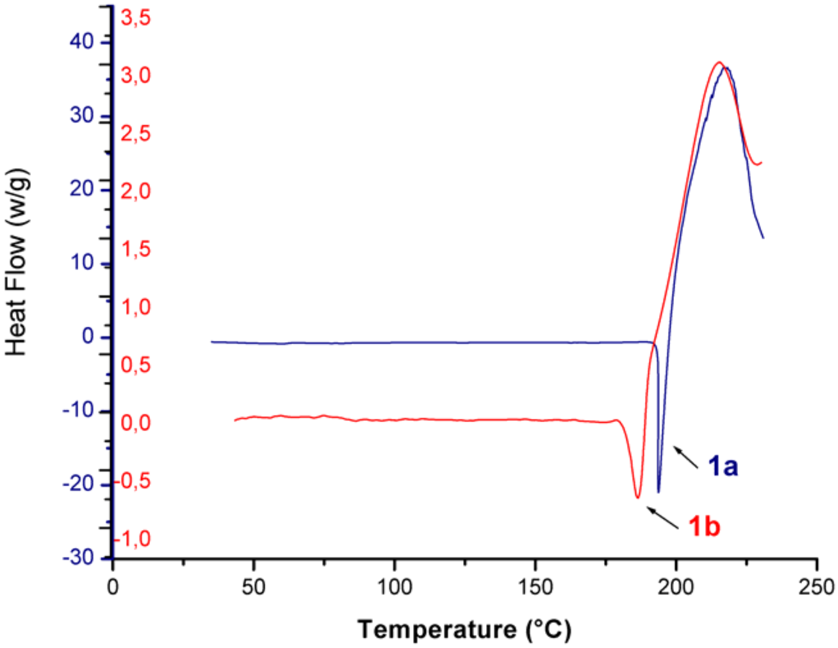

Figure 2-15. DSC curves of structures 1a and 1b

DSC method is also very helpful in testing the relative stability of structures with isomeric molecules as inclusion compounds, as well as the different crystal forms with the same inclusion compound. DSC measurements suggested the stability of the structures with isomeric inclusion molecules to be in the sequence *para* > *ortho* > *meta:*

- *p*-difluorobenzene (**1-8**) (12.7 Kcal/mol) > *o*-difluorobenzene (**1-6**) (12 Kcal/mol) > *m*-difluorobenzene (**1-7**) (10.7 Kcal/mol).
- *p*-fluorotoluene (**1-20**) (15.4 Kcal/mol) > *o*-fluorotoluene (**1-21**) (12.2 Kcal/mol)
- *p*-fluoronitrobenzene (**1-25**) (8.1 Kcal/mol) > *o*-fluoronitrobenzene (**1-24**) (3.4 Kcal/mol) > *m*-fluoronitrobenzene (**1-23**) (2.5 Kcal/mol).

The same results have been found from the theoretical calculations of the lattice energy. The guest molecules with *para* substitution pattern fit much better into the holes between the host molecules than the *ortho* and *meta* substitution pattern producing stronger intermolecular interactions with the host molecules as well as with the other guest molecules and consequently more stable packing.

Additionally, DSC measurements proved the first structure with phenol 1 (**1-11**) (host: guest = 2:1), to be more stable than the second one with phenol 2 (**1-12**) (host: guest = 1:2), the second structure with γ-picoline 2 (**1-31**) (host: guest = 1:1.5), to be more stable than the first one with γ-picoline 1 (**1-30**) (host: guest = 1:1), and the second structure with *p*-xylene 2 (**1-35**) (host: guest = 2:1/2), to be more stable than the first one with *p*-xylene 1 (**1-18**) (host: guest = 1:1). In other words, the close packing structure is always more stable than the other structure. These results are also in a good agreement with the theoretical calculations as we will see in the next chapter.

Conclusion 2

- in agreement with the results in conclusion 1, high dissolution energies E_{diss} (which prove higher host-guest interaction) are needed for structures, which have host-guest intermolecular hydrogen bonds [as structure with hydroquinone (**1-17**) (stable till melting), DMF (**1-16**), acetic acid (**1-37**), formic acid (**1-36**)], structures with solvates that have methyl group in the *para* position [as *p*-xylene 2 (**1-35**), *p*-fluorotoluene (**1-20**), *p*-chlorotoluene (**1-34),** γ-picoline 2 (**1-31**)], and structures with benzonitrile (**1-14**) and nitroethane (**1-26**). No measurements could be perform for the structure with benzaldhyde (**1-28**).

- dimoph **1a** is more stable than dimorph **1b**.
- stability of the structures with isomeric inclusion molecules are in the sequence of: covolvates with *para* > *ortho* > *meta* substitution pattern.
- If there are more than one structure with the same inclusion molecule, then the close packing structure is always more stable than the other structure.

2-5 Powder diffraction

What has really happened to the inclusion structures after the evaporation of the solvent? From the DSC curves, one noticed that a stable structure formed after the dissolution of the solvent, which then, if we continued heating , start to melt or decompose at certain temperature. But which structure is this? To be able to answer this question a performance of powder diffraction is necessary.

For every inclusion structure three powder diffraction measurements have been performed, at room temperature (structure with inclusion molecule), at temperature higher than the guest dissolution temperature (structure without inclusion molecule, at high temperature), and after leaving the sample to cool down another room temperature measurement (room temperature 2) has performed to see if any changes will occur in the structure upon cooling. (Figure 2-16) show, as an example, the powder diffraction data of these measurements for the structure with nitroethane (**1-26**). The different in the output curve between the first room temperature measurement and the two others measurements and the similarity between the last two ones can be clearly seen (Figure 2-16). In the all measurements we have done no difference has been found between the last two measured curves, which mean that the host structure after the evaporation of the solvent is the same at high and room temperature. But again which structure of the host is that?.

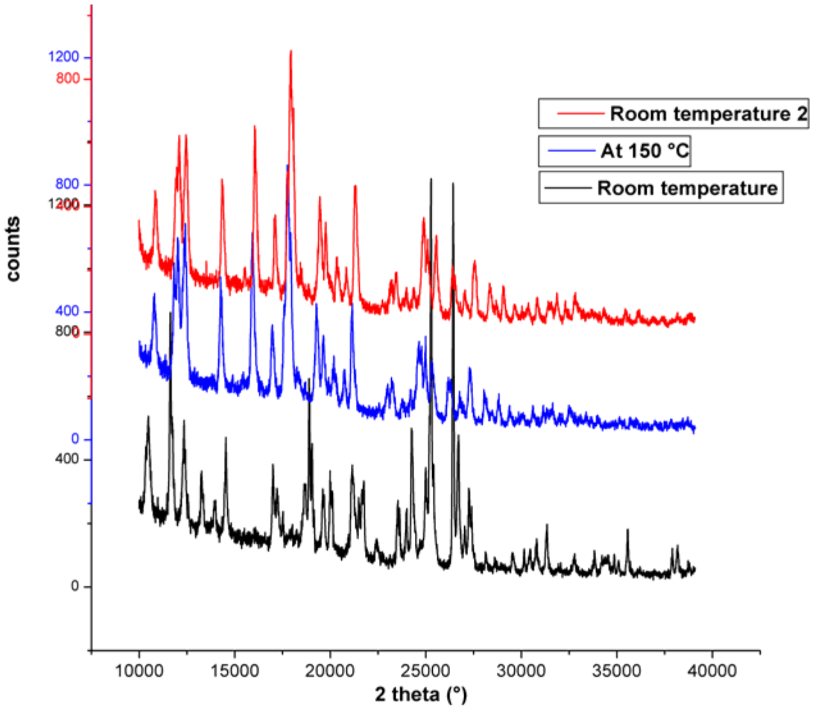

Figure(2-16). Powder diffractions data of the structure with nitroethane (1-26)

To answer this question we have to compare the room temperature 2 diffraction data for each inclusion structure with that of **1a** and **1b** to see if it matches one of them (Figure 2-17).

All the cosolvates structures change to structure **1a** (Figure 2-17) after the evaporation of the solvent, except that of anisole which change to structure **1b**. The anisole structure, as we have seen before, has a unique packing arrangement (Figure 2-9).

The changing of the most cosolvates structures to structure **1a** is consistent with the fact that form **1a** is more stable than form **1b**.

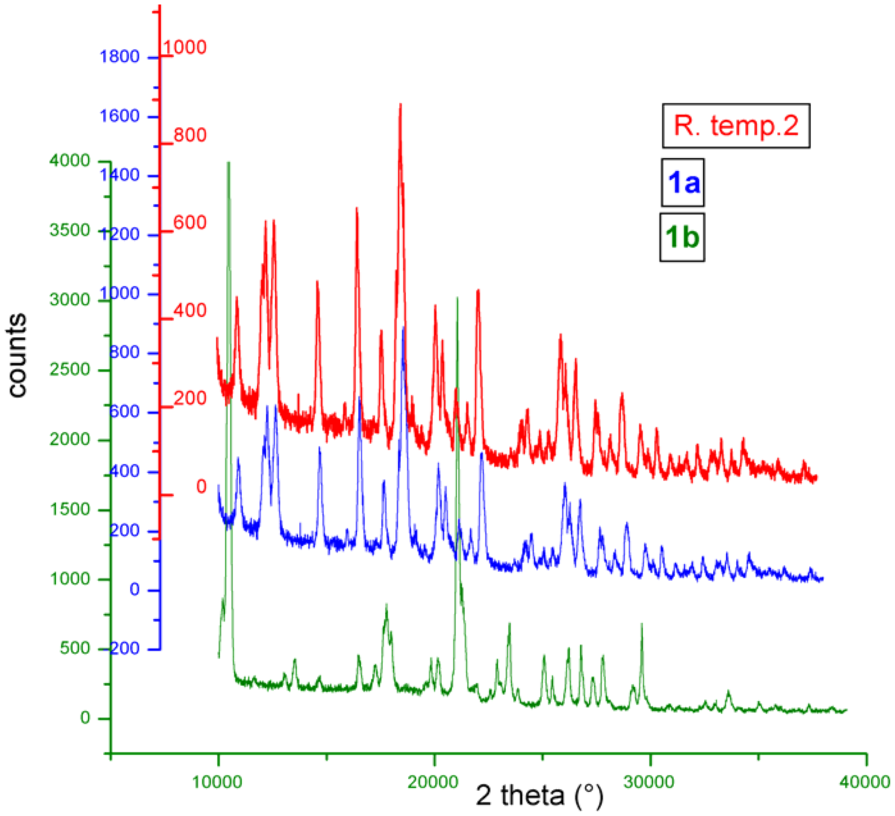

Figure 2-16. Powder diffractions data of 1a, 1b, and room temperature 2 (R. temp. 2) of structure with nitroethane (1-26)

For the structures, as structures with benzonitrile (**1-14**) (Figure 2-14) and ethylbenzene (**1-2**), in which two peaks have been found in the DSC curve while only one step in TG curve at this temperature range, fourth powder diffraction measurement has been performed at temperature range between the first and the second peak in the DSC curve. This measurement proved another structure to perform (phase change) at this temperature range.

3 Energy calculations

3-1 Method

The density functional method within the program DMOL3 (2.2)[11,12] have been used to optimized the positions of the hydrogen atoms in the molecular experimental structures of **1** in the different cosolvates structures, and then to calculate the molecular energy in these conformations (ET). DMOL3 uses numerical orbitals for the basis functions. Each function corresponds to an atomic orbital. The generation of an entire second set of functions leads to a double basis set; this is referred to as a double-numerical (DN) set. This notation is used in analogy with Gaussian double-zeta (DZ) sets, *N* is used to emphasize the numerical nature of these orbitals. Additional basis functions, including polarization, are also used. We have performed the calculations using a DNP (Double Numerical plus Polarization) basis set which includes a polarization p-function on all hydrogen atoms, and GGA-blyp [13,14] as exchange–correlation potential. The size of the DNP basis set is comparable to Gaussian 6-31G**. The "total energy" (ET) of a molecule refers to the energy of a specific arrangement of atoms. The zero of energy, however, is taken to be the infinite separation of all electrons and nuclei, so the total energy is generally negative, corresponding to a bound state. The "binding energy" (EB) is the energy required to separate the individual atoms.

The atomic Coulomb charges have been derived, using the density function method, by fitting the charge to reproduce the electrostatic potential (ESP) which calculated at a large number of grid points around the molecule from the positions of the atomic nuclei α and the electron density ρ. The ESP-derived charges can reproduce the intermolecular interaction properties of molecules well with a simple two-body additive potential.

The molecular structures of **1** and that of the solvate molecules, with the ESP derived charges, have been used to calculate the crystal energy (EC), the lattice energy (EL), and the molecular energy (EM) using the force field method within the program Discover[15] with COMPASS[16,17] force field (Table 4). COMPASS include parameters for high-energy nitro functional which is very important to our molecule. The parameters were derived with an emphasis on the nonbonded parameters, which include a Lennard-Jones 9-6 function for the van der Waals term and a Coulombic term for an electrostatic interaction. Although the main part of the hydrogen bond comes from electrostatic attraction between the positively charged hydrogen and negatively charged heteroatom, additional stabilization may be modelled by assigning special deep and short van der Waals interactions.

The crystal energy refers to the total energy of the crystal including molecular energies, while lattice energy is the summation of the non-bond interaction energies between the different molecules in the crystal.

The lattice energy/molecule (ELM) is calculated using the relation :

$$ELM = EL/N = (EC - N*EM)/N$$

where N is the number of molecules in unit cell .

The non-bond interaction energy (ENB) is the summation of the electrostatic (E_{el}) and van der Waals (E_{vdw}) interaction energies, while van der Waals interaction is the summation of the repulsive (E_{re}) and dispersion (E_{dis}) energies.

3-2 Results and discussion

3-2-1 The DFT calculations on the molecular level

DFT method has been used to perform a single point energy calculation of the total energy (ET) and the binding energy (EB) for the molecular structures of **1** in the dimorph and the cosolvates structures. Additionally, the energy corresponding to the total optimized structures (**1opt**) for the molecular structures of **1** in each structure have also been calculated, Table (6).

These calculations show that, for the dimorph, the stabilities of the different molecular conformations of **1** are in the order **1opt** > **1a1** > **1a2** > **1b**. In other words, the stabilities of the molecules are in the order, isolated molecule > molecule free of intermolecular hydrogen-bond > molecule connected with one intermolecular hydrogen-bond > molecule connected with two intermolecular hydrogen bonds, which illustrate the effect of the packing patterns on the molecular structure. This relation is not applied for the conformations of **1** in the different inclusion structures, the reason is simply that in this structures we have in addition host-guest interactions, which also have influence on the conformation of **1**.

Figures (3-1, 3-2 and 3-3) show an overlap between the optimised structure **1opt** and that of **1a1**, **1a2**, **1b** respectively. The good agreement between **1a1** and **1opt** is very clear. On the other hand, the difference, in the position of the nitro group free of intramolecular hydrogen bonds and the two neighbouring isopropylamino groups, between **1a2**, **1opt** (Figure 3-2), and **1b** , **1opt** (Figure 3-3) is also very clear, suggesting more stability of the molecular conformation of **1** when the carbon atom connected to nitro group free of intramolecular hydrogen bond has less twisting and the methyl groups of the neighbouring isopropylamino groups are far from each other.

For the pseudopolymorphs of **1** within the solvates, the molecular energies (ET) range between (-857020.1 Kcal/mol) for cocrystal structure with benzonitrile (**1-14)** and (-857033.0 Kcal/mol) for cocrystal structure with *o*-difluorobenzene **(1-6)** with a difference of 12.9 Kcal/mol, with the exception of one of the two independent molecules of anisole that have much lower energy (-856858.1 Kcal/mol).

This clear difference in the molecular energy of the host molecule **1** in the structure with anisole than its molecular energy in all the other structures should be the reason why only this structure change to dimorph **1b** after the evaporation of the solvent.

The ET of the optimized structures are nearly the same, the difference between the average value and the maximum and minimum values is 1.8 Kcal/mol. The ET of **1** in the cosolvates is always higher than its energy in the dimorphs. This prove more stability of the molecular structure of **1** in the cosolvates than in the dimorph.

Table 6. Total and binding energy of 1

	Molecular experimental structure		**Optimized structure 1opt**	
	Total Energy (ET)	Binding Energy (EB)	Total Energy (ET)	Binding Energy (EB)
1a1	-856843.9	-4944.7	-857035.8	-5136.6
1a2	-856822.8	-4923.5	-857035.2	-5136.0
1b	-856778.2	-4879.4	-857035.8	-5136.6
1-1 benzene	-857028.1	-5128.9	-857034.8	-5135.6
1-2 ethylbenzene	-857027.8	-5128.5	-857035.1	-5135.8
1-3 cumene	-857028.5	-5129.3	-857035.0	-5135.7
1-4 fluorobenzene	-857028.2	-5129.0	-857034.8	-5135.6
1-5 chlorobenzene	-857025.2	-5126.0	-857035.1	-5135.9
1-6 *o*-difluorobenzene	-857033.0	-5133.8	-857033.8	-5134.5
1-7 *m*-difluorobenzene	-857026.8	-5127.5	-857033.9	-5134.7
1-8 *p*-difluorobenzene	-857028.6	-5129.4	-857035.1	-5135.8
1-9 1,2,4-trifluorobenzene	-857023.6	-5124.4	-857034.1	-5134.8
1-10m1 hexafluorobenzene	-857025.0	-5125.8	-857034.8	-5135.6
1-10m2 hexafluorobenzene	-857024.9	-5125.7	-857034.4	-5135.2
1-11m1 phenol 1	-857026.2	-5127.0	-857035.7	-5136.4
1-11m2 phenol 1	-857026.0	-5126.7	-857035.8	-5136.5
1-12 phenol 2	-857026.1	-5126.8	-857034.7	-5135.5
1-13m1 anisole	-857026.8	-5127.59	-857035.7	-5136.4
1-13m2 anisole	-856858.1	-4958.9	-857035.6	-5136.3
1-14 benzonitrile	-857020.1	-5125.8	-857034.8	-5135.6
1-15 trifluorotoluene	-857022.3	-5123.0	-857034.1	-5134.8
1-16 DMF	-857023.3	-5124.0	-857034.8	-5135.6

	Molecular experimental structure		**Optimized structure 1opt**	
	Total Energy (ET)	Binding Energy (EB)	Total Energy (ET)	Binding Energy (EB)
1-17 hydroquinone	-857026.9	-5127.7	-857035.7	-5136.4
1-18 *p*-xylene 1	-857026.9	-5127.7	-857034.1	-5134.9
1-19 *p*-nitophenol	-857026.3	-5127.1	-857035.6	-5136.4
1-20 *p*-fluorotoluene	-857025.6	-5126.4	-857033.9	-5134.6
1-21 *o*-fluorotoluene	-857027.5	-5128.3	-857033.9	-5134.7
1-22 *p*-chlorofluorobenzene	-857023.9	-5124.7	-857032.2	-5133.0
1-23 *m*-fluoronitrobenzene	-857028.3	-5129.1	-857034.4	-5135.2
1-24 *o*-fluoronitrobenzene	-857027.4	-5128.1	-857035.3	-5136.0
1-25 *p*-fluoronitrobenzene	-857027.3	-5128.0	-857034.7	-5135.5
1-26 nitroethane	-857028.2	-5128.9	-857034.7	-5135.5
1-27 **1-**nitropropane	-857026.5	-5127.3	-857032.8	-5133.6
1-28 benzaldhyde	-857025.7	-5126.4	-857034.7	-5135.5
1-29 dioxene	-857027.1	-5127.8	-857034.7	-5135.5
1-30 γ-picoline 1	-857024.6	-5125.4	-857033.9	-5134.7
1-31 γ-picoline 2	-857023.7	-5124.4	-857034.8	-5135.6
1-32 toluene	-857025.4	-5126.2	-857035.0	-5135.8
1-33 nitrobenzene	-857026.1	-5126.9	-857034.9	-5135.6
1-34 *p*-chlorotoluene	-857029.4	-5130.2	-857035.0	-5135.8
1-35m1 *p*-xylene 2	-857027.1	-5127.9	-857035.7	-5136.4
1-35m2 *p*-xylene 2	-857025.6	-5126.4	-857035.3	-5136.1
1-36 formic acid	-857026.6	-5127.4	-857034.6	-5135.4
1-37 acetic acid	-857025.1	-5125.9	-857034.7	-5135.5
1-39 acetonitrile	-857021.4	-5122.2	-857034.8	-5135.5

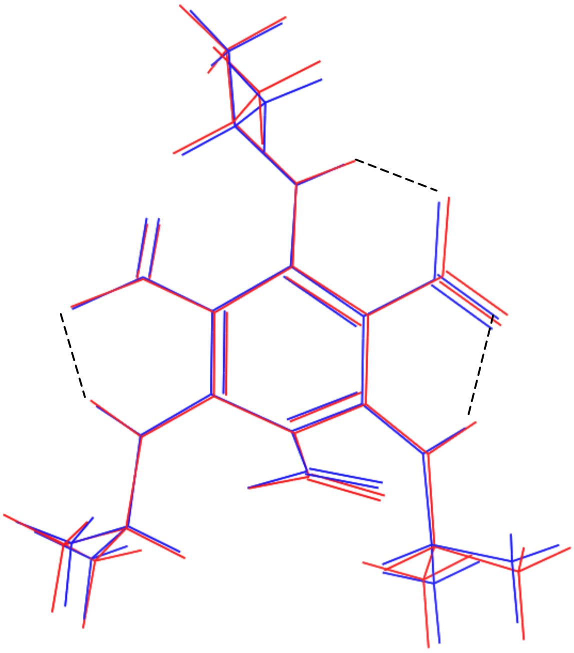

Figure 3-1. 1a1 blue molecule, 1opt red molecule

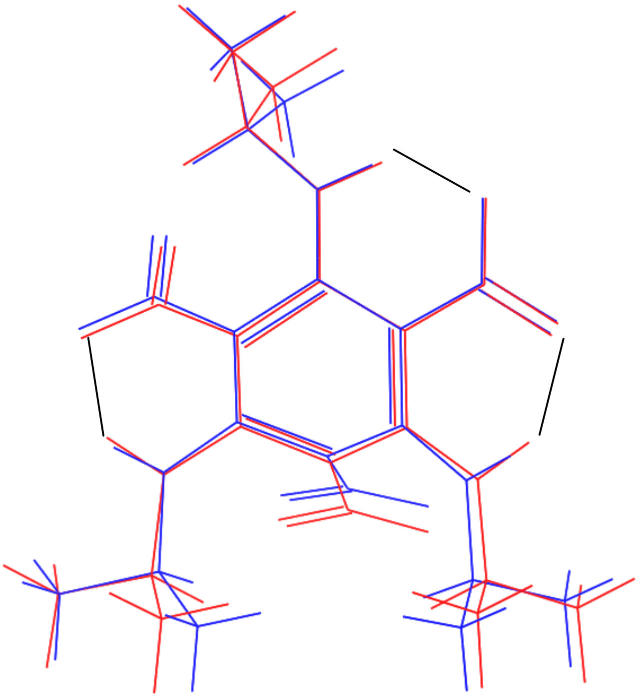

Figure 3-2 . 1a2 blue molecule, 1opt red molecule

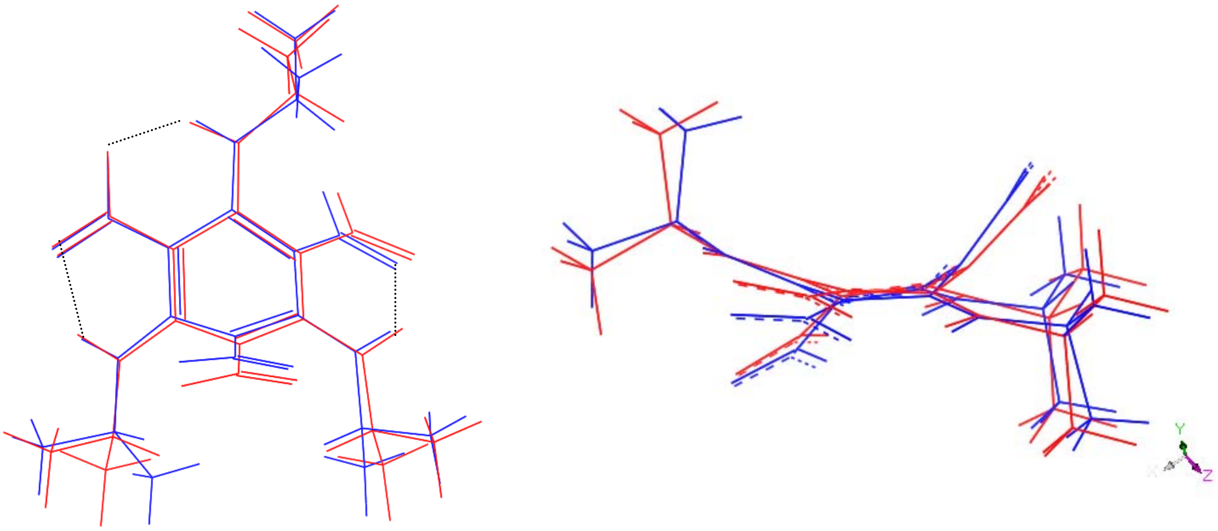

Figure 3-3. 1b blue molecule, 1opt red molecule

3-2-2 Force Field calculations in three dimension (on the crystal level)

Table (7) summarizes the force field calculation results of the crystal energy (EC), total non-bond energy (ENB), Lattice energy (EL), and Lattice energy/molecule (ELM) of the dimorph and the different inclusion structures. High lattice energies per molecule (ELM) (more than 25 Kcal/mol) have been calculated for structures;

- which have intermolecular hydrogen bonds. These structures can be divided into two groups:
    1. structures that have both host-host and host-guest intermolecular hydrogen bonds as structures with: phenol 1 (**1-11**) (ELM= -29.5 Kcal/mol), hydroquinone (**1-17**) (ELM= -32.7 Kcal/mol), DMF (**1-16**) (ELM= -31.9 Kcal/mol), benzaldhyde (**1-28**) (ELM= -28.4 Kcal/mol), acetic acid (**1-37**) (ELM= -33.5 Kcal/mol), and formic acid (**1-36**) (ELM= -32.2 Kcal/mol).
    2. structures that have only host-host intermolecular hydrogen bonds as structures with: anisole (**1-13**) (ELM= -31.4 Kcal/mol), benzonitrile (**1-14**) (ELM= -25.4 Kcal/mol), γ-picoline 2 (**1-31**) (ELM= -30.5 Kcal/mol), and p-xylene 2 (**1-35**) (ELM= -30.7 Kcal/mol).

  It is clear to notice that the first group, which contains both host-host and host-guest intermolecular hydrogen bond, has higher range of ELM (between -28.4 Kcal/mol and -33.5 Kcal/mol) than the second group, which contains only host-host intermolecular hydrogen bond (between –25.4 Kcal/mol and -31.4 Kcal/mol). The reason for the high ELM for structures with anisole and γ-picoline 2 is that in these structures we have more than one (two for anisole and three for γ-picoline 2) host-host intermolecular hydrogen bonds.
- structures with solvates that have methyl group in the para position, as structures with; *p*-chlorotoluene (**1-34**) (ELM= -26.8 Kcal/mol) and *p*-xylenen 1 and 2 (**1-18**) (**1-35**) (ELM= -30.7 and –26.1 Kcal/mol) except with *p*-fluorotoluene (**1-20**) (ELM= -23.5 Kcal/mol).
- structure with nitroethane (1-26) (ELM= -26.2 Kcal/mol), and 1-nitopopane (1-27) (ELM= -28.4 Kcal/mol).

This all results are in a good agreement with the results from (DSC) measurements.

Table 7. Force field calculations results

	Total crystal energy EC Kcal/mol	Total non-bond energy ENB Kcal/mol	Lattice energy EL Kcal/mol	Lattice energy/molecule ELM Kcal/mol
1a	-11188.2	-15159.5	-594.9	-37.2
1b	-5732.3	-6375.6	-260.6	-32.6
1-1 benzene	-2868.2	-3128.0	-161.5	-20.2
1-2 ethylbenzene	-3544.7	-3879.6	-197.4	-24.7
1-3 cumene	-3234.7	-3688.9	-191.5	-23.9
1-4 fluorobenzene	-2926.4	-3197.7	-138.9	-17.4
1-6 *o*-difluorobenzene	-3025.7	-3277.3	-149.3	-18.7
1-7 *m*-difluorobenzene	-3318.8	-3596.9	-150.7	-18.8
1-8 *p*-difluorobenzene	-3622.9	-3897.5	229.3	-28.7
1-9 1,2,4-trifluorobenzene	-3510.4	-3796.8	-176.2	-22.0
1-10 hexafluorobenzene	-7327.6	-7887.0	-362.4	-22.6
1-11 phenol 1	-4315.9	-4597.6	-176.7	-29.5
1-12 phenol 2	-2350.7	-2502.9	-122.7	-20.5
1-13 anisole	-3103.9	-3691.3	-188.3	-31.4
1-14 benzonitrile	-2265.8	-2407.2	-101.8	-25.4
1-15 trifluorotoluene	-3560.5	-3906.0	-178.4	-22.3
1-16 DMF	-1722.8	-1894.9	-127.7	-31.9
1-17 hydroquinone	-2025.9	-2169.9	-98.2	-32.7
1-18 *p*-xylene 1	-3790.9	-4042.4	-209.2	-26.1
1-19 *p*-nitophenol	-1958. 9	-2083. 5	-93.2	-23.3
1-20 *p*-fluorotoluene	-3694.4	-4059.6	-187.6	-23.5
1-21 *o*-fluorotoluene	-2836.4	-3111.2	-175.4	-21.9
1-22 *p*-chlorofluorobenzene	-3862.3	-4194.3	-185.3	-23.2
1-23 *m*-fluoronitrobenzene	-1628.4	-1756.8	-92.4	-23.1
1-24 *o*-fluoronitrobenzene	-4403.8	-4692.3	-196.0	-24.5
1-25 *p*-fluoronitrobenzene	-2144.0	-2271.7	-103.8	-25.9
1-26 nitroethane	-4689.0	-4950.7	-209.4	-26.2
1-27 **1-**nitropropane	-4618.4	-4862.4	-227.3	-28.4
1-28 benzaldhyde	-2321.3	-2456.5	-113.5	-28.4
1-29 dioxene	-2100.4	-2230.7	-100.5	-25.1
1-30 γ-picoline 1	-4119.0	-4396.7	-175.3	-21.9
1-31 γ-picoline 2	-9139.9	-9637.5	-454.6	-30.3
1-32 toluene	-3534.9	-3807.8	-198.6	-24.8
1-33 nitrobenzene	-2247.1	-2449.3	-100.6	-25.1
1-34 *p*-chlorotoluene	-3999.8	-4267.2	-214.4	-26.8
1-35 *p*-xylene 2	-5961.2	-6467.1	-368.1	-30.7
1-36 formic acid	-2452.4	-2613.5	-96.6	-32.2
1-37 acetic acid	-2486.9	-2642.3	-100.4	-33.5
1-39 acetonitrile	-1906.3	-2046.2	-82.4	-20.6

A good test for the reliability of our calculations is to examine how good is the agreement between the theoretical calculated ELM and the experimental measured dissolution energy E_{diss} (DSC measurements). A direct comparison between calculations and experiment can be done for the dimorph, structures with isomeric molecules as inclusion compounds, and different crystals forms with same inclusion compound. Table (8) summarizes these results. The good agreement between experimental results and theoretical calculations is clear.

Table 8. Comparison between the experimental and the theoretical results

Inclusion compound	Dissolution Energy kcal/mol	Lattice energy/molecule Kcal/mol
1a	7.6	-37.2
1b	2.9	-32.6
p-difluorobenzene	12.7	-28.7
o-difluorobenzene	12.0	-18.7
m-difluorobenzene	10.7	-18.8
p-fluorotoluene	15.4	-23.5
o-fluorotoluene	12.2	-21.9
p-fluoronitrobenzene	8.1	-25.9
o-fluoronitrobenzene	3.4	-24.5
m-fluoronitrobenzene	2.5	-23.1
phenol 1	12.7	-29.5
phenol 2	7.8	-20.5
γ-picoline 1	8.6	-21.5
γ-picoline 2	13.4	-30.3
p-xylene 1	5.1	-26.1
p-xylene 2	15.3	-30.7

In the case of structures with *o*- and *m*-difluorobenzene difference between the calculation and the measurements have been found. DSC method measured more energy for structure with *o*-difluorobenzene than the structure with *m*-difluorobenzene, while the calculated values are nearly equal. The disorder in both structures with *o*-difluorobenzene and *m*-difluorobenzene, should be the reason for that difference.

Conclusion 3

- in agreement with the experimental results (conclusions 1 and 2), high ELM have been calculated for structures, which have host-guest intermolecular hydrogen bonds [as structures with phenol 1 (**1-11**), hydroquinone (**1-17**), DMF (**1-16**), benzaldhyde (**1-28**), acetic acid (**1-37**), formic acid (**1-36**)], structures with solvates that have methyl group in the *para* position [as *p*-xylene 1 and 2 (**1-18**) (**1-35**), *p*-chlorotoluene (**1-34),** γ-picoline 2 (**1-31**) except *p*-fluorotoluene (**1-20**)], and structures with benzonitrile (**1-14**), nitroethane (**1-26**), and 1-nitropropane (**1-27**).

- dimorph **1a** is more stable than dimorph **1b**.
- stability of the structures with isomeric inclusion molecules are in the sequence of covolvates with *para* > *ortho* > *meta* substitution pattern.
- If there are more than one structure with the same inclusion molecule, then the close packing structure is always more stable than the other structure.
- high ELM have been calculated for the structures with phenol 1 (**1-11**) and anisole (**1-13**) although the measured dissolution energy are not high. The high ELM calculated energy for these structures comes mainly from the strong host-host interactions, which is not measured by the DSC experiment.

3-2-3 Calculation of intermolecular interactions

Which kind of interaction plays the main role in each structure? To answer this question properly, the interactions energy between the different molecules in each crystal should be examined in detail. This will also help to gain more inside each structure trying to understand more about the factors determining the packing and its influence on the molecular parameters.

Table 9. Intermolecular interactions in the cosolvate structures

Group	Inclusion compound	Molecule	E_{el}	E_{vdw}		$E_{non\text{-}bond}$
				E_{re}	E_{dis}	
Dimorph	**1a**	1a2(0)···1a2(1)	-9.62	13.03	-18.65	-15.24
		1a2(0)···1a1(0)	-0.31	11.20	-19.70	-8.82
		1a2(0)···1a1(1)	-4.53	6.74	-10.55	-8.34
		1a2(0)···1a1(3)	-3.75	10.58	-19.39	-12.56
		1a1(1)···1a1(3)	0.48	9.79	-17.15	-6.88
		1a1(1)···1a1(0)	-4.14	6.65	-12.18	-9.66
		1a1(1)···1a2(2)	-0.36	3.31	-7.17	-4.22
		1a1(1)···1a1(2)	-0.92	0.01	-0.03	-0.96
	1b	1b(0)···1b(1)	-10.31	15.00	-22.15	-17.29
		1b(0)···1b(2)	-4.16	17.14	-28.07	-15.09
		1b(0)···1b(3)	-0.04	2.22	-4.65	-2.03
		1b(0)···1b(5)	0.04	1.50	-4.73	-3.03
		1b(0)···1b(6)	-0.03	4.30	-7.08	-3.35
		1b(2)···1b(7)	-1.75	1.57	-2.88	-3.06
		1b(6)···1b(7)	0.18	1.98	-2.97	-0.82
Group 1 (Cc)	**1-1** benzene	Host(1)···Host(2)	-3.28	7.66	-11.57	-7.18
		Host(1)···Host(3)	-5.32	11.65	-20.51	-14.17
		Host(1)···Guest(1)	0.16	6.39	-10.45	-3.91
		Host(1)···Guest(2)	-0.72	5.63	-9.68	-4.77
		Guest(1)···Guest(2)	0.06	0.49	-1.25	-0.82
	1-2 ethylbenzene	Host(1)···Host(2)	-3.32	5.19	-9.02	-7.27
		Host(1)···Host(3)	-5.64	14.05	-23.69	-15.29
		Host(1)···Guest(1)	-0.21	7.12	-11.94	-4.62
		Host(1)···Guest(2)	-0.78	7.04	-11.36	-5.10
		Guest(1)···Guest(2)	-0.04	0.83	-2.02	-1.24
	1-3 cumene	Host(1)···Host(2)	-2.87	3.96	-7.72	-6.64
		Host(1)···Host(3)	-5.68	13.06	-22.44	-15.05
		Host(1)···Guest(1)	-1.05	6.28	-10.94	-4.74
		Host(1)···Guest(2)	-0.83	9.22	-14.90	-5.89
		Guest(1)···Guest(2)	0.03	1.28	-2.60	-1.36
	1-4 fluorobenzene	Host(1)···Host(2)	-3.47	7.11	-10.98	-7.00
		Host(1)···Host(3)	-5.32	12.08	-20.98	-14.22
		Host(1)···Guest(1)	-0.15	7.03	-11.28	-4.40
		Host(1)···Guest(2)	-0.17	5.69	-9.82	-4.30
		Guest(1)···Guest(2)	-0.56	1.09	-1.84	-1.30
	1-6 *o*-difluorobenzene	Host(1)···Host(2)	-2.83	9.12	-12.04	-5.75
		Host(1)···Host(3)	-4.77	13.73	-21.88	-12.92
		Host(1)···Guest(1)	-0.26	6.50	-11.02	-4.79
		Host(1)···Guest(2)	-0.16	0.00	-0.10	-0.25
		Guest(1)···Guest(2)	0.69	1.69	-2.38	-1.39
	1-7 m-difluorobenzene	Host(1)···Host(2)	-2.99	6.69	-10.55	-6.85
		Host(1)···Host(3)	-5.44	12.45	-21.47	-14.46
		Host(1)···Guest(1)	-1.62	7.59	-12.23	-6.27
		Host(1)···Guest(2)	-0.08	5.36	-9.41	-4.13

Group	Inclusion compound	Molecule	E_{el}	E_{vdw}		$E_{non\text{-}bond}$
				E_{re}	E_{dis}	
		Guest(1)···Guest(2)	-2.82	1.96	-2.34	-0.20
	1-8 *p*-difluorobenzene	Host(1)···Host(2)	-3.11	7.55	-13.25	-8.81
		Host(1)···Host(3)	-5.76	12.21	-22.54	-16.09
		Host(1)···Guest(1)	-1.89	6.02	-14.25	-10.12
		Host(1)···Guest(2)	-0.36	3.53	-8.65	-5.48
		Guest(1)···Guest(2)	-3.58	1.54	-2.55	-4.59
	1-9 1,2,4-trifluorobenzene	Host(1)···Host(2)	-3.18	6.50	-10.35	-7.038
		Host(1)···Host(3)	-5.50	11.91	-21.21	-14.82
		Host(1)···Guest(1)	-0.80	4.42	-8.62	-5.00
		Host(1)···Guest(2)	-1.89	7.63	-12.17	-6.44
		Guest(1)···Guest(2)	-0.64	1.40	-2.37	-1.62
	1-15 trifluorotoluene	Host(1)···Host(2)	-3.13	4.94	-8.84	-7.03
		Host(1)···Host(3)	-5.37	11.43	-20.78	-14.66
		Host(1)···Guest(1)	0.43	7.05	-12.02	-5.12
		Host(1)···Guest(2)	-0.85	6.10	-10.37	-5.63
		Guest(1)···Guest(2)	0.00	1.18	-2.30	-1.13
	1-18 *p*-xylene 1	Host(1)···Host(2)	-3.04	4.79	-8.60	-6.85
		Host(1)···Host(3)	-5.94	15.26	-24.87	-15.55
		Host(1)···Guest(1)	-0.06	1.41	-2.59	-1.23
		Host(1)···Guest(2)	-0.00	0.00	-0.02	0.01
		Guest(1)···Guest(2)	-0.12	1.58	-2.92	-1.46
	1-20 *p*-fluorotoluene	Host(1)···Host(2)	-3.29	5.37	-9.32	-7.24
		Host(1)···Host(3)	-5.62	13.55	-23.24	-15.31
		Host(1)···Guest(1)	-1.36	5.61	-10.39	-6.14
		Host(1)···Guest(2)	0.02	1.93	-2.69	-0.74
		Guest(1)···Guest(2)	0.02	0.49	-1.49	-0.99
	1-21 *o*-fluorotoluene	Host(1)···Host(2)	-2.96	6.13	-10.09	-6.93
		Host(1)···Host(3)	-5.17	11.83	-20.64	-13.97
		Host(1)···Guest(1)	-0.05	8.16	-12.62	-4.51
		Host(1)···Guest(2)	-0.08	0.01	-0.11	-0.18
		Guest(1)···Guest(2)	-0.53	1.92	-3.06	-1.68
	1-22 *p*-chlorofluorobnezene	Host(1)···Host(2)	-3.24	5.57	-9.59	-7.25
		Host(1)···Host(3)	-5.35	13.21	-22.90	-15.17
		Host(1)···Guest(1)	-0.63	1.14	-2.18	-0.91
		Host(1)···Guest(2)	-0.75	0.00	-0.01	-0.01
		Guest(1)···Guest(2)	-0.06	0.55	-2.29	-1.23
	1-30 γ-picoline 1	Host(1)···Host(2)	-3.23	6.49	-10.42	-7.17
		Host(1)···Host(3)	-5.28	11.66	-20.57	-14.19
		Host(1)···Guest(1)	-2.20	8.43	-13.40	-7.18
		Host(1)···Guest(2)	-0.24	5.51	-9.67	-4.40
		Guest(1)···Guest(2)	-0.79	0.92	-1.99	-1.69
	1-32 toluene	Host(1)···Host(2)	-4.39	6.52	-10.23	-8.09
		Host(1)···Host(3)	-6.71	14.85	-24.63	-16.49
		Host(1)···Guest(1)	0.56	7.17	-11.47	-1.93
		Host(1)···Guest(2)	-1.72	7.07	-11.43	-4.54
		Guest(1)···Guest(2)	-0.27	0.89	-1.79	-1.17
	1-34 *p*-chlorotoluene	Host(1)···Host(2)	-3.54	4.56	-8.44	-7.42
		Host(1)···Host(3)	-6.53	13.37	-22.94	-16.10
		Host(1)···Guest(1)	-2.21	6.17	-11.71	-7.74
		Host(1)···Guest(2)	-0.08	8.47	-12.99	-4.44
		Guest(1)···Guest(2)	-0.11	1.72	-3.19	-1.59
Group 2 Subgroup 2-1	**1-14** benzonitrile	Host(1)···Host(2)	-5.590	18.91	-31.13	-17.20
		Host(2)···Host(3)	-2.12	5.20	-8.09	-5.02
		Host(1)···Guest(1)	-2.12	3.37	-5.57	-4.32
		Host(1)···Guest(2)	-1.57	6.84	-11.96	-6.70
		Guest(1)···Guest(2)	-1.39	5.34	-8.86	-4.92

Group	Inclusion compound	Molecule	E_{el}	E_{vdw}		$E_{non\text{-}bond}$
				E_{re}	E_{dis}	
	1-28 benzaldhyde	Host(1)···Host(2)	-6.86	22.54	-33.74	-18.05
		Host(2)···Host(3)	-2.73	4.50	-7.58	-5.80
		Host(3)···Guest(1)	-3.09	4.91	-7.16	-5.34
		Host(1)···Guest(2)	-0.51	0.75	-1.82	-1.58
		Guest(1)···Guest(2)	0.49	2.75	-5.82	-3.55
	1-29 dioxane	Host(1)···Host(2)	-6.45	16.54	-27.91	-17.88
		Host(2)···Host(3)	-2.30	6.97	-10.09	-5.48
		Host(2)···Guest(1)	-1.99	4.76	-13.32	-1.99
		Host(2)···Guest(2)	-2.82	2.78	-2.07	-2.11
	1-33 nitrobenzene	Host(1)···Host(2)	-5.69	18.96	-31.13	-17.92
		Host(2)···Host(3)	-5.28	5.14	-7.97	-8.11
		Host(3)···Guest(1)	-2.77	3.05	-5.00	-4.71
		Host(1)···Guest(2)	0.45	1.01	-2.32	-0.86
		Guest(1)···Guest(2)	-0.63	0.14	-0.58	-0.19
	1-16 DMF	Host(1)···Host(2)	-6.21	17.69	-29.58	-18.10
		Host(2)···Host(3)	-3.92	6.50	-9.60	-7.01
		Host(2)···Guest(2)m1	-8.46	7.83	-9.62	-10.25
		Host(2)···Guest(1)m2	-3.11	13.58	-16.88	-6.42
		Guest(2)m1···Guest(2)m2	-4.06	7.64	-11.16	-7.59
	1-17 hydrochinon	Host(1)···Host(2)	-5.48	18.32	-29.65	-16.80
		Host(2)···Host(3)	-4.89	6.70	-9.76	-7.58
		Host(3)···Host(4)	-4.70	9.73	-19.33	-13.93
		Host(3)···Guest(1)	-6.60	5.75	-7.78	-8.63
		Host(1)···Guest(1)	-2.68	9.51	-13.38	-6.56
	1-19 *p*-nitrophenol	Host(1)···Host(2)	-5.26	16.26	-28.41	-17.45
		Host(2)···Host(3)	-3.77	4.75	-7.51	-6.40
		Host(3)···Host(4)	-2.17	9.21	-14.71	-7.71
		Host(3)···Guest(1)	-8.60	3.08	-4.46	-9.98
		Host(1)···Guest(2)	-0.84	7.96	-11.73	-4.62
		Guest(1)···Guest(2)	-2.22	5.62	-9.42	-6.02
	1-25 *p*-fluoronitrobenzene	Host(1)···Host(2)	-4.92	17.84	-30.01	-17.10
		Host(2)···Host(3)	-1.23	4.74	-7.43	-3.93
		Host(3)···Host(4)	-2.15	10.61	-16.88	-8.43
		Host(3)···Guest(1)	0.52	0.14	-1.05	-1.43
		Host(1)···Guest(2)	-2.57	3.43	-5.16	-4.30
		Guest(1)···Guest(2)	-0.93	6.07	-9.88	-4.75
Group 2 Subgroup 2-2	**1-11** phenol 1	Host(1)m1···Host(1)m2	-3.94	6.08	-9.20	-7.06
		Host(1)m1···Host(3)m1	-2.20	0.15	-1.14	-3.18
		Host(1)m1···Host(2)m2	1.53	2.69	-4.96	-1.06
		Host(1)m2···Guest(1)	-7.78	5.87	-7.67	-9.58
	1-23 *m*-fluoronitrobenzene	Host(1)···Host(2)	-4.10	6.47	-9.74	-7.36
		Host(1)···Host(3)	0.86	2.20	-4.52	-1.46
		Host(1)···Guest(1)	-1.94	9.35	-14.86	-7.46
		Host(1)···Guest(3)	-3.89	3.86	-6.17	-6.20
		Guest(1)···Guest(2)	-0.87	3.24	-6.91	-4.54
	1-39 acetonitrile	Host(1)···Host(2)	-4.50	5.65	-8.83	-7.72
		Host(1)···Host(3)	-5.00	12.61	-21.55	-13.77
		Host(1)···Guest(1)	-0.32	4.33	-6.74	-2.79
		Host(1)···Guest(3)	-2.12	6.47	-9.92	-5.57
		Guest(1)···Guest(2)	-3.86	2.92	-3.81	-4.75
	1-37 acetic acid	Host(1)···Host(2)	-3.52	5.96	-9.05	-6.61
		Host(1)···Host(3)	-5.24	14.72	-26.00	-16.44
		Host(1)···Guest(1)	-4.35	9.34	-11.81	-6.82
		Host(1)···Guest(3)	-6.13	2.77	-3.71	-7.07
		Guest(1)···Guest(2)	-1.50	5.81	-7.07	-2.66
	1-36 formic acid	Host(1)···Host(2)	-4.94	6.21	-9.25	-7.99

Group	Inclusion compound	Molecule	E_{el}	E_{vdw}		$E_{non\text{-}bond}$
				E_{re}	E_{dis}	
		Host(1)···Host(3)	-3.29	11.47	-21.99	-13.62
		Host(1)···Guest(1)	-2.52	6.70	-8.92	-4.73
		Host(1)···Guest(3)	-8.67	3.39	-3.94	-9.21
		Guest(1)···Guest(2)	0.03	0.00	-0.03	0.00
Group 2 Subgroup 2-3	**1-13** anisole	Host(1)m2···Host(2)m2	-5.25	6.92	-10.22	-8.55
		Host(1)m1···Host(2)m1	-3.90	13.23	-25.23	-15.90
		Host(2)m1···Host(1)m2	-0.37	6.18	-11.91	-6.11
		Host(1)m2···Host(3)m1	-2.85	8.35	-15.34	-9.84
		Host(1)m2···Guest(2)	-2.19	11.46	-16.29	-7.02
		Host(1)···Guest(1)	-0.12	1.76	-3.71	-2.07
		Guest(1)···Guest(3)	-0.49	0.10	-0.63	-1.02
Group 3	**1-10** hexafluorobenzene	Host(1)m2···Host(2)m1	-6.68	11.37	-18.02	-13.33
		Host(1)m2···Host(3)m1	-0.29	1.34	-3.24	-1.62
		Host(2)m1···Guest(1)m1	-2.40	6.15	-11.17	-7.42
		Guest(1)m1···Guest(2)m1	-0.37	0.03	-0.28	-0.62
	1-12 phenol 2	Host(1)···Host(2)	-5.28	6.09	-9.31	-8.48
		Host(1)···Host(3)	-3.19	4.69	-12.77	-10.86
		Host(1)···Guest(1)m1	-1.52	7.63	-11.59	-5.48
		Host(3)···Guest(1)m1	-6.82	5.20	-6.59	-8.23
		Guest(1)m1···Guest(1)m2	-4.68	2.59	-4.86	-4.94
	1-24 *o*-fluoronitrobenzene	Host(1)···Host(2)	-7.27	12.53	-19.19	-13.92
		Host(1)···Host(3)	0.91	0.90	-2.64	-0.83
		Host(1)···Guest(2)	0.31	3.88	-6.70	-2.31
		Host(2)···Guest(2)	-3.31	8.96	-13.85	-8.00
	1-26 nitroethane	Host(1)···Host(3)	-5.60	19.89	-31.53	-17.23
		Host(1)···Host(2)	-7.80	12.60	-18.54	-14.01
		Host(1)···Guest(1)	-4.69	6.94	-9.94	-7.70
		Host(1)···Guest(2)	-1.22	1.81	-3.37	-2.78
		Guest(1)···Guest(2)	-0.70	0.06	-0.25	-0.89
	1-27 1-nitropropane	Host(1)···Host(3)	-5.16	19.42	-31.31	-17.05
		Host(1)···Host(2)	-7.21	13.57	-20.15	-13.80
		Host(1)···Guest(1)	0.87	2.63	-3.94	-0.44
		Host(1)···Guest(2)	-1.04	1.31	-2.13	-1.85
		Guest(1)···Guest(2)	-0.91	0.41	-0.80	-1.30
	1-35 *p*-xylene 2	Host(1)m2···Host(1)m1	-5.99	8.16	-11.58	-9.41
		Host(1)m2···Host(2)m1	-6.49	10.98	-18.99	-14.88
		Host(1)m1···Host(3)m1	-2.56	7.84	-13.36	-8.07
		Host(1)m2···Guest(1)	-0.11	0.74	-2.21	-1.58
Group 4	**1-31** γ-picoline 2	Host(1)···Host(2)	-5.31	9.91	-15.28	-10.67
		Host(1)···Host(3)	-9.90	13.31	-19.56	-16.34
		Host(1)···Guest(1)m2	-.94	6.91	-12.35	-0.51
		Guest(1)m1···Guest(1)m2	0.66	2.53	-4.52	-1.33

For structures that have disorder, the values in Table 9 have been calculated by taking the average of two calculations, in each we have considered only one disorder position.

(I)- *For crystal form **1a**:* the largest intermolecular interaction is between the molecules **1a2(0)···1a2(1)** (Figure 3-4) at –15.24 Kcal/mol (Table 9), which also has the largest electrostatic interaction (-9.62 Kcal/mol) in the crystal. The largest component of this interaction energy is the dispersion interaction (-18.65 Kcal/mol), but the net van der Waals interaction

(E_{re}+E_{dis} = -5.62 Kcal/mol) is smaller than the electrostatic interaction. This interaction can be attributed to the intermolecular hydrogen bond (blue line) between these two molecules. The contribution of the hydrogen bond in the intermolecular interaction is mainly of electrostatic type, but it has a considerable contribution in the van der Waals interaction as well.

The second largest intermolecular interaction energy in this crystal is calculated for the **1a2(0)**···**1a1(3)** pair (Figure 3-4) at -12.56 Kcal/mol (Table 9). The major component of this interaction is again the dispersion term (-19.39 Kcal/mol), and the net van der Waals interaction (E_{re}+E_{dis} = -8.81 Kcal/mol) is higher than the electrostatic interaction (-3.75 Kcal/mol). This can be attributed to the many close contact between the methyl groups and the methyl···nitro groups of both molecules, such as the close contact between a methyl group of **1a1(3)** and two different methyl groups **1a2(0)** ($H_3C\cdots CH_3$ = 4.0 Å and 4.05 Å). In addition to another close contact between a methyl group of **1a1(3)** and a nitro group of **1a2(0)** ($H_3C\cdots N$ = 3.35 Å)

The largest intermolecular dispersion interaction energy in this crystal is calculated for the **1a2(0)**···**1a1(0)** pair (the two independent molecules) at -19.70 Kcal/mol (Table 9). This can be attributed to the many close contact between the methyl groups and the methyl···nitro groups of both molecules, such as the close contact between a methyl group of **1a2(0)** and an isopropylamino group of **1a1(0)** ($H_3C\cdots CH_3$ = 4.11 Å and $H_3C\cdots NH$ =4.02 Å), in addition to a close contact between another methyl group of **1a1(0)** and a nitro group of **1a2(0)** ($H_3C\cdots N$ = 4.17 Å).

We can conclude that, for packing **1a**, the interactions between the molecules **1a2** that are connected with intermolecular hydrogen bonds are stabilized with electrostatic interactions, this molecules are laying perpendicular to each other, while the interactions between the two independent molecules **1a1** and **1a2** are stabilized with dispersion interactions, this molecules are laying parallel to each others. The parallel orientation of these molecules to each other gives chance for many methyl···methyl or methyl nitro groups interactions, or in other words, because of the nature of the molecular conformations of molecule **1**, the parallel orientation of these molecules to each others is preferable because of the many methyl…methyl or methyl nitro groups interactions

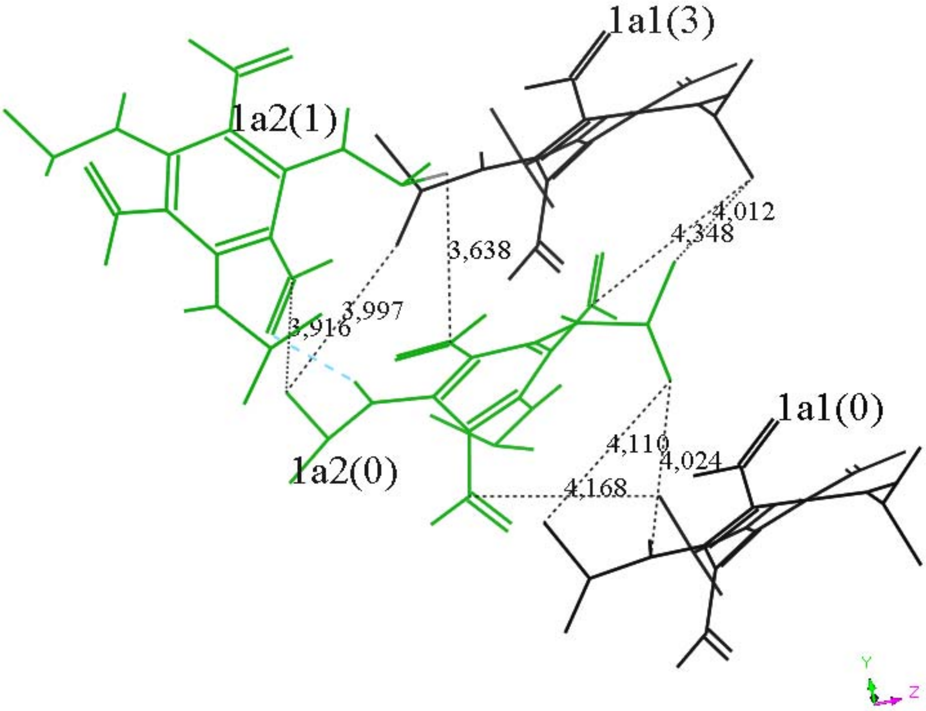

Figure 3-4. Intermolecular interactions in 1a

(II)- *For crystal form **1b**:* the largest interaction is between the molecules **1b(0)**···**1b(1)** (Figure 3-5) at –17.29 Kcal/mol (Table 9), which also has the largest electrostatic interaction (-10.31 Kcal/mol) in the crystal. Again the largest component of the interaction energy is the dispersion interaction (-22.15 Kcal/mol), but the net van der Waals interaction ($E_{re}+E_{dis}$ = -7.15 Kcal/mol) is smaller than the electrostatic interaction. Both interactions can be attributed largely to the two symmetry equivalent hydrogen bonds, (Figure 3-5). The second largest interaction energy is calculated for the **1b(0)**···**1b(2)** pair (Figure 3-5) (-15.09 Kcal/mol) (Table 9). The major component of this interaction is the dispersion term (-28.07 Kcal/mol), which is the largest dispersion interaction between all the pairs in the crystal and this can be attributed to the many close contact between the methyl groups, methyl···nitro and nitro···nitro groups of both molecules, such as the close contact between a methyl group of **1b(2)** and two methyl groups of **1b(0)** ($H_3C\cdots CH_3$ = 3.78 Å and 4.30 Å). In addition to the close contact between a methyl group of **1b(0)** and a nitro group of **1b(2)** ($H_3C\cdots N$ = 4.43 Å) and another close contact between two nitro groups (**1b(0)**N···O**1b(2)** = 3.45 Å, and 3.18 Å). All these interactions can be found twice because of the symmetry equivalence.

Studying the packing **1b** we can see that there are only two strong interactions in the crystal, all the other interactions are relatively small. One of this strong interaction is between the dimer (two neighbouring molecules that are connected with intermolecular hydrogen bonds), these are stabilized with electrostatic interactions and the second one between the different dimers of molecules which are stabilized with dispersion interactions.

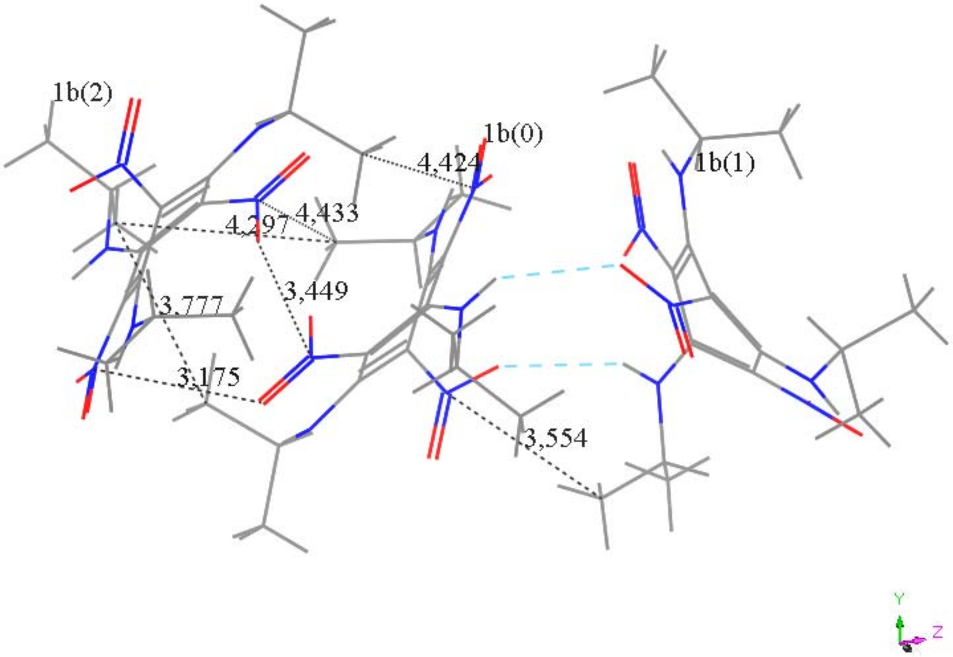

Figure 3-5. Intermolecular interactions in 1b

(III)- *For the first group (group 1) of the inclusion crystals,* in which no intermolecular hydrogen bond has been found, the largest interaction (between –12.92 Kcal/mo for the structure with *o*-difluorobenzene (**1-6**) and –16.49 Kcal/mol for the structure with toluene (**1-32**)), in all inclusion crystals of this group is between Host(1)···Host(3) (Table 9). The largest component of this interaction energy is the dispersion interaction. This can be attributed to the many close contact between the methyl···nitro groups and nitro···nitro groups of both molecules, such as the close contact (O···C ≈ 3.8 Å) between a nitro group of Host(1) and a methyl group of Host (3), in addition to another close contact between two nitro groups (N···O ≈ 3.32 Å), (Figure 3-6).

The second largest interaction energy (between –5.75 Kcal/mo for the structure with *o*-difluorobenzene (**1-6**) and –8.81 Kcal/mol for the structure with *p*-difluorobenzene (**1-8**)), between the host molecules in all inclusion crystal of this group, is calculated for

Host(1)···Host(2), again the largest component of the interaction energy is the dispersion interaction. This can be attributed to the many close contact between the methyl groups and the methyl…nitro groups of both molecules, such as the close contact between two methyl groups (C···C ≈ 3.7 Å), (Figure 3-6), in addition to another close contact between methyl group of Host (2) and nitro group of Host (2) (H3C…N = 3.96 Å).

Strong host-guest and guest-guest interactions have been calculated for structure with *p*-difluorobenzene (**1-8**). This explains why this structure is more stable than the structures with *m*- and *o*-difluorobenzene (**1-7**) and (**1-6**). On the other hand, very weak host-host and host-guest intermolecular interactions have been calculated for the structure with *p*-xylene 1 (**1-18**). This explain why this structure is less stable than the structure with *p*-yxlene 2 (**1-35**).

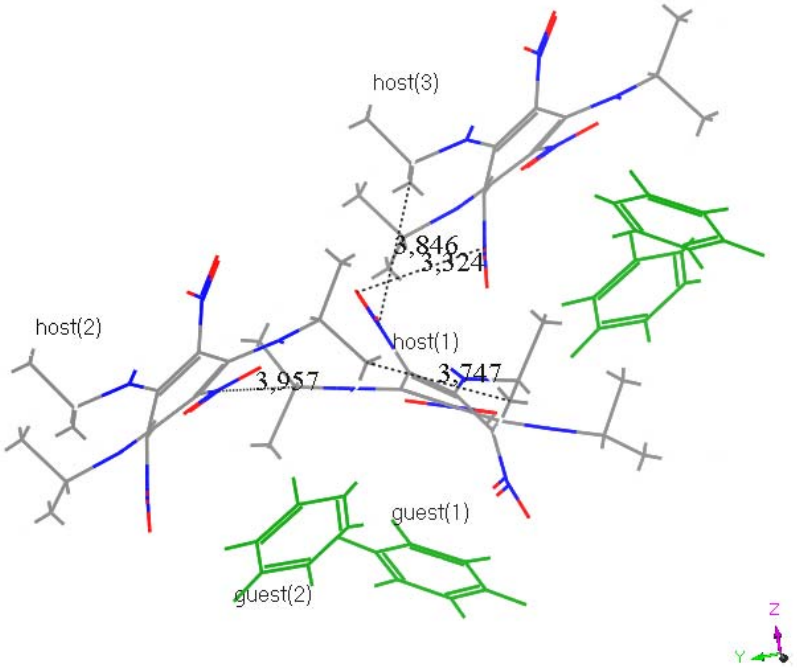

Figure 3-6. intermolecular interactions in structure with fluorobenzene 1-4

(**IV**)- *For the subgroup 2-1 of the inclusion crystals*, the largest interaction (between –16.80 Kcal/mo for the structure with hydroquinone (**1-17**) and –18.10 Kcal/mol for the structure with DMF (**1-16**)) is between the host molecules Host(1)···Host(2) (Table 9). The largest component of this interaction energy is the dispersion interaction. This high interaction can be attributed to the many close contact between the methyl groups and the methyl…nitro groups of both molecules, such as the close contact between the oxygen of nitro group and a methyl group (O···C ≈ 3.5 Å), in addition to another close contact between two methyl groups (C···C ≈ 4.35 Å) (Figure 3-7).

The second largest interaction energy (between –3.93 Kcal/mo for the structure with *p*-fluoronitrobenzene (**1-25**) and –8.11 Kcal/mol for the structure with nitrobenzene (**1-33**)) between the host molecules for the first five structures in this group is calculated for Host(2)···Host(3), while the third largest interaction for the structures with hydroquinone (**1-17**), *p*-nitrophenol (**1-19**) and *p*-fluoronitrobenzene (**1-25**). The largest component of this interaction energy is the dispersion interaction, but the net van der Waals interaction is smaller than the electrostatic one, which is expected because of the intermolecular hydrogen bonds between these two molecules.

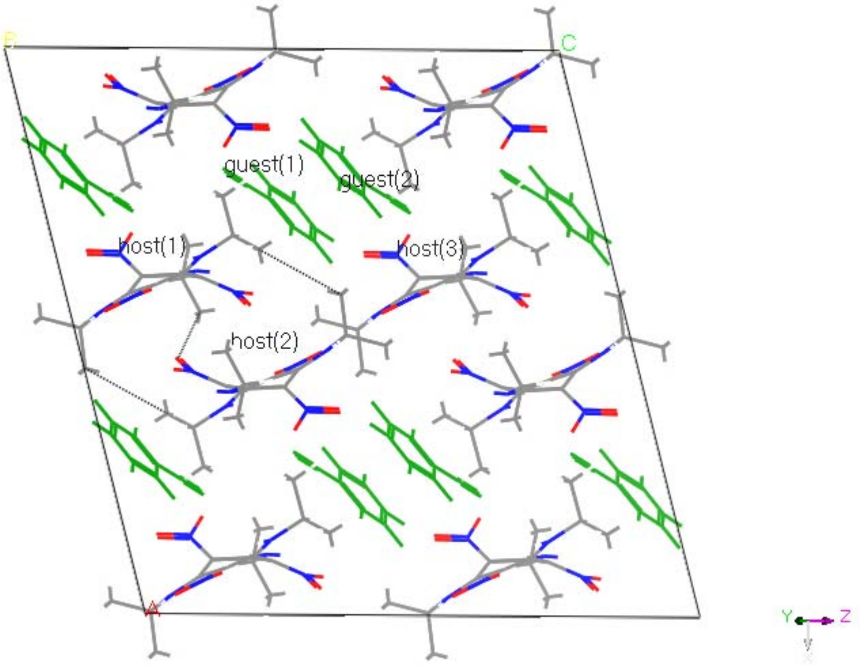

Figure 3-7. Intermolecular interactions in the structure with benzonitrile 1-14

Although these two molecules (Host(2)…Host(3)) are, in most of the cases, connected with two intermolecular hydrogen bonds, the interaction between them is not the strongest interaction in the crystal. The reason for that is the intermolecular hydrogen bonds between these two molecules are of week type, their length (NH···O) range between 3.20 Å and 3.43 Å.

The second largest interaction energy between the host molecules for structures with hydroquinone (1-17), p-nitrophenol (1-19) and p-fluoronitrobenzene (1-25) is between Host(3)···Host(4) (Table 9). These two molecules lie in two different layers; the parallel orientation of the guest molecules to the host molecules in these structures gives chance for stronger interactions between the different layers of host molecules.

The strong host-guest and guest-guest interactions for the structures in this group, except the structure with dioxane (**1-29**), explain the stability of these structures.

(**V**)- *In the subgroup 2-2 of inclusion crystals,* for both structures with phenol (**1-11**) and *m*-fluoronitrobenzene (**1-23**) only one strong interaction between the host molecules has been found. This is between the dimer that are connected with double hydrogen bonds (Host(1)m1···Host(1)m2 for phenol and Host(1)···Host(2) for *m*-fluoronitrobenzene). This interaction can be attributed to the hydrogen bonds between the two molecules. For the other three structures of this group there are two large interactions between the host molecules. The largest interaction is between Host(1)···Host(2) (Table 9), the largest component of this interaction energy is the dispersion interaction. This strong interaction can be attributed to the many close contact between the methyl groups and the methyl···nitro groups of both molecules, such as the close contact (O···C ≈ 3.3 Å) between a nitro group and a methyl group, in addition to another close contact between two methyl groups (C···C ≈ 3.9 Å).

The second largest interaction energy between the host molecules is calculated for Host(2)···Host(3). The largest component of this interaction energy is the dispersion interaction, but the net van der Waals interaction is smaller than the electrostatic interaction, this interaction can be attributed to the intermolecular hydrogen bonds between these two molecules.

(**VI**)- *For structure with anisole subgroup 2-3,* four large interactions between the host molecules have been found. The largest interaction is between Host(1)m···Host(2)m1 (Table 9), the largest component of this interaction energy is the dispersion interaction. There is no intermolecular hydrogen bond between these two molecules. This strong interaction can be attributed to the close contact (O···C ≈ 3.7 Å) between a nitro group and a methyl group, in addition to another close contact between two methyl groups (C···C ≈ 4.2 Å) (Figure 3-8).

(**VII**)- *For the group 3*; the largest interaction is between Host(1)m2…Host(2)m1 for the structure with hexafluorobenzene (**1-10**) and *p*-xylene 2 (**1-35**), while between Host(1)···Host(3) for the other structures (Table 9), except for structure with *o*-fluoronitrobenzene, the largest component of this interaction energy is the dispersion interaction, which again can be contributed to the close contact (O···C ≈ 3.5 Å) between a nitro group and a methyl group, in addition to another close contact between two methyl groups (C···C ≈ 4 Å) (Figure 3-9).

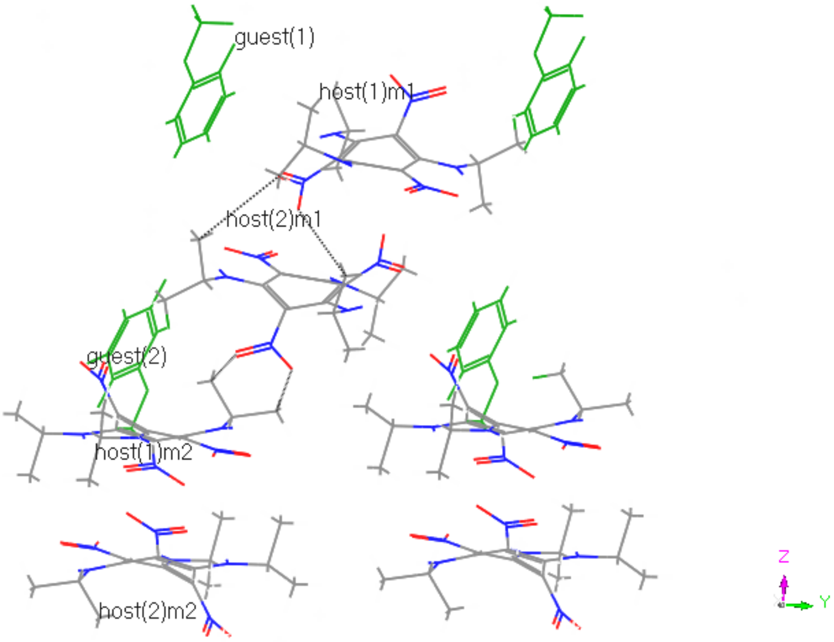

Figure 3-8. Intermolecular interactions in the structure with anisole 1-13

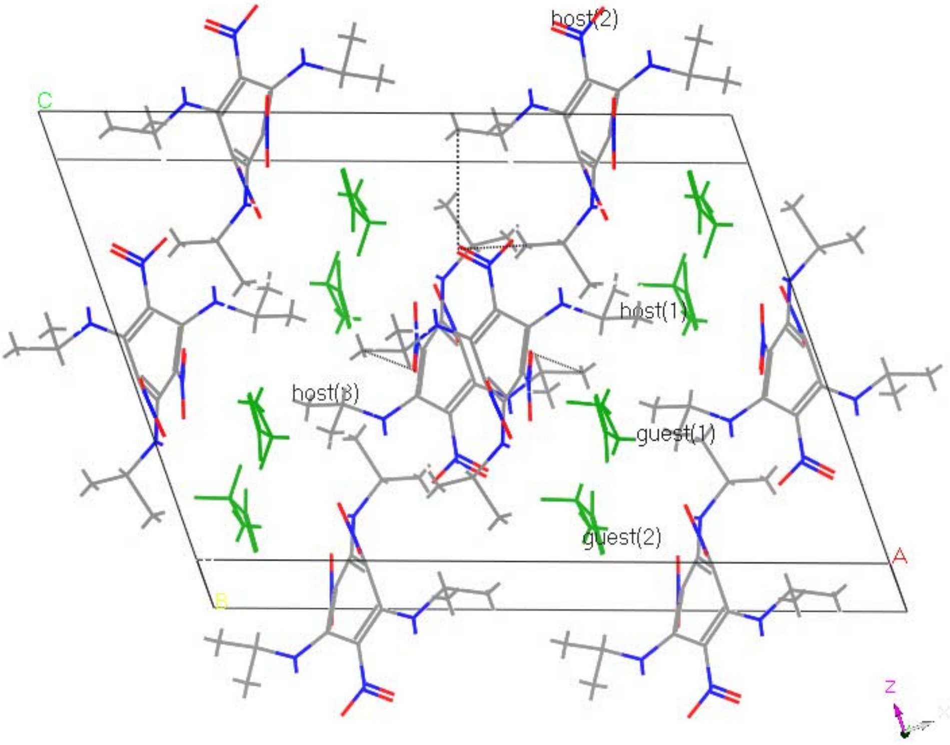

Figure 3-9. Intermolecular interactions in the structure with nitroethane 1-26

In general we can conclude that:

- in the structures without solvent (the dimorphs) the largest interaction in the crystal has been calculated to be between the pair of molecules that connected with intermolecular hydrogen bond. The length of the hydrogen bonds in these cases are 2.97 Å for **1a** and 3.16 Å for **1b**.

- for the cosolvate structures in group 2, there are a dimer (two neighbouring molecules that are connected with intermolecular hydrogen bonds) or a pair (two neighbouring molecules sitting in the analogue position as the dimer but not connected with intermolecular hydrogen bonds) character structures of the host molecules. The largest interaction has been calculated to be between the host molecules of different dimers or pairs, which are not connected with intermolecular hydrogen bonds. This is because the intermolecular hydrogen bonds within the dimer are of week type, their lengths (NH—O) range between 3.20 Å and 3.43 Å. On the other hand, strong dispersion interactions in addition to a considerable electrostatic interactions, have been calculated between the molecules of the different dimers or pairs, which can be attributed to the many close contacts between the methyl···methyl, nitro···methyl and nitro···nitro groups of these molecules. The nitro group free of intramolecular hydrogen bond and the methyl groups of the neighbouring isopropylamino groups are generally the groups that responsible for this interaction.
- the twist or the twisted boat six-membered ring conformations of the host **1**, which are the forms adopted by **1** in the most cosolvates structures, are very suitable for the generation of many van der Waals interactions between the different layers within the packing patterns of our cosolvates structures.

Now we can explain why high ELM has been calculated for structure with nitropropane although the measured dissolution energy of the solvent was not so high (Table 5). This is because, as we can see in table 9, the host- guest intermolecular interactions are very week for this structure. The high ELM calculated energy for this structure comes mainly from the strong host-host interactions, which is not measure by the DSC experiment.

4 Deprotonated structures

4-1 Discussion of the packing

Several attempts to get inclusion structures of 2,4,6-tris(cyclopropylamino)-1,3,5-trinitrobenzenes (**2**), 2,4,6-tris(t-butylamino)-1,3,5-trinitrobenzenes (**3**), and 2,4,6-tris(2-butyllamino)-1,3,5-trinitrobenzenes (**4**), have been done. No inclusion structures with these molecules could be found, but deprotonated structures with isopropylamine and/or t-butylamine (Scheme 4-1), which could be established as a general phenomenon for non-planar 2,4,6-tris-monoalkylamino-1,3,5-trinitrobenznenes. In the deprotonated structure of the host, one hydrogen atom of the three amine groups leaves its group and is transfered to the amine group of the guest forming negatively charged host molecules and positively charged inclusion molecules.

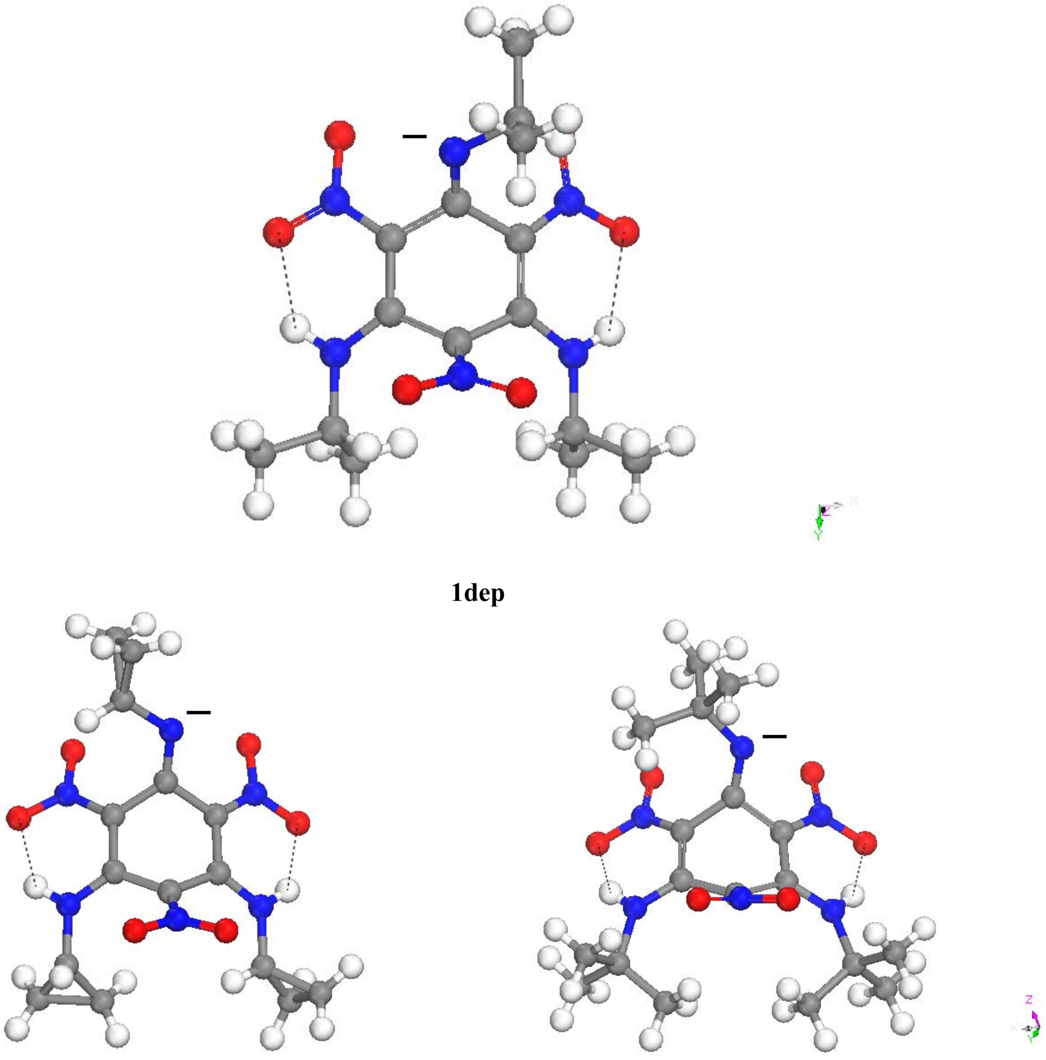

1dep

2dep **3dep**

Figure 4-1. Molecular structure of 1dep, 2dep and 3dep

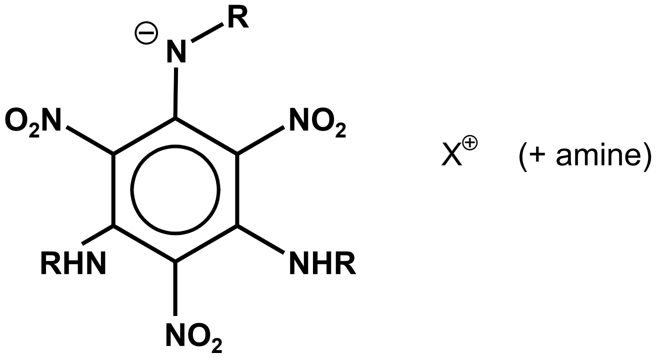

scheme 4-1. 1 dep 1: R = ^{i}Pr; x = (^{i}Pr)$_2$NH$_2^+$; 2 × (^{i}Pr)$_2$NH,
1 dep 2: R = ^{i}Pr; x = (^{i}Pr)$_2$NH$_2^+$,
1 dep 3: R = ^{i}Pr; x = (^{t}Bu)NH$_3^+$,
2 dep 1: R = cyclopropyl; x = (^{t}Bu)NH$_3^+$,
3 dep 1: R = (^{t}Bu)NH$_2$; x = (^{t}Bu)NH$_3^+$; 4 × (^{t}Bu)NH$_2$

A new deprotonated (dep) structure of 2,4,6-tris(isopropylamino)-1,3,5-trinitrobenzenes, **1dep** (Figure 4-1), with isopropylamine has been found **1dep-1**. This structure adopt the space group P-1, Figure (4-2) shows its packing arrangement. In this packing type dimer character of the host molecules has been found (each two host molecules are connected with two intermolecular hydrogen bonds forming with the intramolecular hydrogen bonds a square or parallelogram form). Each host molecule is connected with hydrogen bonds with two guest molecules. A stable unit, of two host molecules and four guest molecules, is then repeated in both b and c directions.

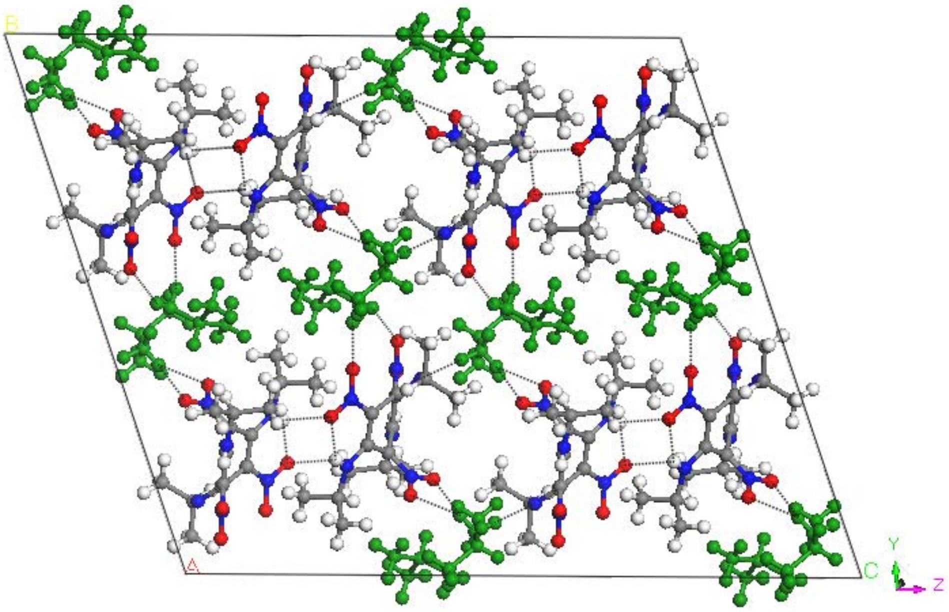

Figure 4-2.The packing arrangement of (1 dep-1)

Additionally, new refinement of the known structures with isoproplyamine[45] **1dep-2,** and t-butylamine **1dep-3**, have been done, which proved these two structures to be deprotonated as well.

The deprotonated structure of 2,4,6-tris(cyclopropylamino)-1,3,5-trinitrobenzenes **2dep** (Figure 4-1) with t-butylamine **2dep-1**, has been found to adopt the space group P2$_1$/c, Figure (4-3). Here we have a layer structure perpendicular to c direction. In each layer the guest molecules are connected with the host molecules through hydrogen bonds.

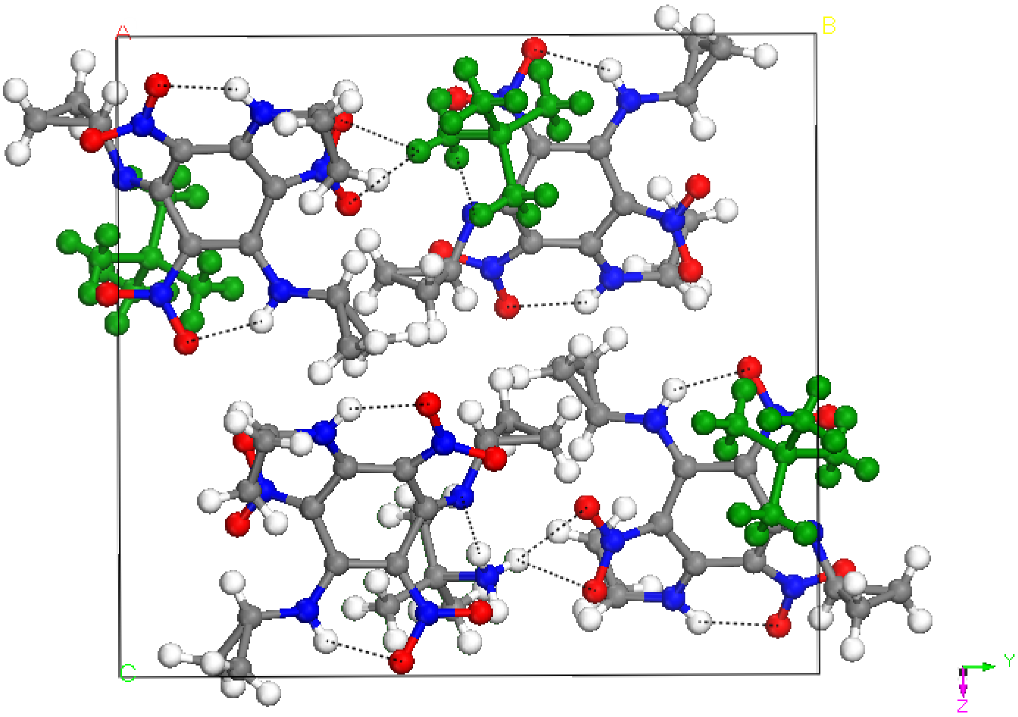

Figure 4-3.The packing arrangement of (2dep-1)

The structure of 2,4,6-tris(t-butylamino)-1,3,5-trinitrobenzenes **3dep** with t-butylamine **3dep-1**, has been found to adopt the space group P-1, Figure (4-4). Here there are a chain character of hydrogen bonds system running in the b direction. In the chain both host and guest molecules are connected by hydrogen bonds.

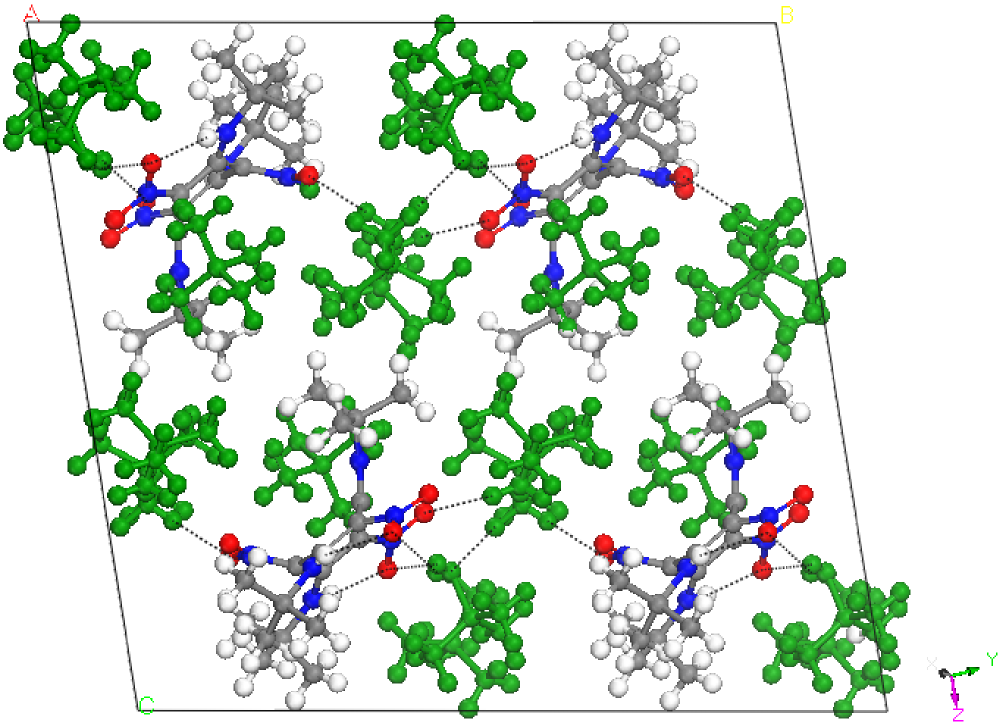

Figure 4-4.The packing arrangement of (3dep-1)

In this structure every host molecule is enclosed with guest molecules, the host: guest ratio is 1 host molecule: 5 guest molecules. One can even look at this structure as a structure of t-butylamine with 2,4,6-tris(t-butylamino)-1,3,5-trinitrobenzenes as inclusion molecule.

4-2 Ring conformation

The calculated ring conformations of all the deprotonated structures are summarized in Table 10.

Table 10. Six membered ring conformation

Inclusion Compound	**Twist form**	**Boat form**	$\sum\lvert_{\text{Tors}}\rvert$ [°]	**Q / θ [°] / P_2 [°]**	**$\Delta(P_2)$ from ideal form**
1dep.-1		☒	180.4	0.74 / -85.2 / 91.8	1.8
1dep.-2		☒	160.9	0.78 / -87.2 / 32.5	2.5
1dep.-3		☒	164.1	0.68 / -85.8 / 92.0	2.0
2dep.-1		☒	193.9	0.76 / -75.6 / 90.5	0.5
3dep.1		☒	162.6	0.67 / -85.1 / 91.0	1.0

All the deprotonated molecules have been found to adopt nearly ideal boat form (Table 10, Figure 4-5). The absent of the third intermolecular hydrogen bond gives more freedom for the ring to adapt the boat conformation.

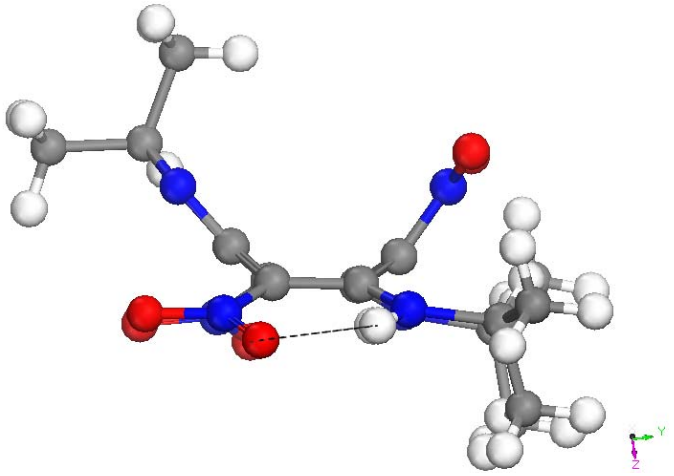

1dep

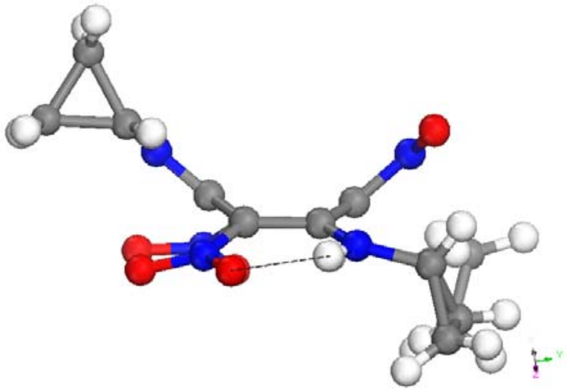

2dep

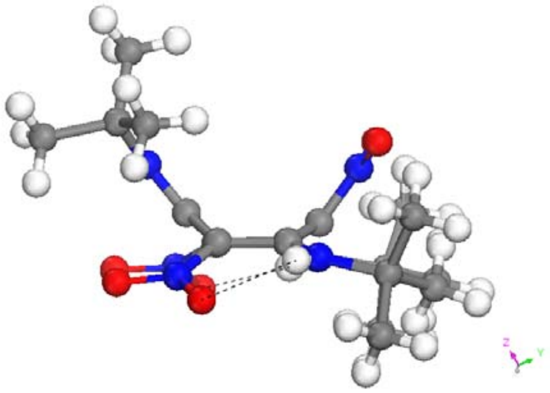

3dep

Figure 4-5. Ring conformation of 1dep, 2dep and 3dep

The average of the two short (C—C short)$_{ave}$ and the four long (C—C long)$_{ave}$ bonds in the ring for the structures **1dep-1**, **2dep-1** and **3dep-**1 are given in Table 11.

Table 11. The average C—C bond lengths in ring of 1dep-1, 2dep-1 and 3dep-1

	1dep-1	**2dep-1**	**3dep-1**
(C—C short)$_{ave}$/ (C—C long)$_{ave}$	1.400/1.484	1.419/1.483	1.420/1.469

It is clear to notice the high difference between (C—C short)$_{ave}$ and (C—C long)$_{ave}$. Additionally, the bond lengths between the carbon atoms in the ring and the nitrogen atoms (C$_{ring}$—N) show the formation of two shorter bond lengths (between C_2—N_2 & C_5—N_5 for 1dep-1 and 3dep-1, and between C_3—N_3 & C_6—N_6 for 2dep-1). These results prove the formation of the quinonoid form in these structures.

5 Synthesis and X-ray structure analysis of 2,4,6-tris(2(S)-butylamino)-1,3,5-trinitrobenzenes

5-1 Synthesis

5-1-1 Synthesis of 2,4,6-tris(2(S)-butylamino)-1,3,5-trinitrobenzenes 5

Dry (2(S)-butylamino) [1 ml (13.7 mmol)] was added, through the dropping funnel, to a solution of 1,3,5-trichloro-2,4,6-trinitrobenznene [0.7 g (2.3 mmol))] in toluene (ml) with stirring at 0° C. The solution immediately turned yellow. The mixture was stirred for 12 hours and then dilute hydrochloric acid was added. After the separation of the organic phase, it has been dried using Na_2SO_4. The mixture was then distilled to get rid of the solution (toluene) and yellow, very small crystals were formed, which recrystallized again out of acetone to get a suitable crystal for X-ray measurements.

Mp.: 120.4°C
^{1}H-NMR:
(CD_2Cl_2, 300 MHz): δ = 0.92 (t, 9 H, CH_3), 1.31(d, 9 H, CH_3), 1.68 (dp, 6 H, CH_2), 3.64 (br., 3H, CH), 10.80 (br., 3 H, NH)

Quantitative analysis (Nr. 14638)
$C_{18}H_{30}N_6O_6$ calculated: C 50.69%, H 7.09%, N 19.71%.
Found: C 49.43%, H 6.66%, N 19.03%.

5-2 X-ray structure analyses of 5

The three intramolecular hydrogen bonds also can be found here for **5**, which have been established as a general phenomenon in non-planar 2,4,6-tris-monoalkylamino-1,3,5-trinitrobenzenes. One nitro group is connected with both neighbouring NH groups by hydrogen bonds, and the second nitro group takes part in only one intramolecular hydrogen bond leaving the third nitro group free from intramolecular hydrogen bonding (Figure 5-1).

Structure **5** was found to adopt the non centrosymmetric space group $P2_1$ with 4 molecules in the unit cell (two independent molecules in the asymmetric unit, Figure 5-2).

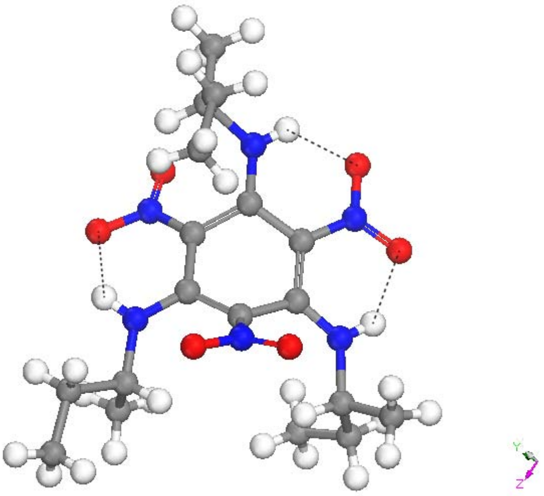

5

Figure 5-1. Molecular structure of 5

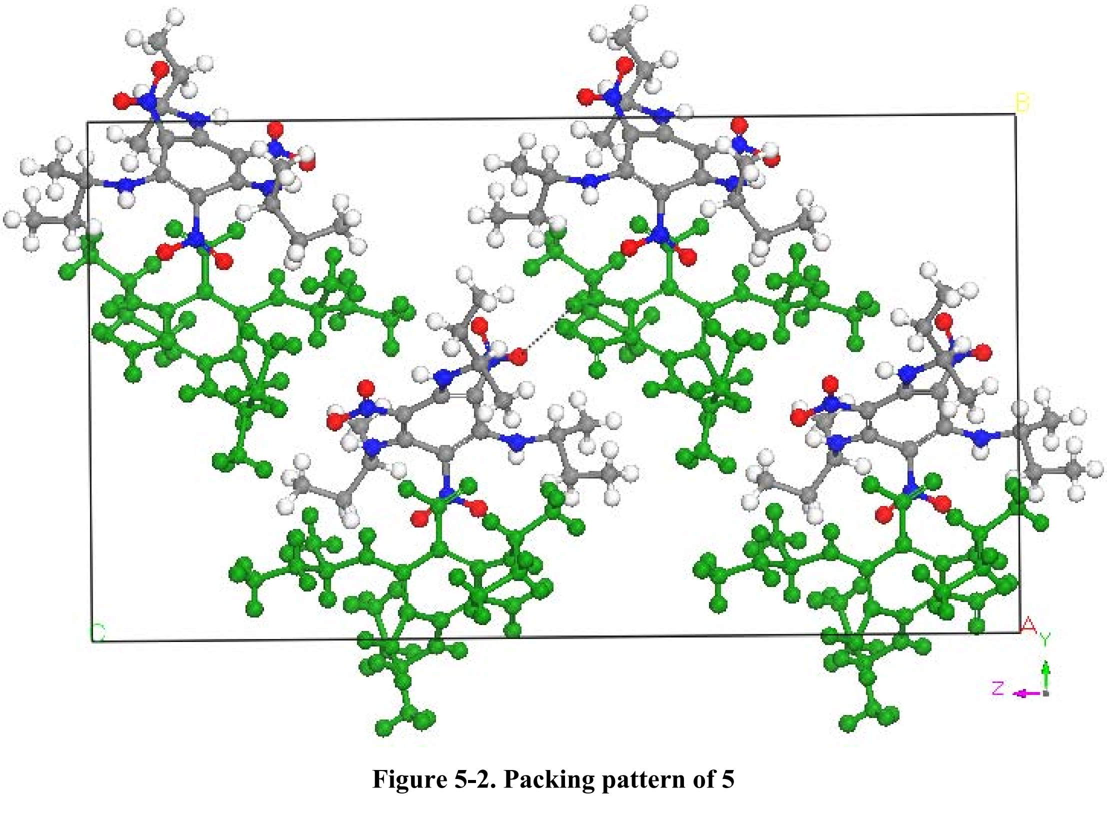

Figure 5-2. Packing pattern of 5

For structure **5** a Zig-Zag channel character packing have been found. The units of the channel is the two independent molecules pair. Intermolecular hydrogen bonds between the two independent molecules, in different symmetry positions, have also been found.

6 Crystallographic data

Intensities, for structures with benzene (**1-1**), cumene (**1-3**), fluorobenzene (**1-4**), and hydroquinone (**1-17**), were collected on Bruker SMART 1000-diffractometer with Mo-K_{∇} radiation (⇔ = 0.71073 Å).

Intensities, for structures with ethylbenzene (**1-2**), *o*- *m*- and *p*-difluorobenzene (**1-6**) (**1-7**) (**1-8**), hexafluoronbenzene (**1-10**), DMF (**1-16**), p-chlorofluorobenzne (**1-22**), *m*-fluoronitrobenzen (**1-23**), nitroethane (**1-26**), nitropropane (**1-27**), benzaldhyde (**1-28**), and dioxane (**1-29**), were collected on NONIUS kappa with Mo-K_{∇} radiation (⇔ = 0.71073 Å).

Intensities, for structures with chlorobenznene (**1-5**), 1,2,4-trifluorobenzene ((**1-9**), phenol 1 (**1-11**), benzonitrile (**1-14**), p-nitrophenol (**1-19**), p-fluorotoluene (**1-20**), p-fluoronitrobnezene (**1-25**), and γ-picoline 1 (**1-30**), were collected on NONIUS CAD4 with Mo-K_{∇} radiation (⇔ = 0.71073 Å).

For all the previous structures, structure solution were carried out with SHELXS-97[46] while the refinements was performed with SHELXL-97[47].

All the other data were collected on Bruker SMART APEX-diffractometer with Mo-K_{∇} radiation (⇔ = 0.71073 Å), highly oriented graphite-crystal monochromator. For these structures data collection and reduction were performed with the BRUKER SMART and SAINT software[48]. Structure solution and refinements were performed within SHELXTL[49] .

All measurements have been performed at temperature lower than –60° C using liquid nitrogen.

dimorph 1a

Crystal data	
empirical formula	$(C_{15}H_{24}O_6N_6)$
formula wt	384.40
crystal size [mm]	0.45, 0.24, 0.15
crystal colour	yellow
solvent	ethanol
temperature	100(2) K
crystal system	monoclinic
space group	C 2/c
a (Å)	18.453(1)
b (Å)	11.652(1)
c (Å)	36.214(2)
β (deg)	103.777(1)
Z	16
V ($Å^3$)	7563.0(8)
D_{calc} (mg/m^3)	1.35
F(000)	3264
μ [mm^{-1}]	0.106

Data colection	
Θ range [°]	1.16 /28.33
h	-24/20
k	-15/15
l	-48/44
Reflection collected	27688
Reflection unique	9426
Reflection observed $[I > 2\sigma(I)]$	7970
R_{int}	0.036

Refinement	
R_1	0.039
wR_2	0.099
Goof	1.024
No. of parameters	679
$(\Delta\rho)_{max/min}$	0.437/ -0.257

Bond lengths Å

C1-C6	1.425(2)	C20-C25	1.452(2)
C1-C2	1.453(2)	C20-C21	1.460(2)
C2-C3	1.450(2)	C21-C22	1.448(2)
C3-C4	1.450(2)	C22-C23	1.441(2)
C4-C5	1.447(2)	C23-C24	1.451(2)
C5-C6	1.445(2)	C24-C25	1.425(2)

Torsion angles (°)

C1 - C2 - C3 - C4	-25.31(14)	C20 - C21 - C22 - C23	16.31(14)
C2 - C3 - C4 - C5	- 7.88(14)	C21 - C22 - C23 - C24	18.40(15)
C3 - C4 - C5 - C6	36.05(14)	C22 - C23 - C24 - C25	-29.74(15)
C4 - C5 - C6 - C1	-28.84(15)	C23 - C24 - C25 - C20	4.27(15)
C5 - C6 - C1 - C2	6.20 (15)	C21 - C20 - C25 - C24	32.24(14)
C6 - C1 - C2 - C3	33.14(15)	C25 - C20 - C21 - C22	42.81(14)

Hydrogen bonds

D - H ··· A	d(H···A)	d(D···A)	
N2-H2···O4	1.882	2.567	
N4-H4···O3	1.781	2.544	
N6-H6···O2	1.875	2.586	
N21-H21···O22	1.987	2.605	
N21-H21···O20	2.188	2.968	[-x+3/2, y+1/2, -z+1/2]
N23-H23···O23	1.790	2.554	
N25-H25···O25	1.942	2.625	

dimorph 1b

Crystal data	
empirical formula	($C_{15}H_{24}O_6N_6$)
formula wt	384.40
crystal size [mm]	0.06, 0.07, 0.30
crystal colour	yellow
solvent	methylacetate
temperature	100(2) K
crystal system	monoclinic
space group	C 2/c
a (Å)	13.185(3)
b (Å)	16.807(3)
c (Å)	17.347(5)
β (deg)	92.35(2)
Z	8
V ($Å^3$)	3840(2)
D_{calc} (mg/m^3)	1.26
F(000)	1632
μ [mm^{-1}]	0.108

Data colection	
Θ range [°]	2.0/28.3
h	-17/16
k	-12/22
l	-22/22
Reflection collected	13714
Reflection unique	4622
Reflection observed [$I > 2\sigma(I)$]	3103
R_{int}	0.065

Refinement	
R_1	0.044
wR_2	0.144
Goof	1.040
No. of parameters	309
$(\Delta\rho)_{max/min}$	0.249 /-0.242

Bond lengths Å

C1-C6	1.433(2)	C3-C4	1.424(2)
C1-C2	1.458(2)	C4-C5	1.462(2)
C2-C3	1.439(2)	C5-C6	1.445(2)

Torsion angles (°)

C1 - C2 - C3 - C4	31.34(14)
C2 - C3 - C4 - C5	7.69(14)
C3 - C4 - C5 - C6	-37.69(14)
C4 - C5 - C6 - C1	27.90(14)
C5 - C6 - C1 - C2	9.41(15)
C6 - C1 - C2 - C3	-40.68(15)

Hydrogen bonds

D - H ··· A	d(H···A)	d(D···A)	
N1-H1···O5	1.882	2.622	
N3-H3···O3	1.859	2.592	
N5-H5···O6	2.069	2.602	
N5-H5···O2	2.360	3.160	[-x, y, -z+1/2]

benzene as inclusion compound (1-1)

Crystal data	
empirical formula	$(C_{15}H_{24}O_6N_6)$. (C_6H_6)
formula wt	462.5
crystal size [mm]	0.44, 0.40, 0.30
crystal colour	yellow
solvent	benzene
temperature	173(2) K
crystal system	monoclinic
space group	C c
a (Å)	16.813(1)
b (Å)	16.052(1)
c (Å)	11.762(1)
β (deg)	129.88(1)
Z	4
V (Å^3)	2436.1(2)
D_{calc} (mg/m^3)	1.26
F(000)	984
μ [mm^{-1}]	0.09

Data colection	
Θ range [°]	2.03 - 28.31
h	-22/22
k	0/21
l	-15/15
Reflection collected	16350
Reflection unique	5871
Reflection observed [$I > 2\sigma(I)$]	5451
R_{int}	0.04

Refinement	
R_1	0.032
wR_2	0.084
Goof	1.035
No. of parameters	418
$(\Delta\rho)_{max/min}$	0.260/-0.187

Bond lengths Å

C1-C6	1.444(2)	C3-C4	1.420(2)
C1-C2	1.448(2)	C4-C5	1.454(2)
C2-C3	1.448(2)	C5-C6	1.451(2)

Torsion Angles (°)

C1 - C2 - C3 - C4	31.60(16)
C2 - C3 - C4 - C5	1.55(16)
C3 - C4 - C5 - C6	-27.14(16)
C4 - C5 - C6 - C1	20.04(16)
C5 - C6 - C1 - C2	11.70(16)
C6 - C1 - C2 - C3	-38.19(16)

Hydrogen bonds

D - H ··· A	d(H···A)	d(D···A)
N1-H1···O6	1.935	2.606
N3-H3···O3	1.914	2.566
N5-H5···O5	1.888	2.559

ethylbenzene as inclusion compound (1-2)

Crystal data	
empirical formula	$(C_{15}H_{24}O_6N_6)$. $(C_6H_5(CH_2CH_3)$
formula wt	490.6
crystal size [mm]	0.17, 0.15, 0.10
crystal colour	yellow
solvent	ethylbenzene
temperature	200(2) K
crystal system	monoclinic
space group	C c
a (Å)	17.3029(3)
b (Å)	17.1664(5)
c (Å)	11.3104(3)
β (deg)	130.342(1)
Z	4
V (Å^3)	2560.6(1)
D_{calc} (mg/m^3)	1.270
F(000)	1048
μ [mm^{-1}]	0.093

Data colection	
Θ range [°]	2.0/ 27.9
h	-22/19
k	-20/22
l	-13/14
Reflection collected	7061
Reflection unique	4474
Reflection observed [$I > 2\sigma(I)$]	3430
R_{int}	0.04

Refinement	
R_1	0.059
wR_2	0.124
Goof	1.050
No. of parameters	347
$(\Delta\rho)_{max/min}$	0.41/-0.20

Bond lengths Å

C1-C6	1.455(5)
C1-C2	1.433(4)
C2-C3	1.426(4)
C3-C4	1.453(4)
C4-C5	1.445(4)
C5-C6	1.445(5)

Torsion angles (°)

C1 - C2 - C3 - C4	8.18(41)
C2 - C3 - C4 - C5	-29.80(39)
C3 - C4 - C5 - C6	15.98(38)
C4 - C5 - C6 - C1	17.23(39)
C5 - C6 - C1 - C2	-39.99(40)
C6 - C1 - C2 - C3	26.94(41)

Hydrogen bonds

D - H ··· A	d(H···A)	d(D···A)
N2-H2···O3	1.978	2.607
N4-H4···O5	1.871	2.573
N6-H6···O6	1.888	2.582

cumene as inclusion compound (1-3)

Crystal data	
empirical formula	$(C_{15}H_{24}O_6N_6)$. $(C_6H_5C(CH_3)_2)$
formula wt	502.60
crystal size [mm]	0.22, 0.33, 0.44
crystal colour	yellow
solvent	cumene
temperature	173(2) K
crystal system	monoclinic
space group	C c
a (Å)	16.679(4)
b (Å)	17.323(4)
c (Å)	11.566(3)
β (deg)	127.72(2)
Z	4
V ($Å^3$)	2643.3(1)
D_{calc} (mg/m^3)	1.268
F(000)	1080
μ [mm^{-1}]	0.090

Data colection	
Θ range [°]	1.9/ 28.3
h	-22/22
k	0/23
l	-15/15
Reflection collected	17688
Reflection unique	6261
Reflection observed [$I > 2\sigma(I)$]	5866
R_{int}	0.04

Refinement	
R_1	0.034
wR_2	0.085
Goof	1.035
No. of parameters	475
$(\Delta\rho)_{max/min}$	0.26/-0.27

Bond lengths Å

C1-C6	1.442(2)	C3-C4	1.421(2)
C1-C2	1.452(2)	C4-C5	1.449(2)
C2-C3	1.442(2)	C5-C6	1.451(2)

Torsion Angles

C1 - C2 - C3 - C4	14.90
C2 - C3 - C4 - C5	18.00
C3 - C4 - C5 - C6	-40.80
C4 - C5 - C6 - C1	28.30
C5 - C6 - C1 - C2	6.40
C6 - C1 - C2 - C3	-28.10

Hydrogen bonds

D - H ··· A	d(H···A)	d(D···A)
N1-H1···O6	1.944	2.567
N3-H3···O3	1.928	2.615
N5-H5···O5	1.859	2.577

fluorobenzene as inclusion compound (1-4)

Crystal data	
empirical formula	$(C_{15}H_{24}O_6N_6)$. (C_6H_5F)
formula wt	480.5
crystal size [mm]	0.30, 0.30, 0.40
crystal colour	yellow
solvent	fluorobenzene
temperature	173(2) K
crystal system	monoclinic
space group	C c
a (Å)	16.8105(5)
b (Å)	15.9195(4)
c (Å)	11.7425(3)
β (deg)	128.936(2
Z	4
V ($Å^3$)	2444.36(3)
D_{calc} (mg/m^3)	1.306
F(000)	1016
μ [mm^{-1}]	0.102

Data colection	
Θ range [°]	2.0 / 28.3
h	-22/22
k	0/21
l	-15/15
Reflection collected	16428
Reflection unique	5865
Reflection observed $[I > 2\sigma(I)]$	5449
R_{int}	0.023

Refinement	
R_1	0.033
wR_2	0.084
Goof	1.055
No. of parameters	423
$(\Delta\rho)_{max/min}$	0.23/-0.23

Bond lengths Å

C1-C6	1.416(2)	C3-C4	1.434(2)
C1-C2	1.448(2)	C4-C5	1.453(2)
C2-C3	1.455(2)	C5-C6	1.457(2)

Torsion angles (°)

C1 - C2 - C3 - C4	-38.50
C2 - C3 - C4 - C5	12.30
C3 - C4 - C5 - C6	19.10
C4 - C5 - C6 - C1	-26.90
C5 - C6 - C1 - C2	1.90
C6 - C1 - C2 - C3	31.50

Hydrogen bonds

D - H ··· A	d(H···A)	d(D···A)
N1-H1···O6	1.935	2.606
N3-H3···O3	1.914	2.566
N5-H5···O5	1.888	2.599

chlorobenzene as inclusion compound (1-5)

Crystal data	
empirical formula	$(C_{15}H_{24}O_6N_6)$. $\frac{1}{2}(C_6H_5Cl)$
formula wt	440.68
crystal size [mm]	0.35, 0.35, 0.20
crystal colour	yellow
solvent	chlorobenzene
temperature	213(2) K
crystal system	monoclinic
space group	C c
a (Å)	17.144(9)
b (Å)	16.854(5)
c (Å)	11.376(7)
β (deg)	129.89(3)
Z	4
V ($Å^3$)	2522(2)
D_{calc} (mg/m^3)	1.16
F(000)	932
μ [mm^{-1}]	0.139

Data colection	
Θ range [°]	2.2/28.0
h	0/22
k	0/22
l	-15/11
Reflection collected	3118
Reflection unique	3118
Reflection observed $[I > 2\sigma(I)]$	2247
R_{int}	-

Refinement	
R_1	0.066
wR_2	0.178
Goof	1.030
No. of parameters	318
$(\Delta\rho)_{max/min}$	0.62/-0.28

Bond lengths Å

C1-C6	1.421(6)	C3-C4	1.438(6)
C1-C2	1.447(5)	C4-C5	1.453(6)
C2-C3	1.446(6)	C5-C6	1.448(6)

Torsion angles (°)

C1 - C2 - C3 - C4	-16.78
C2 - C3 - C4 - C5	-17.38
C3 - C4 - C5 - C6	40.99
C4 - C5 - C6 - C1	-27.78
C5 - C6 - C1 - C2	-8.37
C6 - C1 - C2 - C3	30.86

Hydrogen bonds

D - H ··· A	d(H···A)	d(D···A)
N2-H2···O3	1.866	2.555
N4-H4···O4	1.886	2.572
N6-H6···O1	2.015	2.602

m-difluorobenzene as inclusion compound (1-6)

Crystal data	
empirical formula	$(C_{15}H_{24}O_6N_6)$. $(C_6H_4F_2)$
formula wt	498.5
crystal size [mm]	0.50, 0.30, 0.10
crystal colour	yellow
solvent	1,3-difluorobenzen
temperature	200(1) K
crystal system	monoclinic
space group	C c
a (Å)	16.644(3)
b (Å)	16.031(3)
c (Å)	11.677(2)
β (deg)	128.04(3)
Z	4
V (Å^3)	2453.8
D_{calc} (mg/m^3)	1.35
F(000)	1048
μ [mm^{-1}]	0.110

Data colection	
Θ range [°]	2.5/27.9
h	-18/21
k	-20/20
l	-15/15
Reflection collected	6336
Reflection unique	4117
Reflection observed $[I > 2\sigma(I)]$	3619
R_{int}	0.039

Refinement	
R_1	0.044
wR_2	0.099
Goof	1.02
No. of parameters	353
$(\Delta\rho)_{max/min}$	0.25/-0.23

Bond lengths Å

C1-C6	1.446(3)	C3-C4	1.455(3)
C1-C2	1.447(3)	C4-C5	1.449(3)
C2-C3	1.429(3)	C5-C6	1.417(3)

Torsion angles (°)

C1 - C2 - C3 - C4	13.19(31)
C2 - C3 - C4 - C5	17.79(29)
C3 - C4 - C5 - C6	-26.36(29)
C4 - C5 - C6 - C1	2.47(30)
C5 - C6 - C1 - C2	30.36(31)
C6 - C1 - C2 - C3	-38.51(31)

Hydrogen bonds

D - H ··· A	d(H···A)	d(D···A)
N2-H2···O3	1.875	2.606
N4-H4···O4	1.803	2.557
N6-H6···O6	1.832	2.561

o-difluorobenzene as inclusion compound (1-7)

Crystal data	
empirical formula	$(C_{15}H_{24}O_6N_6)$ $(C_6H_4F_2)$
formula wt	498.49
crystal size [mm]	0.35, 0.25, 0.25
crystal colour	yellow
solvent	1,2-difluorobenzen
temperature	245(2) K
crystal system	monoclinic
space group	C c
a (Å)	16.817(3)
b (Å)	15.746(3)
c (Å)	11.720(2)
β (deg)	128.38(3)
Z	4
V ($Å^3$)	2432.8(8)
D_{calc} (mg/m^3)	1.361
F(000)	1048
μ [mm^{-1}]	0.111

Data colection	
Θ range [°]	2.2/27.9
h	-22/22
k	-18/20
l	-15/15
Reflection collected	4697
Reflection unique	4696
Reflection observed [$I > 2\sigma(I)$]	4033
R_{int}	0.032

Refinement	
R_1	0.040
wR_2	0.090
Goof	1.03
No. of parameters	412
$(\Delta\rho)_{max/min}$	0.35/-0.25

Bond lengths Å

C1-C6	1.448(3)	C3-C4	1.456(3)
C1-C2	1.449(3)	C4-C5	1.448(3)
C2-C3	1.420(3)	C5-C6	1.439(3)

Torsion angles (°)

C1 - C2 - C3 - C4	-0.05(27)
C2 - C3 - C4 - C5	25.18(27)
C3 - C4 - C5 - C6	-18.54(26)
C4 - C5 - C6 - C1	-12.10(26)
C5 - C6 - C1 - C2	38.41(25)
C6 - C1 - C2 - C3	-32.11(26)

Hydrogen bonds

D - H ··· A	d(H···A)	d(D···A)
N2-H2···O3	1.950	2.563
N4-H4···O5	1.883	2.558
N6-H6···O6	1.902	2.601

p-difluorobenzene as inclusion compound (1-8)

Crystal data	
empirical formula	$(C_{15}H_{24}O_6N_6)$. $(C_6H_4F_2)$
formula wt	498.49
crystal size [mm]	0.50, 0.35, 0.12
crystal colour	yellow
solvent	1,4-difluorobenzen
temperature	200(2) K
crystal system	monoclinic
space group	C c
a (Å)	16.9675(2)
b (Å)	16.6954(4)
c (Å)	11.3477(3)
β (deg)	130.05
Z	4
V (Å^3)	2460.66(9)
D_{calc} (mg/m^3)	1.346
F(000)	1048
μ [mm^{-1}]	0.110

Data colection	
Θ range [°]	2.2 / 27.9
h	-22/22
k	-21/18
l	-9/14
Reflection collected	6479
Reflection unique	3866
Reflection observed [$I > 2\sigma(I)$]	3461
R_{int}	0.027

Refinement	
R_1	0.034
wR_2	0.075
Goof	1.05
No. of parameters	428
$(\Delta\rho)_{max/min}$	0.20/-0.21

Bond lengths Å

C1-C6	1.445(3)	C3-C4	1.442(3)
C1-C2	1.451(3)	C4-C5	1.456(3)
C2-C3	1.441(3)	C5-C6	1.418(3)

Torsion angles (°)

C1 - C2 - C3 - C4	17.94(26)
C2 - C3 - C4 - C5	17.17(26)
C3 - C4 - C5 - C6	-31.89(26)
C4 - C5 - C6 - C1	9.12(27)
C5 - C6 - C1 - C2	27.69(26)
C6 - C1 - C2 - C3	-41.67(25)

Hydrogen bonds

D - H ··· A	d(H···A)	d(D···A)
N2-H2···O3	1.825	2.573
N4-H4···O4	1.827	2.567
N6-H6···O6	1.846	2.608

1,2,4-trifluorobenzene as inclusion compound (1-9)

Crystal data	
empirical formula	$(C_{15}H_{24}O_6N_6).(C_6H_3F_3)$
formula wt	516.5
crystal size [mm]	0.50, 0.50, 0.45
crystal colour	yellow
solvent	1,2,4-trifluorobnezene
temperature	223(2) K
crystal system	monoclinic
space group	C c
a (Å)	16.849(8)
b (Å)	16.538(3)
c (Å)	11.626(7)
β (deg)	128.97
Z	4
V (Å^3)	2518.57(2)
D_{calc} (mg/m^3)	1.360
F(000)	1080
μ [mm^{-1}]	0.115

Data colection	
Θ range [°]	2.2 / 28.0
h	0/22
k	0/21
l	-15/11
Reflection collected	3127
Reflection unique	3127
Reflection observed [$I > 2\sigma(I)$]	2483
R_{int}	-

Refinement	
R_1	0.048
wR_2	0.138
Goof	1.03
No. of parameters	347
$(\Delta\rho)_{max/min}$	0.37/-0.25

Bond lengths Å

C1-C6	1.453(4)	C3-C4	1.445(4)
C1-C2	1.444(4)	C4-C5	1.443(4)
C2-C3	1.444(4)	C5-C6	1.416(4)

Torsion angles (°)

C1 - C2 - C3 - C4	-16.12(40)
C2 - C3 - C4 - C5	40.69(38)
C3 - C4 - C5 - C6	-29.85(39)
C4 - C5 - C6 - C1	-5.11(40)
C5 - C6 - C1 - C2	28.60(40)
C6 - C1 - C2 - C3	-17.11(40)

Hydrogen bonds

D - H ··· A	d(H···A)	d(D···A)
N1-H1···O1	1.892	2.555
N3-H3···O2	1.759	2.559
N5-H5···O5	1.802	2.596

hexafluorobenzene as inclusion compound (1-10)

Crystal data	
empirical formula	$(C_{15}H_{24}O_6N_6).(C_6H_6)_2$
formula wt	570.46
crystal size [mm]	0.20, 0.15, 0.14
crystal colour	yellow
solvent	hexafluorobenzene
temperature	190(2) K
crystal system	monoclinic
space group	P 2_1/a
a (Å)	14.944(2)
b (Å)	22.122(3)
c (Å)	15.132(2)
β (deg)	93.60(3)
Z	8
V (Å^3)	4992.4(1)
D_{calc} (mg/m^3)	1.518
F(000)	2352
μ [mm^{-1}]	0.141

Data colection	
Θ range [°]	1.84 /25.00
h	-17/17
k	-26/26
l	-16/17
Reflection collected	36104
Reflection unique	36111
Reflection observed [$I > 2\sigma(I)$]	21682
R_{int}	-

Refinement	
R_1	0.069
wR_2	0.1815
Goof	0.907
No. of parameters	745
$(\Delta\rho)_{max/min}$	0.421/ -0.421

Bond lengths Å

C1-C2	1.442(4)	C20-C21	1.439(4)
C1-C6	1.454(4)	C20-C25	1.443(4)
C2-C3	1.441(4)	C21-C22	1.449(4)
C3-C4	1.441(4)	C22-C23	1.447(4)
C4-C5	1.428(4)	C23-C24	1.425(4)
C5-C6	1.446(4)	C24-C25	1.425(4)

Torsion angles (°)

C1 - C2 - C3 - C4	39.18(39)	C20 - C21 - C22 - C23	16.31(37)
C2 - C3 - C4 - C5	-26.99(38)	C21 - C22 - C23 - C24	18.40(37)
C3 - C4 - C5 - C6	-9.93(39)	C22 - C23 - C24 - C25	-29.74(41)
C4 - C5 - C6 - C1	34.45(38)	C23 - C24 - C25 - C20	4.27(41)
C5 - C6 - C1 - C2	-21.60(37)	C21 - C20 - C25 - C24	32.24(38)
C6 - C1 - C2 - C3	-13.32(38)	C25 - C20 - C21 - C22	42.81(38)

Hydrogen bonds

D - H ··· A	d(H···A)	d(D···A)
N2-H2···O2	1.818	2.545
N4-H4···O5	1.975	2.554

N4-H4···F55	2.505	3.219	[x-1/2, -y+1/2, z]
N6-H6···O1	1.929	2.601	
N21-H21···O22	1.813	2.579	
N23-H23···O23	1.855	2.623	
N25-H25···O25	2.059	2.591	
N25-H25···F44	2.406	3.3983	[x+1/2, -y+1/2, z]

phenol 1 as inclusion compound (1-11)

Crystal data	
empirical formula	$(C_{15}H_{24}O_6N_6)$. (C_6H_5OH)
formula wt	431.46
crystal size [mm]	0.35, 0.30, 0.25
crystal colour	yellow
solvent	mesitylene
temperature	193(2) K
crystal system	triclinic
space group	P –1
a (Å)	10.604(4)
b (Å)	11.522(6)
c (Å)	18.907(8)
α (deg)	84.55(4)
β (deg)	80.18(3)
γ (deg)	69.31(3)
Z	4
V ($Å^3$)	2127.9(2)
D_{calc} (mg/m^3)	1.347
F(000)	916
μ [mm^{-1}]	0.104

Data colection	
Θ range [°]	2.1 / 27.9
h	0/13
k	-14/15
l	-24/24
Reflection collected	10791
Reflection unique	10244
Reflection observed $[I > 2\sigma(I)]$	6173
R_{int}	0.025

Refinement	
R_1	0.054
wR_2	0.116
Goof	1.01
No. of parameters	750
$(\Delta\rho)_{max/min}$	0.28/-0.29

Bond lengths Å

C1-C6	1.454(3)	C16-C21	1.438(3)
C1-C2	1.433(3)	C16-C17	1.443(3)
C2-C3	1.421(3)	C17-C18	1.463(3)
C3-C4	1.448(3)	C18-C19	1.437(3)
C4-C5	1.440(3)	C19-C20	1.413(3)
C5-C6	1.446(3)	C20-C21	1.453(3)

Torsion angles (°)

C1 - C2 - C3 - C4	-18.08(25)	C16 - C17 - C18 - C19	41.83(24)
C2 - C3 - C4 - C5	36.83(25)	C17 - C18 - C19 - C20	22.46(24)
C3 - C4 - C5 - C6	-15.24(25)	C18 - C19 - C20 - C21	16.42(25)
C4 - C5 - C6 - C1	-21.84(24)	C19 - C20 - C21 - C16	-35.84(19)
C5 - C6 - C1 - C2	41.49(24)	C20 - C21 - C16 - C17	15.10(25)
C6 - C1 - C2 - C3	-21.15(25)	C21 - C16 - C17 - C18	21.53(24)

Hydrogen bonds

D - H ··· A	d(H···A)	d(D···A)
N2-H2···O4	1.967	2.620

N4-H4···O6	1.802	2.572	
N6-H6···O5	1.940	2.589	
N6-H6···O7	2.490	3.276	[x, y+1, z]
N8-H8···O7	1.909	2.583	
N8-H8···O5	2.520	3.294	[x, y-1, z]
N10-H10···O11	1.9042	2.622	
N12-H12···O8	1.838	2.568	

phenol 2 as inclusion compound (1-12)

Crystal data	
empirical formula	$(C_{15}H_{24}O_6N_6)$. $(C_6H_5OH)_2$
formula wt	572.62
crystal size [mm]	0.26, 0.25, 0.16
crystal colour	yellow
solvent	anisol+phenol
temperature	200(2) K
crystal system	triclinic
space group	P –1
a (Å)	10.977(2)
b (Å)	10.930(3)
c (Å)	13.339(3)
α (deg)	100.35(2)
β (deg)	97.96(8)
γ (deg)	106.22(6)
Z	2
V (Å^3)	1481.3(6)
D_{calc} (mg/m^3)	1.284
F(000)	608
μ [mm^{-1}]	0.096

Data colection	
Θ range [°]	2/28
h	-14/12
k	-12/14
l	-17/17
Reflection collected	10013
Reflection unique	7011
Reflection observed [$I > 2\sigma(I)$]	5593
R_{int}	0.024

Refinement	
R_1	0.040
wR_2	0.096
Goof	1.03
No. of parameters	514
$(\Delta\rho)_{max/min}$	0.30/-0.26

Bond lengths Å

C1-C6	1.438(2)	C3-C4	1.421(2)
C1-C2	1.466(2)	C4-C5	1.462(2)
C2-C3	1.449(2)	C5-C6	1.443(2)

Torsion angles (°)

C1 - C2 - C3 - C4	28.96(16)
C2 - C3 - C4 - C5	10.28(16)
C3 - C4 - C5 - C6	-36.36(16)
C4 - C5 - C6 - C1	22.05(16)
C5 - C6 - C1 - C2	15.31(16)
C6 - C1 - C2 - C3	-42.44(15)

Hydrogen bonds

D - H ··· A	d(H···A)	d(D···A)	
N1-H1···O5	1.852	2.581	
N3-H3···O3	1.942	2.619	
N5-H5···O6	1.927	2.593	
N5-H5···O6	2.442	3.248	[-x+2, -y+2, -z]
O20-H20···O1	1.698	2.609	
O30-H30···O20	1.881	2.757	

anisole as inclusion compound (1-13)

Crystal data	
empirical formula	$(C_{15}H_{24}O_6N_6)_2.(C_6H_5OCH_3)$
formula wt	438.47
crystal size [mm]	0.50, 0.35, 0.25
crystal colour	yellow
solvent	anisole
temperature	193(2) K
crystal system	triclinic
space group	P –1
a (Å)	10.724(2)
b (Å)	12.018(3)
c (Å)	18:676(4)
α (deg)	86.50(2)
β (deg)	77.52(2)
γ (deg)	68.54(2)
Z	4
V (Å^3)	2186.8(8)
D_{calc} (mg/m^3)	1.33
F(000)	932
μ [mm^{-1}]	0.102

Data colection	
Θ range [°]	2.1/28.0
h	0/14
k	-14/15
l	-24/24
Reflection collected	11058
Reflection unique	10504
Reflection observed [$I > 2\sigma(I)$]	7856
R_{int}	0.020

Refinement	
R_1	0.043
wR_2	0.124
Goof	1.05
No. of parameters	650
$(\Delta\rho)_{max/min}$	0.36/-0.37

Bond lengths Å

C1-C6	1.419(2)	C20-C21	1.444(2)
C1-C2	1.450(2)	C20-C25	1.451(2)
C2-C3	1.439(2)	C21-C22	1.422(2)
C3-C4	1.444(2)	C22-C23	1.455(2)
C4-C5	1.448(2)	C23-C24	1.450(2)
C5-C6	1.442(2)	C24-C25	1.434(2)

Torsion angles (°)

C1 - C2 - C3 - C4	-21.81	C20 - C21 - C22 - C33	-2.93
C2 - C3 - C4 - C5	-10.19	C21 - C22 - C23 - C24	32.48
C3 - C4 - C5 - C6	35.45	C22 - C23 - C24 - C25	-25.74
C4 - C5 - C6 - C1	-26.07	C23 - C24 - C25 - C20	-9.26
C5 - C6 - C1 - C2	-7.80	C24 - C25 - C20 - C21	40.15
C6 - C1 - C2 - C3	31.90	C25 - C20 - C21 - C22	-33.80

Hydrogen bonds

D - H ··· A	d(H···A)	d(D···A)
N2-H2···O3	1.847	2.555
N4-H4···O4	1.832	2.570
N6-H6···O1	2.015	2.631

N6-H6···O21	2.492	3.195	
N21-H21···O22	1.882	2.588	
N23-H23···O24	1.873	2.574	
N25-H25···O25	1.843	2.579	
N25-H25···O25	2.373	3.153	[-x+2, -y+1, -z]

benzonitrile as inclusion compound (1-14)

Crystal data	
empirical formula	$(C_{15}H_{24}O_6N_6)$. (C_6H_5CN)
formula wt	487.52
crystal size [mm]	0.40, 0.40, 0.35
crystal colour	yellow
solvent	benzonitrile
temperature	223(2) K
crystal system	triclinic
space group	P -1
a (Å)	11.259(2)
b (Å)	11.299(3)
c (Å)	11.715(5)
α (deg)	61.99(2)
β (deg)	70.44(2)
γ (deg)	74.65(2)
Z	2
V (Å^3)	1229.4(7)
D_{calc} (mg/m^3)	1.317
F(000)	516
μ [mm^{-1}]	0.098

Data colection	
Θ range [°]	2/28
h	0/14
k	-14/14
l	-14/15
Reflection collected	6219
Reflection unique	5919
Reflection observed [$I > 2\sigma(I)$]	4359
R_{int}	0.013

Refinement	
R_1	0.043
wR_2	0.113
Goof	1.04
No. of parameters	432
$(\Delta\rho)_{max/min}$	0.21/-0.31

Bond lengths Å

C1-C6	1.432(2)	C3-C4	1.441(2)
C1-C2	1.427(2)	C4-C5	1.443(2)
C2-C3	1.452(2)	C5-C6	1.461(2)

Torsion angles (°)

C1 - C2 - C3 - C4	36.90(17)
C2 - C3 - C4 - C5	-19.87(17)
C3 - C4 - C5 - C6	-16.14(16)
C4 - C5 - C6 - C1	39.18(16)
C5 - C6 - C1 - C2	-23.19(16)
C6 - C1 - C2 - C3	-14.83(17)

Hydrogen bonds

D - H ··· A	d(H···A)	d(D···A)	
N1-H1···O2	1.927	2.613	
N3-H3···O4	1.928	2.583	
N5-H5···O3	1.889	2.585	
N5-H5···O3	2.572	3.374	[-x+2, -y+1, -z]

trifluorotoluene as inclusion compound (1-15)

Crystal data	
empirical formula	$(C_{15}H_{24}O_6N_6)$. $(C_6H_5CF_3)$
formula wt	530.5
crystal size [mm]	0.45, 0.35, 0.20
crystal colour	yellow
solvent	trifluorotoluene
temperature	223 K
crystal system	monoclinic
space group	C c
a (Å)	17.177(11)
b (Å)	16.964(9)
c (Å)	11.587(9)
α (deg)	90
β (deg)	129.58(4)
γ (deg)	90
Z	4
V ($Å^3$)	2602(3)
D_{calc} (mg/m^3)	1.350
F(000)	1112
μ [mm^{-1}]	0.110

Data colection	
Θ range [°]	2.1/28
h	0/22
k	0/22
l	-15/11
Reflection collected	3245
Reflection unique	3245
Reflection observed [$I > 2\sigma(I)$]	2281
R_{int}	-

Refinement	
R_1	0.059
wR_2	0.124
Goof	1.050
No. of parameters	354
$(\Delta\rho)_{max/min}$	0.34/-0.40

Bond lengths Å

C1-C6	1.450(6)	C3-C4	1.456(5)
C1-C2	1.437(6)	C4-C5	1.450(6)
C2-C3	1.416(5)	C5-C6	1.431(6)

Torsion angles (°)

C1 - C2 - C3 - C4	-7.65(58)
C2 - C3 - C4 - C5	30.03(55)
C3 - C4 - C5 - C6	-17.76(56)
C4 - C5 - C6 - C1	-15.05(58)
C5 - C6 - C1 - C2	38.81(55)
C6 - C1 - C2 - C3	-27.34(56)

Hydrogen bonds

D - H ··· A	d(H···A)	d(D···A)
N2-H2···O3	1.983	2.604
N4-H4···O5	1.833	2.560
N6-H6···O6	1.786	2.563

DMF as inclusion compound (1-16)

Crystal data	
empirical formula	$(C_{15}H_{24}O_6N_6).(C_6H_7ON)$
formula wt	487.52
crystal size [mm]	0.35, 0.35, 0.30
crystal colour	yellow
solvent	DMF
temperature	193(2) K
crystal system	triclinic
space group	P –1
a (Å)	10.935(2)
b (Å)	11.038(3)
c (Å)	12.300(4)
α (deg)	109.61(2)
β (deg)	98.56(2)
γ (deg)	94.05(1)
Z	2
V ($Å^3$)	1371.2(5)
D_{calc} (mg/m^3)	1.280
F(000)	568
μ [mm^{-1}]	0.099

Data colection	
Θ range [°]	2.2/28
h	0/14
k	-14/14
l	-16/16
Reflection collected	6950
Reflection unique	6608
Reflection observed [$I > 2\sigma(I)$]	4897
R_{int}	0.026

Refinement	
R_1	0.049
wR_2	0.140
Goof	1.05
No. of parameters	390
$(\Delta\rho)_{max/min}$	0.37/-0.40

Bond lengths Å

C1-C6	1.460(2)	C3-C4	1.468(2)
C1-C2	1.428(2)	C4-C5	1.414(2)
C2-C3	1.452(2)	C5-C6	1.449(2)

Torsion angles (°)

C1 - C2 - C3 - C4	31.60(19)
C2 - C3 - C4 - C5	-38.13(20)
C3 - C4 - C5 - C6	5.66(20)
C4 - C5 - C6 - C1	33.40(20)
C5 - C6 - C1 - C2	-39.52(20)
C6 - C1 - C2 - C3	5.51(20)

Hydrogen bonds

D - H ··· A	d(H···A)	d(D···A)	
N1-H1···O2	1.918	2.591	
N1-H1···O2	2.492	3.218	[-x+1, -y, -z]
N3-H3···O1	2.147	2.675	
N3-H3···O60	2.442	2.937	[-x+1, -y+1, -z]
N3-H3···O50	2.650	3.080	
N5-H5···O3	1.903	2.600	

hydroquinone as inclusion compound (1-17)

Crystal data	
empirical formula	$(C_{15}H_{24}O_6N_6).(C_6H_6O_2)$
formula wt	439.46
crystal size [mm]	0.50, 0.20, 0.13
crystal colour	yellow
solvent	hydroquinone
temperature	173(2) K
crystal system	triclinic
space group	P –1
a (Å)	10.717(2)
b (Å)	10.991(3)
c (Å)	11.455(3)
α (deg)	115.33(2)
β (deg)	110.87(1)
γ (deg)	98.79(2)
Z	2
V ($Å^3$)	1062.5(4)
D_{calc} (mg/m^3)	1.374
F(000)	466
μ [mm^{-1}]	0.107

Data colection	
Θ range [°]	2.2/28.4
h	-14/14
k	-14/14
l	-15/15
Reflection collected	17872
Reflection unique	17872
Reflection observed [$I > 2\sigma(I)$]	13420
R_{int}	-

Refinement	
R_1	0.058
wR_2	0.163
Goof	1.01
No. Of parameters	389
$(\Delta\rho)_{max/min}$	0.29/-0.28

Bond lengths Å

C1-C6	1.421(2)	C3-C4	1.442(2)
C1-C2	1.437(2)	C4-C5	1.447(2)
C2-C3	1.468(2)	C5-C6	1.453(2)

Torsion angles (°)

C1 - C2 - C3 - C4	43.50(13)
C2 - C3 - C4 - C5	-24.37(13)
C3 - C4 - C5 - C6	-13.71(13)
C4 - C5 - C6 - C1	37.12(14)
C5 - C6 - C1 - C2	-18.83(14)
C6 - C1 - C2 - C3	-21.48(14)

Hydrogen bonds

D - H ··· A	d(H···A)	d(D···A)	
N1-H1···O6	2.044	2.641	
N3-H3···O3	1.847	2.592	
N3-H3···O3	2.432	3.228	[-x, -y+1, -z]
N5-H5···O4	1.846	2.583	
O7-H7···O2	1.816	2.718	

p-xylene 1 as inclusion compound (1-18)

Crystal data	
empirical formula	$(C_{15}H_{24}O_6N_6)$. (C_8H_{10})
formula wt	490.6
crystal size [mm]	0.20, 0.17, 0.10
crystal colour	yellow
solvent	p-xylene
temperature	100(2) K
crystal system	monoclinic
space group	Cc
a (Å)	16.555(6)
b (Å)	16.849(6)
c (Å)	11.241(4)
β (deg)	125.959(5)
Z	4
V ($Å^3$)	2538.1(15)
D_{calc} (mg/m^3)	1.28
F(000)	1048
μ [mm^{-1}]	0.094

Data colection	
Θ range [°]	2.2/28.5
h	-22/17
k	-19/22
l	-14/15
Reflection collected	9224
Reflection unique	5397
Reflection observed $[I > 2\sigma(I)]$	5135
R_{int}	0.052

Refinement	
R_1	0.045
wR_2	0.109
Goof	1.06
No. of parameters	452
$(\Delta\rho)_{max/min}$	0.34/-0.22

Bond lengths Å

C1-C6	1.445(3)	C3-C4	1.444(2)
C1-C2	1.447(3)	C4-C5	1.422(3)
C2-C3	1.458(3)	C5-C6	1.453(2)

Torsion angles (°)

C1 - C2 - C3 - C4	-41.82(23)
C2 - C3 - C4 - C5	28.28(25)
C3 - C4 - C5 - C6	8.41(27)
C4 - C5 - C6 - C1	-31.05(26)
C5 - C6 - C1 - C2	16.53(25)
C6 - C1 - C2 - C3	18.03(24)

Hydrogen bonds

D - H ··· A	d(H···A)	d(D···A)
N2-H2···O1	1.912	2.582
N4-H4···O6	1.840	2.591
N6-H6···O2	1.908	2.577

p-nitrophenol as inclusion compound (1-19)

Crystal data	
empirical formula	$(C_{15}H_{24}O_6N_6)$. $(C_6H_4\,OHNO_2)$
formula wt	523.51
crystal size [mm]	0.35, 0.35, 0.20
crystal colour	yellow
solvent	mesitylene
temperature	193(2) K
crystal system	triclinic
space group	P –1
a (Å)	11.016(3)
b (Å)	11.267(4)
c (Å)	11.998(5)
α (deg)	68.06(3)
β (deg)	64.22(2)
γ (deg)	70.45(2)
Z	2
V (Å^3)	1217.1(7)
D_{calc} (mg/m^3)	1.428
F(000)	552
μ [mm^{-1}]	0.113

Data colection	
Θ range [°]	2.1/27.9
h	0/14
k	-14/14
l	-14/15
Reflection collected	6154
Reflection unique	5855
Reflection observed $[I > 2\,\sigma\,(I)]$	4516
R_{int}	0.0171

Refinement	
R_1	0.046
wR_2	0.104
Goof	1.02
No. of parameters	450
$(\Delta\,\rho)_{max/min}$	0.33/-0.31

Bond lengths Å

C1-C6	1.437(2)	C3-C4	1.417(2)
C1-C2	1.454(2)	C4-C5	1.453(2)
C2-C3	1.446(2)	C5-C6	1.445(2)

Torsion angles (°)

C1 - C2 - C3 - C4	25.87(19)
C2 - C3 - C4 - C5	8.75(20)
C3 - C4 - C5 - C6	-32.89(20)
C4 - C5 - C6 - C1	22.13(20)
C5 - C6 - C1 - C2	10.58(20)
C6 - C1 - C2 - C3	-35.89(19)

Hydrogen bonds

D - H ··· A	d(H···A)	d(D···A)	
N1-H1···O5	1.851	2.567	
N3-H3···O4	1.945	2.584	
N5-H5···O6	1.911	2.616	
O50-H50···O2	1.895	2.716	[x-1, y, z]

p-fluorotoluene as inclusion compound (1-20)

Crystal data	
empirical formula	$(C_{15}H_{24}O_6N_6)$. (C_7H_7F)
formula wt	494.53
crystal size [mm]	0.40, 0.30, 0.20
crystal colour	yellow
solvent	*p*-fluorotoluene
temperature	203(2) K
crystal system	monoclinic
space group	C c
a (Å)	17.107(9)
b (Å)	16.895(7)
c (Å)	11.351(6)
β (deg)	129.23
Z	4
V (Å^3)	2541(2)
D_{calc} (mg/m^3)	1.293
F(000)	1048
μ [mm^{-1}]	0.100

Data colection	
Θ range [°]	2.2/28.0
h	0/22
k	0/22
l	-14/11
Reflection collected	3152
Reflection unique	3152
Reflection observed [$I > 2\sigma(I)$]	2387
R_{int}	-

Refinement	
R_1	0.059
wR_2	0.169
Goof	1.03
No. of parameters	313
$(\Delta\rho)_{max/min}$	0.57/-0.44

Bond lengths Å

C1-C6	1.458(2)	C3-C4	1.457(2)
C1-C2	1.441(2)	C4-C5	1.439(2)
C2-C3	1.434(2)	C5-C6	1.421(2)

Torsion angles (°)

C1 - C2 - C3 - C4	-17.01(53)
C2 - C3 - C4 - C5	41.48(51)
C3 - C4 - C5 - C6	-28.59(54)
C4 - C5 - C6 - C1	-7.78(57)
C5 - C6 - C1 - C2	31.11(54)
C6 - C1 - C2 - C3	-17.53(53)

Hydrogen bonds

D - H ··· A	d(H···A)	d(D···A)
N1-H1···O1	1.880	2.566
N3-H3···O2	1.887	2.571
N5-H5···O6	1.991	2.601

o-fluorotoluene as inclusion compound (1-21)

Crystal data	
empirical formula	$(C_{15}H_{24}O_6N_6)$. (C_7H_7F)
formula wt	494.53
crystal size [mm]	0.25, 0.20, 0.20
crystal colour	yellow
solvent	*o*-fluorotoluene
temperature	200(2) K
crystal system	monoclinic
space group	C c
a (Å)	17.295(1)
b (Å)	15.789(2)
c (Å)	11.830(1)
β (deg)	129.94(3)
Z	4
V (Å^3)	2477.0(4)
D_{calc} (mg/m^3)	1.326
F(000)	1048
μ [mm^{-1}]	0.103

Data colection	
Θ range [°]	3.1/27.9
h	-22/22
k	-16/20
l	-15/15
Reflection collected	4544
Reflection unique	4544
Reflection observed $[I > 2\sigma(I)]$	3273
R_{int}	-

Refinement	
R_1	0.059
wR_2	0.131
Goof	1.02
No. of parameters	347
$(\Delta\rho)_{max/min}$	0.4/-0.24

Bond lengths Å

C1-C6	1.452(5)	C3-C4	1.427(5)
C1-C2	1.453(5)	C4-C5	1.448(5)
C2-C3	1.445(5)	C5-C6	1.410(5)

Torsion angles (°)

C1 - C2 - C3 - C4	10.57(48)
C2 - C3 - C4 - C5	-37.00(46)
C3 - C4 - C5 - C6	31.63(47)
C4 - C5 - C6 - C1	0.24(42)
C5 - C6 - C1 - C2	-25.48(48)
C6 - C1 - C2 - C3	19.70(48)

Hydrogen bonds

D - H ··· A	d(H···A)	d(D···A)
N1-H1···O1	1.787	2.545
N3-H3···O2	1.810	2.544
N5-H5···O5	1.958	2.604

p-chlorofluorobenzene as inclusion compound (1-22)

Crystal data	
empirical formula	$(C_{15}H_{24}O_6N_6)$. (C_6H_4FCl)
formula wt	514.94
crystal size [mm]	0.30, 0.35, 0.45
crystal colour	yellow
solvent	*p*-chlorofluorobenzene
temperature	203(2) K
crystal system	monoclinic
space group	C c
a (Å)	17.025(5)
b (Å)	16.684(3)
c (Å)	11.402(3)
β (deg)	128.76(2)
Z	4
V (Å^3)	2525.4(1)
D_{calc} (mg/m^3)	1.354
F(000)	1080
μ [mm^{-1}]	0.206

Data colection	
Θ range [°]	2.2/28.0
h	0/22
k	0/22
l	-15/11
Reflection collected	3134
Reflection unique	3134
Reflection observed $[I > 2\,\sigma\,(I)]$	2629
R_{int}	-

Refinement	
R_1	0.035
wR_2	0.086
Goof	1.05
No. of parameters	364
$(\Delta\,\rho)_{max/min}$	0.19/-0.22

Bond lengths Å

C1-C6	1.441(3)	C3-C4	1.415(3)
C1-C2	1.452(3)	C4-C5	1.448(3)
C2-C3	1.445(2)	C5-C6	1.441(3)

Torsion angles (°)

C1 - C2 - C3 - C4	-27.68(30)
C2 - C3 - C4 - C5	-8.82(31)
C3 - C4 - C5 - C6	31.65(30)
C4 - C5 - C6 - C1	-17.31(30)
C5 - C6 - C1 - C2	-17.43(29)
C6 - C1 - C2 - C3	41.16(28)

Hydrogen bonds

D - H ··· A	d(H···A)	d(D···A)
N1-H1···O5	1.899	2.569
N3-H3···O4	1.870	2.603
N5-H5···O6	1.881	2.565

m-fluoronitrobenzene as inclusion compound (1-23)

Crystal data	
empirical formula	$(C_{15}H_{24}O_6N_6)$. $(C_6H_4NO_2F)$
formula wt	525.50
crystal size [mm]	0.42, 0.31, 0.25
crystal colour	yellow
solvent	*m*-fluoronitrobenzene
temperature	148(2) K
crystal system	triclinic
space group	P –1
a (Å)	10.6400(2)
b (Å)	10.8262(2)
c (Å)	11.9471(2)
α (deg)	72.495(1)
β (deg)	71.553(1)
γ (deg)	82.409(1)
Z	2
V (Å^3)	1243.99(4)
D_{calc} (mg/m^3)	1.403
F(000)	552
μ [mm^{-1}]	0.114

Data colection	
Θ range [°]	2.0/27.9
h	-13/11
k	-14/14
l	-15/15
Reflection collected	8178
Reflection unique	5837
Reflection observed [$I > 2\sigma(I)$]	4737
R_{int}	0.026

Refinement	
R_1	0.042
wR_2	0.103
Goof	1.02
No. of parameters	446
$(\Delta\rho)_{max/min}$	0.26/-0.25

Bond lengths Å

C1-C6	1.450(2)	C3-C4	1.427(2)
C1-C2	1.448(2)	C4-C5	1.441(2)
C2-C3	1.445(2)	C5-C6	1.454(2)

Torsion angles (°)

C1 - C2 - C3 - C4	-27.52(18)
C2 - C3 - C4 - C5	3.91(18)
C3 - C4 - C5 - C6	29.18(17)
C4 - C5 - C6 - C1	-37.74(16)
C5 - C6 - C1 - C2	13.02(18)
C6 - C1 - C2 - C3	18.21(17)

Hydrogen bonds

D - H ··· A	d(H···A)	d(D···A)	
N2-H2···O2	1.780	2.545	
N4-H4···O4	1.908	2.612	
N6-H6···O1	2.447	3.252	[-x+2, -y+1, -z+1]
N6-H6···O1	1.860	2.576	

o-fluoronitrobenzene as inclusion compound (1-24)

Crystal data	
empirical formula	$(C_{15}H_{24}O_6N_6)$. $(C_6H_4NO_2F)$
formula wt	525.50
crystal size [mm]	0.42, 0.31, 0.25
crystal colour	yellow
solvent	m-fluoronitrobenzene
temperature	100(2) K
crystal system	monoclinic
space group	P2(1)/c
a (Å)	11.2502(7)
b (Å)	15.0397(9)
c (Å)	14.9582(9)
α (deg)	90.00
β (deg)	104.2540(10)
γ (deg)	90.00
Z	4
V (Å^3)	2453.0(3)
D_{calc} (mg/m^3)	1.432
F(000)	1104
μ [mm^{-1}]	0.115

Data colection	
Θ range [°]	2.31/28.32
h	-15/15
k	-20/20
l	-19/19
Reflection collected	33108
Reflection unique	6088
Reflection observed [$I > 2\sigma(I)$]	4901
R_{int}	0.026

Refinement	
R_1	0.043
wR_2	0.120
Goof	1.07
No. of parameters	436
$(\Delta\rho)_{max/min}$	0.51/-0.51

Bond lengths Å

C1-C6	1.450(2)	C3-C4	1.427(2)
C1-C2	1.448(2)	C4-C5	1.441(2)
C2-C3	1.445(2)	C5-C6	1.454(2)

Torsion angles (°)

C1 - C2 - C3 - C4	-27.52(17)
C2 - C3 - C4 - C5	3.91(17)
C3 - C4 - C5 - C6	29.18(16)
C4 - C5 - C6 - C1	-37.74(16)
C5 - C6 - C1 - C2	13.02(16)
C6 - C1 - C2 - C3	18.21(17)

Hydrogen bonds

D - H ··· A	d(H···A)	d(D···A)	
N2-H2···O2	1.780	2.599	
N4-H4···O4	1.908	2.593	
N6-H6···O1	2.447	3.255	[-x+2, -y+1, -z+1]
N6-H6···O1	1.860	2.569	

p-fluoronitrobenzene as inclusion compound (1-25)

Crystal data	
empirical formula	$(C_{15}H_{24}O_6N_6)$. $(C_6H_4NO_2F)$
formula wt	523.51
crystal size [mm]	0.35, 0.30, 0.15
crystal colour	yellow
solvent	*p*-fluoro nitrobenzene
temperature	193(2) K
crystal system	triclinic
space group	P –1
a (Å)	10.521(2)
b (Å)	11.054(3)
c (Å)	11.963(3)
α (deg)	63.77(2)
β (deg)	84.73(2)
γ (deg)	79.62(2)
Z	2
V (Å^3)	1227.4(5)
D_{calc} (mg/m^3)	1.422
F(000)	552
μ [mm^{-1}]	0.115

Data colection	
Θ range [°]	2.1/27.9
h	0/13
k	-14/14
l	-15/15
Reflection collected	6207
Reflection unique	5890
Reflection observed [$I > 2\sigma(I)$]	4255
R_{int}	0.021

Refinement	
R_1	0.042
wR_2	0.113
Goof	1.02
No. of parameters	446
$(\Delta\rho)_{max/min}$	0.34/-0.34

Bond lengths Å

C1-C6	1.438(2)	C3-C4	1.443(2)
C1-C2	1.424(2)	C4-C5	1.452(2)
C2-C3	1.451(2)	C5-C6	1.453(2)

Torsion angles (°)

C1 - C2 - C3 - C4	33.23(18)
C2 - C3 - C4 - C5	-17.99(19)
C3 - C4 - C5 - C6	-15.42(18)
C4 - C5 - C6 - C1	37.13(18)
C5 - C6 - C1 - C2	-22.95(19)
C6 - C1 - C2 - C3	-12.60(18)

Hydrogen bonds

D - H ··· A	d(H···A)	d(D···A)
N1-H1···O2	1.901	2.607
N3-H3···O3	1.873	2.567
N5-H5···O4	1.862	2.573

nitroethane as inclusion compound (1-26)

Crystal data	
empirical formula	$(C_{15}H_{24}O_6N_6)$. $(C_2H_5NO_2)$
formula wt	459.47
crystal size [mm]	0.43, 0.40, 0.39
crystal colour	yellow
solvent	nitroethane
temperature	200(2) K
crystal system	monoclinic
space group	P 2_1/n
a (Å)	10.7057(2)
b (Å)	14.9258(3)
c (Å)	14.7940(3)
β (deg)	109.829(1)
Z	4
V (Å^3)	2223.79(8)
D_{calc} (mg/m^3)	1.370
F(000)	976
μ [mm^{-1}]	0.110

Data colection	
Θ range [°]	2.0/27.9
h	-14/14
k	-18/19
l	-19/19
Reflection collected	8586
Reflection unique	5269
Reflection observed [$I > 2\sigma(I)$]	3845
R_{int}	0.023

Refinement	
R_1	0.042
wR_2	0.098
Goof	1.03
No. of parameters	405
$(\Delta\rho)_{max/min}$	0.21/-0.28

Bond lengths Å

C1-C6	1.455(2)	C3-C4	1.455(2)
C1-C2	1.430(2)	C4-C5	1.444(2)
C2-C3	1.445(2)	C5-C6	1.450(2)

Torsion angles (°)

C1 - C2 - C3 - C4	27.62(17)
C2 - C3 - C4 - C5	-37.14(17)
C3 - C4 - C5 - C6	10.08(17)
C4 - C5 - C6 - C1	23.29(17)
C5 - C6 - C1 - C2	-34.05(18)
C6 - C1 - C2 - C3	8.17(18)

Hydrogen bonds

D - H ··· A	d(H···A)	d(D···A)	
N2-H2···O2	1.852	2.598	
N4-H4···O5	1.845	2.566	
N6-H6···O6	1.891	2.578	
N6-H6···O3	2.586	3.289	[x+1/2, -y+1/2 ,z+1/2]

1-nitropropane as inclusion compound (1-27)

Crystal data	
empirical formula	$(C_{15}H_{24}O_6N_6)$. $(C_3H_7NO_2)$
formula wt	473.50
crystal size [mm]	0.20, 0.20, 0.15
crystal colour	yellow
solvent	1-nitropropane
temperature	293(2) K
crystal system	monoclinic
space group	$P\,2_1/c$
a (Å)	10.8986(3)
b (Å)	15.1251(3)
c (Å)	14.8456(4)
β (deg)	111.003(1)
Z	4
V (Å^3)	2284.6(1)
D_{calc} (mg/m^3)	1.377
F(000)	1008
μ [mm^{-1}]	0.110

Data colection	
Θ range [°]	2.0/27.9
h	-14/14
k	-17/18
l	-19/19
Reflection collected	9147
Reflection unique	5279
Reflection observed $[I > 2\sigma(I)]$	3589
R_{int}	0.030

Refinement	
R_1	0.044
wR_2	0.093
Goof	1.01
No. Of parameters	422
$(\Delta\rho)_{max/min}$	0.22/-0.27

Bond lengths Å

C1-C6	1.443(2)	C3-C4	1.427(2)
C1-C2	1.449(2)	C4-C5	1.455(2)
C2-C3	1.448(2)	C5-C6	1.451(2)

Torsion angles (°)

C1 - C2 - C3 - C4	-29.96(19)
C2 - C3 - C4 - C5	-6.28(19)
C3 - C4 - C5 - C6	34.63(18)
C4 - C5 - C6 - C1	-26.84(18)
C5 - C6 - C1 - C2	-7.63(18)
C6 - C1 - C2 - C3	37.25(18)

Hydrogen bonds

D - H ··· A	d(H···A)	d(D···A)	
N1-H1···O6	1.832	2.572	
N3-H3···O3	1.901	2.607	
N5-H5···O5	1.919	2.587	
N5-H5···O1	2.586	3.325	[x, -y+1/2 , z+1/2]

benzaldehyde as inclusion compound (1-28)

Crystal data	
empirical formula	$(C_{15}H_{24}O_6N_6)$. (C_6H_5CHO)
formula wt	490.52
crystal size [mm]	0.40, 0.35, 0.35
crystal colour	yellow
solvent	benzaldhyde+ mesitylene
temperature	223(2) K
crystal system	triclinic
space group	P –1
a (Å)	11.1293(2)
b (Å)	11.3454(1)
c (Å)	11.4481(2)
α (deg)	63.5840(5)
β (deg)	78.2320(5)
γ (deg)	72.199(1)
Z	2
V (Å^3)	1228.68(3)
D_{calc} (mg/m^3)	1.263
F(000)	520
μ [mm^{-1}]	0.100

Data colection	
Θ range [°]	1.9/27.9
h	-14/14
k	-14/11
l	-15/12
Reflection collected	8333
Reflection unique	5799
Reflection observed $[I > 2\sigma(I)]$	4334
R_{int}	0.021

Refinement	
R_1	0.049
wR_2	0.124
Goof	1.050
No. of parameters	437
$(\Delta\rho)_{max/min}$	0.29/-0.23

Bond lengths Å

C1-C6	1.445(2)	C3-C4	1.441(2)
C1-C2	1.443(2)	C4-C5	1.420(2)
C2-C3	1.462(2)	C5-C6	1.459(2)

Torsion angles (°)

C1 - C2 - C3 - C4	39.63(18)
C2 - C3 - C4 - C5	-25.12(18)
C3 - C4 - C5 - C6	-13.30(18)
C4 - C5 - C6 - C1	37.12(18)
C5 - C6 - C1 - C2	-21.81(18)
C6 - C1 - C2 - C3	-14.74(18)

Hydrogen bonds

D - H ··· A	d(H···A)	d(D···A)	
N2-H2···O2	1.860	2.588	
N2-H2···O2	2.608	3.420	[-x+1, -y+2, -z]
N4-H4···O5	1.913	2.612	
N6-H6···O1	1.943	2.600	
N6-H6···O50	2.463	3.148	[x+1, y, z]
O7-H7···O2	1.816	2.522	

dioxane as inclusion compound (1-29)

Crystal data	
empirical formula	$(C_{15}H_{24}O_6N_6).(C_4H_8O_2)$
formula wt	428.45
crystal size [mm]	0.30, 0.10, 0.08
crystal colour	yellow
solvent	dioxane
temperature	148(2) K
crystal system	triclinic
space group	P –1
a (Å)	10.3056(3)
b (Å)	11.1027(3)
c (Å)	11.2729(4)
α (deg)	113.658(1)
β (deg)	109.015(1)
γ (deg)	100.564(2)
Z	2
V ($Å^3$)	1040.92(6)
D_{calc} (mg/m^3)	1.367
F(000)	456
μ [mm^{-1}]	0.107

Data colection	
Θ range [°]	2.2/27.9
h	-13/13
k	-14/14
l	-11/14
Reflection collected	6986
Reflection unique	4934
Reflection observed [$I > 2\sigma(I)$]	3426
R_{int}	0.031

Refinement	
R_1	0.062
wR_2	0.102
Goof	1.06
No. of parameters	383
$(\Delta\rho)_{max/min}$	0.26/-0.25

Bond lengths Å

C1-C6	1.436(3)	C3-C4	1.440(2)
C1-C2	1.455(2)	C4-C5	1.452(3)
C2-C3	1.447(3)	C5-C6	1.422(2)

Torsion angles (°)

C1 - C2 - C3 - C4	20.12(22)
C2 - C3 - C4 - C5	16.05(22)
C3 - C4 - C5 - C6	-35.35(21)
C4 - C5 - C6 - C1	15.54(22)
C5 - C6 - C1 - C2	22.60(22)
C6 - C1 - C2 - C3	-40.82(22)

Hydrogen bonds

D - H ··· A	d(H···A)	d(D···A)	
N2-H2···O3	1.879	2.587	
N2-H2···O3	2.434	3.201	[-x+1, -y, -z+1]
N4-H4···O4	1.803	2.569	
N6-H6···O6	1.968	2.636	

γ-picoline 1 as inclusion compound (1-30)

Crystal data	
empirical formula	$(C_{15}H_{24}O_6N_6)$. (C_6H_7N)
formula wt	477.53
crystal size [mm]	0.35, 0.35, 0.30
crystal colour	yellow
solvent	γ-picoline
temperature	223(2) K
crystal system	monoclinic
space group	C c
a (Å)	16.874(9)
b (Å)	16.090(3)
c (Å)	11.800(6)
β (deg)	129.34(3)
Z	4
V ($Å^3$)	2476.7(2)
D_{calc} (mg/m^3)	1.281
F(000)	1016
μ [mm^{-1}]	0.096

Data colection	
Θ range [°]	2.0/28.0
h	0/22
k	0/21
l	-15/12
Reflection collected	3087
Reflection unique	3087
Reflection observed [$I > 2\sigma(I)$]	2387
R_{int}	-

Refinement	
R_1	0.035
wR_2	0.083
Goof	1.05
No. of parameters	351
$(\Delta\rho)_{max/min}$	0.15/-0.20

Bond lengths Å

C1-C6	1.411(3)	C3-C4	1.432(3)
C1-C2	1.447(3)	C4-C5	1.449(3)
C2-C3	1.448(3)	C5-C6	1.453(3)

Torsion angles (°)

C1 - C2 - C3 - C4	38.13(28)
C2 - C3 - C4 - C5	-11.87(29)
C3 - C4 - C5 - C6	-19.46(28)
C4 - C5 - C6 - C1	27.28(29)
C5 - C6 - C1 - C2	-2.32(29)
C6 - C1 - C2 - C3	-30.80(28)

Hydrogen bonds

D - H ··· A	d(H···A)	d(D···A)
N1-H1···O5	1.946	2.597
N3-H3···O3	1.926	2.561
N5-H5···O4	1.843	2.553

γ-picoline 2 as inclusion compound (1-31)

Crystal data	
empirical formula	$(C_{15}H_{24}O_6N_6)$. $(C_6H_7N)_{3/2}$
formula wt	524.09
crystal size [mm]	0.20, 0.25, 0.35
crystal colour	yellow
solvent	γ-picoline
temperature	213(2) K
crystal system	hexagonel
space group	P 3(2)2$_1$
a (Å)	11.3835(4)
b (Å)	11.3835(4)
c (Å)	36.670(3)
α (deg)	90
β (deg)	90
γ (deg)	120
Z	6
V (Å^3)	4115.3(4)
D_{calc} (mg/m^3)	1.269
F(000)	1674
μ [mm^{-1}]	0.093

Data colection	
Θ range [°]	1.7/28.4
h	-14/15
k	-15/6
l	-49/47
Reflection collected	31048
Reflection unique	6851
Reflection observed $[I > 2\sigma(I)]$	4728
R_{int}	0.069

Refinement	
R_1	0.041
wR_2	0.069
Goof	0.87
No. of parameters	473
$(\Delta\rho)_{max/min}$	0.49/-0.20

Bond lengths Å

C1-C6	1.442(2)	C3-C4	1.412(2)
C1-C2	1.456(2)	C4-C5	1.458(2)
C2-C3	1.450(2)	C5-C6	1.438(2)

Torsion angles (°)

C1 - C2 - C3 - C4	28.35(21)
C2 - C3 - C4 - C5	10.62(22)
C3 - C4 - C5 - C6	-34.50(22)
C4 - C5 - C6 - C1	18.36(22)
C5 - C6 - C1 - C2	18.44(21)
C6 - C1 - C2 - C3	-43.49(21)

Hydrogen bonds

D - H ··· A	d(H···A)	d(D···A)	
N1-H1···O6	2.054	2.628	
N1-H1···O1	2.171	2.963	[x-y, -y+1, -z+1/3]
N1-H1···O2	2.475	3.045	[x-y, -y+1, -z+1/3]
N1-H1···N2	2.619	3.400	[x-y, -y+1, -z+1/3]
N3-H3···O4	1.9621	2.619	
N3-H3···O4	2.434	3.239	[y, x, -z]
N5-H5···O5	1.805	2.567	

2,4,6-tris(isopropylamino)-1,3,5-trinitrobenzenes with isopropylamine (1dep-1)

Crystal data	
empirical formula	$(C_{15}H_{18}O_6N_6).(C_3H_9N)^2$
formula wt	502.6
crystal size [mm]	0.18, 0.18, 0.08
crystal colour	yellow
solvent	isopropylamin
temperature	200(2) K
crystal system	triclinic
space group	P –1
a (Å)	9.0040(7)
b (Å)	12.2270(9)
c (Å)	14.2042(10)
α (deg)	104.726(2)
β (deg)	101.120(2)
γ (deg)	105.988(2)
Z	2
V (Å^3)	1394.57(18)
D_{calc} (mg/m^3)	1.20
F(000)	544
μ [mm^{-1}]	0.089

Data colection	
Θ range [°]	2.5/28.3
h	-10/11
k	-16/14
l	-17/18
Reflection collected	10487
Reflection unique	6832
Reflection observed [$I > 2\sigma(I)$]	4459
R_{int}	0.027

Refinement	
R_1	0.044
wR_2	0.096
Goof	0.90
No. of parameters	429
$(\Delta\rho)_{max/min}$	0.37/-0.18

Bond lengths Å

C1-C6	1.398(2)	C3-C4	1.402(2)
C1-C2	1.487(2)	C4-C5	1.476(2)
C2-C3	1.498(2)	C5-C6	1.473(2)
N1-C1	1.389(2)	N4-C4	1.320(2)
N2-C2	1.273(2)	N5-C5	1.350(2)
N3-C3	1.381(2)	N6-C6	1.327(2)

Torsion angles (°)

C1 - C2 - C3 - C4	-45.08(15)
C2 - C3 - C4 - C5	2.34(17)
C3 - C4 - C5 - C6	41.53(16)
C4 - C5 - C6 - C1	-40.06(16)
C5 - C6 - C1 - C2	-5.50(16)
C6 - C1 - C2 - C3	46.76(15)

Hydrogen bonds

D - H ··· A	d(H···A)	d(D···A)
N4-H4···O4	1.970	2.634

N4-H4···O4	2.403	3.178	[-x+2, -y+1, -z+1]
N6-H6···O1	1.894	2.624	
N50-H50A···N53	1.938	2.903	[-x+1, -y+1, -z+1]
N50-H50B···N2	2.095	3.007	[x, y, z+1]
N50-H50C···O6	2.092	2.939	[-x+1, -y+1, -z+1]
N50-H50C···O5	2.400	3.184	[-x+1, -y+1, -z+1]
N53-H53A···O3	2.136	3.012	[x, y+1, z]
N53-H53B···O2	2.472	3.262	[x, y+1, z]

2,4,6-tris(t-butylamino)-1,3,5-trinitrobenzenes with t-butylamine (3dep-1)

Crystal data	
empirical formula	$(C_{18}H_{30}O_6N_6).(C_4H_{11}N)^5$
formula wt	792.2
crystal size [mm]	0.18, 0.18, 0.08
crystal colour	yellow
solvent	t-butylamin
temperature	100(2) K
crystal system	triclinic
space group	P –1
a (Å)	11.378(2)
b (Å)	12.080(2)
c (Å)	20.810(4)
α (deg)	76.391(5)
β (deg)	77.483(4)
γ (deg)	64.793(4)
Z	2
V (Å^3)	2493.0(9)
D_{calc} (mg/m^3)	1.05
F(000)	876
μ [mm^{-1}]	0.072

Data colection	
Θ range [°]	1.0/28.4
h	-15/15
k	-12/16
l	-27/23
Reflection collected	14578
Reflection unique	11389
Reflection observed [$I > 2\sigma(I)$]	5312
R_{int}	0.053

Refinement	
R_1	0.089
wR_2	0.207
Goof	0.96
No. of parameters	563
$(\Delta\rho)_{max/min}$	0.82/-0.36

Bond lengths Å

C1-C6	1.428(4)	C3-C4	1.409(5)
C1-C2	1.485(5)	C4-C5	1.481(5)
C2-C3	1.488(5)	C5-C6	1.478(4)
N1-C1	1.374(4)	N4-C4	1.324(4)
N2-C2	1.259(4)	N5-C5	1.354(4)
N3-C3	1.376(5)	N6-C6	1.324(4)

Torsion angles (°)

C1 - C2 - C3 - C4	51.95(42)
C2 - C3 - C4 - C5	-9.96(45)
C3 - C4 - C5 - C6	-34.63(44)
C4 - C5 - C6 - C1	34.05(43)
C5 - C6 - C1 - C2	10.97(44)
C6 - C1 - C2 - C3	-52.09(41)

Hydrogen bonds

D - H ··· A	d(H···A)	d(D···A)
N4-H4···O4	2.073	2.623
N6-H6···O2	1.868	2.582

N7-H7A···N10	1.840	2.848	[x, y+1, z]
N7-H7B···N8	1.998	2.835	
N7-H7C···O6	1.992	2.877	
N7-H7C···O5	2.573	3.234	
N8-H8A···O1	2.148	3.041	[x, y+1, z]
N8-H8B···O5	2.533	3.116	
N10-H10A···O2	2.417	3.261	
N10-H10B···O4	2.446	3.155	[x-1, y, z]
N11-H11B···O2	2.593	3.574	[x-1, y, z]

2,4,6-tris(cyclopropylamino)-1,3,5-trinitrobenzenes with t-butylamine (2dep-1)

Crystal data	
empirical formula	$(C_{15}H_{18}O_6N_6)$. $(C_4H_{11}N)$
formula wt	451.5
crystal size [mm]	0.37, 0.32, 0.18
crystal colour	yellow
solvent	t-butylamin
temperature	100(2) K
crystal system	monoclinic
space group	P 2_1/c
a (Å)	9.0449(8)
b (Å)	16.4575(14)
c (Å)	15.6444(13)
β (deg)	105.251(2)
Z	4
V ($Å^3$)	2246.8(3)
D_{calc} (mg/m^3)	1.34
F(000)	960
μ [mm^{-1}]	0.101

Data colection	
Θ range [°]	1.8/28.4
h	-11/12
k	-21/20
l	-12/20
Reflection collected	16577
Reflection unique	5592
Reflection observed [$I > 2\sigma(I)$]	4461
R_{int}	0.046

Refinement	
R_1	0.040
wR_2	0.101
Goof	0.98
No. of parameters	405
$(\Delta\rho)_{max/min}$	0.45/-0.24

Bond lengths Å

C1-C6	1.410(2)	C3-C4	1.430(2)
C1-C2	1.482(2)	C4-C5	1.458(2)
C2-C3	1.482(2)	C5-C6	1.452(2)
N1-C1	1.374(2)	N4-C4	1.324(2)
N2-C2	1.314(2)	N5-C5	1.386(2)
N3-C3	1.364(2)	N6-C6	1.274(2)

Torsion angles (°)

C1 - C2 - C3 - C4	-40.45(14)
C2 - C3 - C4 - C5	3.02(15)
C3 - C4 - C5 - C6	36.94(15)
C4 - C5 - C6 - C1	-36.15(14)
C5 - C6 - C1 - C2	-4.34(14)
C6 - C1 - C2 - C3	41.78(14)

Hydrogen bonds

D - H ··· A	d(H···A)	d(D···A)	
N4-H4···O4	1.851	2.857	
N6-H6···O1	1.868	2.571	
N20-H20A···O4	2.091	2.599	
N20-H20B···N2	2.000	2.934	[-x+1, -y, -z+1]

N20-H20B···O3	2.572	2.963	[-x+1, -y, -z+1]
N20-H···O5	2.123	2.918	[x, -y+1/2, z+1/2]
N20-H···O6	2.446	3.253	[x, -y+1/2, z+1/2]

2,4,6-tris(*(S)*2-butylamino)-1,3,5-trinitrobenzenes (5)

Crystal data	
empirical formula	$(C_{18}H_{30}O_6N_6)$
formula wt	426.5
crystal size [mm]	0.50, 0.46, 0.30
crystal colour	yellow
solvent	aceton
temperature	295(2) K
crystal system	monoclinic
space group	P 2_1
a (Å)	8.9457(8)
b (Å)	16.9466(14)
c (Å)	15.1489(13)
β (deg)	90.9006(1)
Z	4
V (Å^3)	1595.8(4)
D_{calc} (mg/m^3)	1.58
F(000)	912
μ [mm^{-1}]	0.094

Data colection	
Θ range [°]	1.34/28.21
h	-10/11
k	-22/11
l	-19/18
Reflection collected	14154
Reflection unique	8210
Reflection observed $[I > 2\sigma(I)]$	5499
R_{int}	0.029

Refinement	
R_1	0.054
wR_2	0.150
Goof	0.95
No. of parameters	552
$(\Delta\rho)_{max/min}$	0.33/-0.17

Bond lengths Å

C1-C6	1.446(4)	C20-C21	1.442(4)
C1-C2	1.452(4)	C20-C25	1.442(4)
C2-C3	1.436(4)	C21-C22	1.397(5)
C3-C4	1.457(4)	C22-C23	1.439(5)
C4-C5	1.416(4)	C23-C24	1.446(4)
C5-C6	1.423(4)	C24-C25	1.445(4)

Torsion angles (°)

C1 - C2 - C3 - C4	-4.61(36)	C20 - C21 - C22 - C33	9.94(52)
C2 - C3 - C4 - C5	35.42(30)	C21 - C22 - C23 - C24	26.41(46)
C3 - C4 - C5 - C6	-30.76(39)	C22 - C23 - C24 -C25	-37.12(40)
C4 - C5 - C6 - C1	-4.40(39)	C23 -C24 - C25 - C20	13.27(39)
C5 - C6 - C1 - C2	13.83(38)	C24 - C25 - C20 - C21	19.20(29)
C6 - C1 - C2 - C3	-28.53(36)	C25 - C20 - C21 - C22	-30.98(48)

Hydrogen bonds

D - H ··· A	d(H···A)	d(D···A)	
N1-H1···O2	1.958	2.597	
N1-H1···O23	2.565	3.197	[-x+2, y-1/2, -z]
N3-H3···O1	1.879	2.577	
N5-H5···O6	2.025	2.596	

N20-H20···O25	1.908	2.573
N22-H22···O21	2.114	2.597
N24-H24···O24	1.860	2.552

Appendix 1

1a1(0)	-x+1, y, -z+1/2
1a1(1)	x-1/2, -y+1/2, z
1a1(3)	-x+3/2, y+1/2, -z+1/2
1a2(0)	-x+1, y, -z+1/2
1a2(1)	x-1/2, y+1/2, z
1a2(2)	-x+1, -y+1, -z+1

1b(0)	-x+1/2, -y+1/2, -z
1b(1)	x+1/2, -y+1/2, z+1/2
1b(2)	x, y, z
1b(3)	-x+1, y, -z+1/2
1b(5)	x+1/2, y+1/2, z
1b(6)	-x+1, -y+1, -z+1
1b(7)	x, -y+1, z+1/2

Group 1

Host(1)	x+1/2, y+1/2, z
Host(2)	x+1, -y+1, z-1/2
Host(3)	x+1/2, -y+1/2, z+1/2

Guest(1)	x+1/2, y+1/2, z
Guest(2)	x, -y+1, z+1/2

Gruop 2
Subgroup 2-1

1-14 benzonitrile

Host(1)	x, y, z
Host(2)	-x+2, -y+2, -z+1
Host(3)	x, y, z+1
Guest(1)	-x+1, -y+1, -z+1
Guest(2)	x, y, z+1

1-28 benzaldhyde

Host(1)	x, y+2, z+1
Host(2)	-x+1, -y+2, -z+1
Host(3)	x, y, z+1
Guest(1)	x+1, y, z+2
Guest(2)	-x+1, -y+2, -z+2

1-29 dioxane

Host(1)	x, y, z+1
Host(2)	-x+1, -y+1, -z+1
Host(3)	x, y+1, z
Guest(1)	x, y+1, z
Guest(2)	-x+1, -y+1, -z+1

1-33 nitrobenzene

Host(1)	-x+2, -y+1, -z+2
Host(2)	x+1, y+1, z+1
Host(3)	-x+1, -y+1, -z+1
Guest(1)	-x, -y+1, -z+1
Guest(2)	x+1, y, z+1

1-16 DMF

Host(1)	x+1, y+1, z+1
Host(2)	-x+1, -y+1, -z+1
Host(3)	x, y+1, z+1
Guest(1)m2	x, y, z+1

1-17 hydrochinon

Host(1)	x, y, z+1
Host(2)	-x+2, -y+1, -z+2
Host(3)	x, y, z
Host(4)	-x+1, -y+1, -z+1

Guest(2)m1	-x+1, -y+1, -z+1
Guest(2)m2	-x+1, -y1, -z

Guest(1)	x, y, z+1
Guest(2)	x, y, z

1-19 *p*-nitrophenol

Host(1)	x, y, z
Host(2)	-x+1, -y+2, -z+1
Host(3)	x, y, z+1
Host(4)	-x+1,-y+1, -z+2
Guest(1)	x, y, z
Guest(2)	-x+1, -y+1, -z+2

1-25 *p*-fluoronitrobenzene

Host(1)	x, y, z
Host(2)	-x+2, -y+1, -z+1
Host(3)	x, y, z+1
Host(4)	-x+1, -y+1, -z+2
Guest(1)	x, y, z+1
Guest(2)	-x+1, -y+1, -z+1

Subgroup 2-2

1-11 phenol 1

Host(1)m1	x, y, z
Host(1)m2	x, y+1, z
Host(2)m2	-x+1, -y+2, -z+1
Host(3)m1	-x+2, -y+1, -z+1
Guest(1)	x-1, y+1, z

1-23 *m*-fluoronitrobenzene

Host(1)	x, y, z
Host(2)	-x+2, -y+1, -z+1
Host(3)	-x+1, -y+1, -z+1
Guest(1)	-x+1, -y, -z+2
Guest(2)	x, y+1, z
Guest(3)	x, y+1, z-1

1-39 acetonitrile

Host(1)	-x+1, -y, -z+1
Host(2)	x, y+1, z
Host(3)	x+1, y+1, z
Guest(1)	-x+1, -y+1, -z+1
Guest(2)	x, y+1, z
Guest(3)	x+1, y, z

1-37 acetic acid

Host(1)	-x+1, -y+1, -z+1
Host(2)	x, y+1, z+1
Host(3)	-x+1, -y+1, -z+2
Guest(1)	-x+1, -y+1, -z+1
Guest(2)	x+1, y+1, z+2
Guest(3)	x+1, y+1, z+1

1-36 formic acid

Host(1)	-x+1, -y+2, -z+1
Host(2)	x, y, z
Host(3)	x+1, y+1, z
Guest(1)	-x, -y+1, -z+1
Guest(2)	x+1, y+1, z+1
Guest(3)	-x+1, -y+1, -z+1

Subgroup 2-3

1-13 anisole

Host(1)m1	x+1, y+1, z
Host(1)m2	-x+1, -y+1, -z+1
Host(2)m1	-x+2, -y+1, -z+1
Host(2)m2	x, y, z+1
Host(3)m1	-x+2, -y, -z+1
Guest(1)	x, y, z
Guest(2)	-x+3, -y+1, -z+1
Guest(3)	-x+2, -y+1, -z+1

Group 3

1-10 hexafluorobenzene

Host(1)m2	-x+1, -y+1, -z+1
Host(2)m1	-x+1, -y+1, -z
Host(3)m1	x, y, z
Guest(1)m1	-x+1, -y+1, -z
Guest(2)m1	-x+1, -y+1, -z+1

1-12 phenol 2

Host(1)	x, y, z+1
Host(2)	-x+2, -y+2, -z+1
Host(3)	-x+1, -y+1, -z+1
Guest(1)m1	-x+1, -y+1, -z+1
Guest(1)m2	x, y, z+1

1-24 *o*-fluoronitrobenzene

Host(1)	-x+1, y+1/2, z+1/2
Host(2)	-x+1, -y+1, -z+1
Host(3)	x+1, -y+1/2, z+1/2
Guest(1)	x, -y+1/2, z+1/2
Guest(2)	-x+1, -y+1, -z+1

1-26 nitroethane

Host(1)	x, y, z
Host(2)	x+1/2, -y+1/2, z+1/2
Host(3)	-x, -y+1, -z+1
Guest(1)	x, y, z
Guest(2)	x+1/2, y+1/2, -z+1/2

1-27 nitropropane

Host(1)	x, y, z
Host(2)	x, -y+1/2, -z+1/2
Host(3)	-x+2, -y+1, z+1
Guest(1)	-x+1, -y+1, -z+1
Guest(2)	x, -y+1/2, z+1/2

1-35 *p*-xylene 2

Host(1)m1	-x+1, -y+2, -z+1
Host(1)m2	-x+1, -y+1, -z+1
Host(2)m1	-x+1, y+1/2, -z+3/2
Host(3)m1	-x+1, -y+3/2, z-1/2
Guest(1)	x, y, z

Group 4

1-31 γ-picoline 2

Host(1)	-x+y+1, -x+1, z+1/3
Host(2)	x-y+1, -y+1, z+1/3
Host(3)	-x+1, -x+y, -z+2/3
Guest(1)m1	-x+y+1, -x+1, z+1/3
Guest(1)m2	-x+y+1, -x+1, z+1/3

References

---

[1] D. S. Coombes, S. L. Price, D. J. Willock, M. Leslie, *J. Phys. Chem.* **1996**, *100*, 7352-7360.

[2] [3a] H. G. Gallagher, K. J. Roberts, J. N. Sherwood, L. A. Smith, *J. Mater. Chem.* **1997**, *7*, 229-235. [3b]R. J. Davey, G. D. Potts, R. Docherty, *J. Am. Chem. Soc.* **1997**, *119*, 1767-1772.

[3] S. L. Price, K. S. Wibley, *J. Phys. Chem.A* **1997**, *101*, 2198-2206.

[4] A. Gavezzotti, *Acc. Chem. Res.* **1994**, *27*, 309-314.

[5] [5a]H. R. Karfunkel, R. J. Gdanitz, *J. Comput. Chem.* **1992**, *13*, 1171-1183. [bb]A. Gavezzotti, *J. Am. Chem. Soc.* **1991**, *113*,4622-4629. [5c]D. W. M. Hofmann, T. Lengauer, *Acta Crys A,* **1997**,*53*,225-235. [5d]B. P. Van Eijck, W. T. M. Mooij, J. Kroon, *Acta, Crys. B.* **1995**, *51*, 99-103. [5e]A. M. Chaka, R. Zaniewski, W. Youngs, C. Tessier, G. Klopman, *Acta, Crys. B.* **1996**, *52*,165-183. [5f]N. Tajima, T. Takayuki, T. Arikawa, T. Sakurai, S. Teramae T. Hirano, *Bull. Chem. Soc. Jpn.* **1995**, *68*, 519. [5g]R. J. Gdanitz, *J. Chem. Phys. Lett.* **1992**, *190*,391-396. [5h]D. E. Williams, *Acta, Crys. A.* **1996**, *52*, 326-328.

[6] J. R. Holden, Z. Du, H. L. Ammon, *J. Comput. Chem.* **1993**, *14*, 422-437.

[7] J. P. M. Lommerse, W. D. S. Motherwell, H. L. Ammon, J. D. Dunitz, A. Gavezzotti, D. W. M. Hofmann, F. J. J. Leusen, W. T. M. Mooij, S. L. Price, B.Schweizer, M. U. Schmidt, B. P. Van Eijck, P. Verwer, D. E. Williams, *Acta Cryst.* **2000**, B56, 697-714.

[8] D. Braga, G. R. Desiraju, J. S. Miller, A. G. Orpen, S. L. Price, *CrystEngComm,* **2002**, 4(83), 500-509.

[9] C. B. Aakeröy, M. Nieuwenhuyzen, S. L. Price, *J. Am. Chem. Soc.* **1998**, *120*, 8986-8993.

[10] L. Yu, G. A. Stephenson, C. A. Mitchell, C. A. Bunnell, S. V. Snorek, J. J. Bowyer, T. B. Borchardt, J. G. Stowell, S. R. Byrn, *J. Am. Chem. Soc.* **2000**, *122*, 585-591.

[11] M. Caira, L. R. Nassimbeni, F. Toda, D. Vujovic, *J. Am. Chem. Soc.* **2000**, *122*, 9367-9372.

[12] J. M. Chance, B. Kahr, A. B. Buda, J. S. Siegel, *J. Am. Chem. Soc.* **1989**, *111*, 5940-5944.

[13] J. J. Wolff, S. F. Nelsen, P. A. Petillo, D. R. Powell, *Chem. Ber*. **1991**, *124*, 1719-1725.

[14] L. R. Nassimbeni, *CrystEngComm*, **2003**, 5(35), 200-203.

[15] U. Burkert, N. L. Allinger, *Molecular Mechanics,* ACS Monographs, American Chemical Society, washington, DC, **1982**.

[16] J. Dale, *Stereochmistry and Conformational analysis,* Verlag Chemie. New York, **1978**.

[17] C. A. Hunter, J. Singh, J. M. Thornton, *J. Mol. Biol.* **1991**, *218*, 837.

[18] S. Tsuzuki, T. Uchimaru, K. Tanabe, *J. Phys. Chem.* **1993**, *97*, 1346.

[19] C. U. Singh, P. A. Kollman, *J. Comp. Chem.* **1984**, *5*, 129.

[20] G. Bakalarski, P. Grochowski, J. S. Kwiatkowski, B. Lesyng, J. Leszczynski, *Chem.*

---

*Phys.***1996,** *204*, 301-311.

[21] C. I. Bayly, P. Cieplak, W. D. Cornell, P. A. Kollman, *J. Phys. Chem.***1993**, *97*, 10269-10280.

[22] B. Delley, *J. Chem. Phys.* **1990,** *92*, 508.

[23] B. Delley, *J. Chem. Phys.* **2000**, *113*, 7756.

[24] J. P. Perdew, Y. Wang, *Phys. Rev.* **1992,** *B45*, 13244.

[25] A. D. J. Becke, *J. Chem. Phys.* **1988**, *88*, 2547.

[26] Accelrys Inc., Materials studio 2.2, San Diaego: Accelrys Inc., **2002**.

[27] H. Sun, *J. Phys. Chem. B* **1998,** *102*, 7338-7364.

[28] S. W. Bunte, *J. Phys. Chem. B* **2000,** *104*, 2477-2489.

[29] P. J. Haines, *Thermal Methods of Analysis, principles, applications and problems,* Blackie Academic and professional, **1995**.

[30] G. Höhne, W. Hemminger, H. J. Flammershein, *Differential Scanning Calorimetry, an introduction for practitioners,* springer-verlag Berlin, Heidelberg, **1996**.

[31] J. O. Hill, *For Better Thermal Analysis and Calorimetry*, III, ICTAC, **1991**.

[32] C. Duval, *Inorganic Thermogravimetric Analysis* (2nd edn), Elsevier, Amsterdam, **1963**.

[33] C. J. Keattch, D. Dollimore, *Introdaction to Thermogravimetry*, Heyden, London, **1975**, Ch. 1.

[34] W. Wendlandt, *J. chem. Educ.*, **1972**, *49*, A571, A623.

[35] K. Honda, *Sci. Rep.* Tohuku Univ., **1915**, *4*, 97.

[36] M. I. Pope, M. D. Judd, *Educ. In Chem.*, **1971**, *8*, 89.

[37] A. R. Leach, *Molecular Modelling, Principles and Applications*, Longman, Harlow, **1996**.

[38] A. I. Kitaigorodsky, *Molecular crystal and molecules,* Academic Pr. **1973**.

[39] W. Koch, M. C. Holthausen, *A Chemist's Guide to Density Functional Theory*, Wiley-VCH, Weinheim, **2000**.

[40] J. J. Wolff, H. Irngartinger, F. Gredel, I. Bolocan*, Chem. Ber.* **1993**, *126*, 2127-2131.

[41] F. Gredel, *dissertation*, Heidelberg, **1997**.

[42] N. S. Zefirov, V. A. Palyulin, E. E. Dashevskaya, *J. Phys. Org. Chem.,* **1990,** *vol. 3*, 147-158.

[43] J. J. Wolff, F. Gredel, T. Oeser, H. Irngartinger, *Chem. Eur. J.* **1999**, *5*, 29-38.

[44] J. Bernstein, *Polymorphism in Molecular Crystals,* Oxford University Press, **2000.**

[45] J. J.Wolff, F.Nelsen, R. Powell, *J. Org. Chem.* **1991**, *56*, 5908-5911.

[46] G. M. Sheldrick, *SHELXS-97*, Universität Göttingen, Germany, **1997.**

[47] G. M. Sheldrick, *SHELXL-97*, Universität Göttingen, Germany, **1997.**

---

[48] *SMART*, *SAINT*: Brucker AXS, Inc., 5465 East Cheryl Parkway, Madison, Wisconsin 53711-5373, USA **2001.**

[49] *SHELXTL 6.1*: Bruker AXS, Inc., 5465 East Cheryl Parkway, Madison, Wisconsin 53711-5373, USA **2000.**

Ich erkläre hiermit, dass ich die vorliegende Dissertation selbst verfasst und mich dabei keiner anderen als den von mir ausdrücklich bezeichneten Quellen und Hilfen bedient habe. Ich habe an keiner anderen Stellen ein Prüfungsverfahren beantragt bzw. die Dissertation in dieser oder anderer Form bereits anderweitig als Prüfungsarbeit verwendet oder einer anderen Fakultät als Dissertation vorgelegt.

Heidelberg, im Oktober 2003

Soheir El-Derby